

# **APPLICATIONS OF INTELLIGENT CONTROL TECHNIQUES FOR IMPROVED PERFORMANCE IN POWER ELECTRONIC CONVERTERS**

**A DISSERTATION**

*Submitted in partial fulfillment of the  
requirements for the award of the degree*

*of*

**INTEGRATED DUAL DEGREE**

**In**

**ELECTRICAL ENGINEERING**

**(With Specialization in Power Electronics)**

**By**

**RAVI KISHORE R**



**DEPARTMENT OF ELECTRICAL ENGINEERING**

**INDIAN INSTITUTE OF TECHNOLOGY ROORKEE**

**ROORKEE – 247 667 (INDIA)**

**MAY, 2016**

## CANDIDATE’S DECLARATION

---

I hereby declare that the work presented in the dissertation report entitled “**Applications of Intelligent Control Techniques for improved performance in Power Electronic Converters**” submitted in partial fulfillment of the requirements for the award of the degree of Integrated Dual Degree in Electrical Engineering with Specialization in Power Electronics, submitted in the Department of Electrical Engineering, Indian Institute of Technology, Roorkee is an authentic record of my work carried out under the guidance and supervision of Dr. Mukesh K. Pathak, Associate Professor, Department of Electrical Engineering, Indian Institute of Technology, Roorkee.

Date: 23<sup>rd</sup> May 2016

Place: Roorkee

(Ravi Kishore R)

## CERTIFICATE

---

This to certify that the above statement made by the candidate is correct to the best of my knowledge.

Dr. Mukesh K. Pathak  
Associate Professor  
Department of Electrical Engineering  
Indian Institute of Technology, Roorkee  
Roorkee – 247667, India

# ACKNOWLEDGEMENTS

---

This report is the result of the project “Applications of Intelligent Control Techniques for improved performance in Converters” for the partial fulfillment of the Master of Technology in Electrical Engineering. I wish to affirm my deep sense of gratitude to my guide Dr. Mukesh Pathak, Department of Electrical Engineering, IIT Roorkee for intuitive and meticulous guidance in completion of this seminar report. I want to express my profound gratitude for his genial and kind co-operation in completing this work and his valuable suggestions throughout the work. I convey my gratitude to Dr. S. P. Srivastava, Head of Department, Electrical Engineering, Indian Institute of Technology Roorkee for providing me this opportunity to pursue this project.

Date: 23<sup>rd</sup> May 2016

(RAVI KISHORE R)

Place: Roorkee

Enrolment No: 11212011

# ABSTRACT

---

Intelligent control techniques based upon Expert Systems, Fuzzy Logic and Artificial Neural Networks are recently having a significant impact on power electronics and motor drives. Neural Networks in particular have created a new and advancing frontier in power electronics, which is already a complex and multidisciplinary technology that is going through dynamic evolution in the recent years.

Converters are evidently the crux of power electronics application. Thus we must experiment, analyze and realize the utility of such intelligent control techniques in this field. Further a comprehensive analysis with respect to the conventional methods can be established.

Neural Networks have proven to be of excellent usage in scenarios involving complex, non-linear and transcendental mathematical models. Providing robust and flexible architectures that can learn in real-time, these networks can be a ready replacement for on-line calculations and storage apparatus. Through this report, we explore how a neural network system can be used in PWM strategies to produce near perfect sinewaves devoid of the harmonics which are sometimes responsible for instabilities. Further we explore how such intelligent control methodologies can be used in applications such as speed control of an induction machine fed by a voltage source inverter. Also through this dissertation, we take steps further from Neural Networks based control to other techniques such as Fuzzy Logic based systems to analyze the utility, advantages and disadvantages of intelligent control techniques for different scenarios. The study ends with a brief description of a successful realization of a hardware prototype.

# TABLE OF CONTENTS

---

<b>CANDIDATE’S DECLARATION</b> .....	<b>ii</b>
<b>ACKNOWLEDGEMENTS</b> .....	<b>iii</b>
<b>ABSTRACT</b> .....	<b>iv</b>
<b>TABLE OF CONTENTS</b> .....	<b>v</b>
<b>LIST OF FIGURES</b> .....	<b>viii</b>
<b>LIST OF ACRONYMS</b> .....	<b>xi</b>
<b>Chapter 1: Introduction</b> .....	<b>1</b>
1.1 Research Motivation .....	1
1.2 Research Objective .....	1
1.3 Literature Review .....	2
1.3.1 Review based on Selective Harmonics Elimination .....	2
1.3.2 Review based on Inverter fed Induction Machine control .....	3
1.4 Introduction to Intelligent Control Techniques.....	4
1.5 Artificial Neural Networks .....	5
1.5.1 Activation Functions.....	6
1.5.2 Network Models .....	7
1.5.3 Training a Backpropagation Network.....	8
1.5.4 Other Neural Network Models .....	10
1.5.5 Neural Networks in Control Systems .....	11
1.5.6 Neural Network Based Control.....	11
1.5.7 Applications of Neural Network Based Control .....	12
1.6 Fuzzy Logic .....	13
1.6.1 Classical Set and Fuzzy Set Comparison.....	13
1.6.2 Fuzzy Systems .....	14
1.6.3 Defuzzification Methods.....	16
1.6.4 Fuzzy Control .....	17
1.6.6 Applications .....	17
1.8 Objective of the Thesis .....	18

1.9 Thesis Organization .....	19
<b>Chapter 2: Selective Harmonics Elimination based PWM Inverter .....</b>	<b>20</b>
2.1 Introduction.....	20
2.2 Harmonics in Inverter Output .....	21
2.3 Switching Angles.....	22
2.4 Fourier Analysis for 2 Level PWM based Inverter Scheme .....	22
2.5 Implementations from Literature .....	24
2.6 ANN based Selective Harmonics Elimination in Inverters .....	24
2.7 Artificial Neural Network Block .....	25
2.8 Block Diagram.....	26
2.9 Selective Harmonics Block.....	27
2.10 Neural Network Training (Offline).....	27
2.11 Switching Waveform Generation Block.....	27
2.12 Inverter Block .....	28
2.13 Results of Simulation.....	28
2.14 Observations .....	30
<b>Chapter 3: Sinusoidal Pulse Width Modulation Based Inverter .....</b>	<b>31</b>
3.1 Two-Level Inverter .....	31
3.1.1 THD Variation with Power Factor.....	34
3.1.2 THD Variation with Frequency .....	34
3.2 Diode-Clamped Three-Level Inverter.....	35
3.2.1 THD Variation with Power Factor.....	38
3.2.2 THD Variation with Frequency .....	38
3.3 Conclusion .....	38
<b>Chapter 4: Multi Level Inverter Based Induction Motor Drive.....</b>	<b>39</b>
4.1 Scalar Control of Multilevel Inverter fed Induction Motor Drive .....	39
4.1.1 Open-Loop v/f Control .....	40
4.1.2 Closed-Loop v/f Control.....	41
4.2 Salient Feature of Scalar Control.....	42
<b>Chapter 5: Performance Evaluation of Inverter Fed Induction Motor Drive .....</b>	<b>44</b>
5.1 General Model using PI based controller.....	44
5.2 Steady State Performance Using PI based controller .....	45
5.2.1 Two Level Inverter fed Induction Motor Drive using PI based controller .....	45

5.2.2	Three-Level Diode-clamped Inverter fed Induction Motor Drive using PI based controller ...	49
5.3	General Model using Neural Network based controller .....	53
5.4	Steady State Performance Using Neural Network based controller .....	54
5.4.1	Two Level Inverter fed Induction Motor Drive using Neural Network based controller .....	54
5.4.2	Three-Level DCI fed Induction Motor Drive using Neural Network based controller .....	57
5.5	General Model using Fuzzy Logic based controller .....	60
5.6	Steady State Performance Using Fuzzy Logic based controller .....	61
5.6.1	Two Level Inverter fed Induction Motor Drive using Fuzzy Logic based controller .....	61
5.6.2	Three-Level DCI fed Induction Motor Drive using Fuzzy Logic based controller .....	64
5.7	Comparison of Performance .....	68
5.8	Recommendation for Future Work .....	72
<b>Chapter 6: System Hardware Development.....</b>		<b>73</b>
6.1	Laboratory Tests .....	73
6.1.1	No Load and Blocked Rotor Test .....	73
6.1.2	Retardation Test .....	75
6.2	Hardware Development .....	77
6.2.1	Development of Power Circuit of Inverter fed Induction motor control .....	77
6.2.2	Snubber Circuit .....	78
6.3	Measurement of System Parameters .....	79
6.4	Control Hardware .....	80
6.4.1	Pulse Amplification and Isolation Circuit.....	81
6.4.2	Controller realization and PWM generation .....	81
6.5	Power Supplies .....	82
6.6	Overall Setup .....	83
<b>References .....</b>		<b>84</b>

# LIST OF FIGURES

---

Figure 1.1: Structure of a biological neuron .....	5
Figure 1.2: Model of Artificial Neuron .....	6
Figure 1.3: Various Activation Functions.....	7
Figure 1.4: General Backpropagation Network .....	8
Figure 1.5: Radial basis function based network topology .....	10
Figure 1.6: Self Organizing Map based Network .....	10
Figure 1.7: Recurrent Neural Network example model .....	11
Figure 1.8: Training a neural controller to emulate actual controller .....	12
Figure 1.9: Example for a Classical Set and Fuzzy Set .....	13
Figure 1.10: Graphs of (a) Triangular (b) Trapezoidal (c) Gaussian and (d) General Bell Curves .....	14
Figure 1.11: Mamdani type of inference method.....	15
Figure 1.12: Larsen type of inference method .....	15
Figure 1.13: Sugeno type of implication method.....	16
Figure 1.14: Structure of a fuzzy control in feedback system.....	17
Figure 2.1: General Inverter leg.....	20
Figure 2.2: Quarter and Half wave symmetry .....	22
Figure 2.3: Block diagram for Neural Network used in the implementation.....	25
Figure 2.4: Block Diagram for Selective Harmonics Elimination using ANN.....	26
Figure 2.5: MATLAB Simulink model for generation of PWM waveform from Switching Angle values.....	27
Figure 2.6: General 3 Phase Inverter Diagram in SIMULINK .....	28
Figure 2.7: Plot fit graph, Modulation Index vs Angles graph and Training Error Plot for 2 Level PWM.....	28
Figure 2.8: PWM waveform showing switching angles in one cycle.....	29
Figure 2.9: Line Voltage waveform Fourier Analysis for 2 Level PWM – 9 Angles at $m = 0.9$ .....	30
Figure 3.1: Simulink Model of 2-Level Inverter .....	31
Figure 3.2: Control Signal Generation for 2-Level Inverter .....	32
Figure 3.3: Carrier and modulating Signals for 2-Level Inverter .....	32
Figure 3.4: Firing Pulses to Six MOSFETS S1, S4, S3, S6, S5, S2 from Top to Bottom .....	32
Figure 3.5: Phase Voltage at $f = 50\text{Hz}$ , $MI = 0.85$ , $fr = 15$ .....	33
Figure 3.6: Line Voltage at $f = 50\text{Hz}$ , $MI = 0.85$ , $fr = 15$ .....	33
Figure 3.7: Line Voltage Harmonic Spectrum at $f = 50\text{Hz}$ .....	33
Figure 3.8: Line Current Waveform and its Harmonic Spectrum at $f = 50\text{Hz}$ (P.F = 0.95) .....	33
Figure 3.9: Variation of THD with Power Factor.....	34
Figure 3.10: Simulink Model of 3-Level Diode-Clamped Inverter .....	35
Figure 3.11: Control Signal Generation for 3-Level Diode-Clamped Inverter.....	36
Figure 3.12: Carrier and modulating Signal for one Phase Leg of 3-Level Diode-Clamped Inverter .....	36



Figure 3.13: Firing Pulses to Four MOSFETS of a Phase Leg of 3-Level Diode-Clamped Inverter .....	36
Figure 3.14: Phase Voltages at $f = 50\text{Hz}$ , $MI = 0.85$ , $fr = 15$ .....	37
Figure 3.15: Line Voltage at $f = 50\text{Hz}$ , $MI = 0.85$ , $fr = 15$ .....	37
Figure 3.16: Line Voltage Harmonic Spectrum at $f = 50\text{Hz}$ .....	37
Figure 3.17: Line Current Waveform and its Harmonic Spectrum at $f = 50\text{Hz}$ (P.F = 0.95) .....	38
Figure 3.18: Variation of THD with Power Factor .....	38
Figure 4.1: Approximate per phase equivalent circuit of an induction machine .....	40
Figure 4.2: Open-Loop Speed Control of Induction Motor Using V/f principle .....	40
Figure 4.3: Closed-Loop Speed Control of Induction Motor Using V/f principle.....	41
Figure 4.4: Speed Drift for (a) Supply Voltage (b) Load Torque Variation .....	42
Figure 5.1: Generalized Simulink Model for Inverter fed Induction Motor Drive using PI based controller.....	44
Figure 5.2: Switching Control Block for the 2-Level Inverter fed Induction Motor Drive .....	45
Figure 5.3: Steady-State Performance using PI when the Motor started with no load .....	46
Figure 5.4: Steady-State Performance using PI when the Motor started with Load ( $Tl = 90\text{N-m}$ ) .....	47
Figure 5.5: Steady-State Performance using PI for Step change in Load ( $Tl = 90\text{N-m}$ ) .....	48
Figure 5.6: Steady-State Performance using PI for Step change in Speed ( $N = 1200$ to $1460$ rpm) .....	48
Figure 5.7: Steady-State Performance using PI for Speed Reversal ( $N = 1460$ to $-1460$ rpm).....	49
Figure 5.8: Switching Control Block for the 3 Level Diode Clamped Inverter fed Induction Motor Drive.....	50
Figure 5.9: Steady-State Performance using PI when the Motor started with-out Load.....	51
Figure 5.10: Steady-State Performance using PI when the Motor started with Load ( $Tl = 90\text{N-m}$ ) .....	51
Figure 5.11: Steady-State Performance using PI for Step change in Load ( $Tl = 90\text{N-m}$ ) .....	52
Figure 5.12: Steady-State Performance using PI for Step change in Speed ( $N = 1200$ to $1460$ rpm) .....	52
Figure 5.13: Steady-State Performance using PI for Speed Reversal ( $N = 1460$ to $-1460$ rpm).....	53
Figure 5.14: Generalized Simulink Model for Inverter fed Induction Motor Drive using Neural Network.....	54
Figure 5.15: Steady-State Performance using NN when the Motor started with no load .....	55
Figure 5.16: Steady-State Performance using NN when the Motor started with Load ( $Tl = 90\text{N-m}$ ) .....	55
Figure 5.17: Steady-State Performance using NN for Step change in Load ( $Tl = 90\text{N-m}$ ) .....	56
Figure 5.18: Steady-State Performance using NN for Step change in Speed ( $N = 1200$ to $1460$ rpm) .....	56
Figure 5.19: Steady-State Performance using NN for Speed Reversal ( $N = 1460$ to $-1460$ rpm) .....	57
Figure 5.20: Steady-State Performance using NN when the Motor started with-out Load .....	58
Figure 5.21: Steady-State Performance using NN when the Motor started with Load ( $Tl = 90\text{N-m}$ ) .....	58
Figure 5.22: Steady-State Performance using NN for Step change in Load ( $Tl = 90\text{N-m}$ ) .....	59
Figure 5.23: Steady-State Performance using NN for Step change in Speed ( $N = 1200$ to $1460$ rpm) .....	60
Figure 5.24: Steady-State Performance using NN for Speed Reversal ( $N = 1460$ to $-1460$ rpm) .....	60
Figure 5.25: Generalized Simulink Model for Inverter fed Induction Motor Drive using Fuzzy Logic.....	61
Figure 5.26: Steady-State Performance using Fuzzy Control when the Motor started with no load .....	62
Figure 5.27: Steady-State Performance when using Fuzzy Control the Motor started with Load ( $Tl = 90\text{N-m}$ ) .....	62

Figure 5.28: Steady-State Performance using Fuzzy Control for Step change in Load ( $T_l = 90\text{N-m}$ ) .....	63
Figure 5.29: Steady-State Performance using Fuzzy Control for Step change in Speed ( $N = 1200$ to $1460$ rpm) .....	63
Figure 5.30: Steady-State Performance using Fuzzy Control for Speed Reversal ( $N = 1460$ to $-1460$ rpm) .....	64
Figure 5.31: Steady-State Performance using Fuzzy Control when the Motor started with-out Load .....	65
Figure 5.32: Steady-State Performance using Fuzzy Control when the Motor started with Load ( $T_l = 90\text{N-m}$ ) .....	65
Figure 5.33: Steady-State Performance using Fuzzy Control for Step change in Load ( $T_l = 90\text{N-m}$ ) .....	66
Figure 5.34: Steady-State Performance using Fuzzy Control for Step change in Speed ( $N = 1200$ to $1460$ rpm) .....	66
Figure 5.35: Steady-State Performance using Fuzzy Control for Speed Reversal ( $N = 1460$ to $-1460$ rpm) .....	67
Figure 5.36: Graphs for 2 Level Inverter fed Induction Machine using different control techniques .....	71
Figure 5.37: Graphs for 3 Level Inverter fed Induction Machine using different control techniques .....	72
Figure 6.1: Nameplate showing the manufacturer stated ratings of Induction Machine.....	73
Figure 6.2: Circuit diagram of (a) No Load test (b) Blocked Rotor test .....	74
Figure 6.3: Coupling diagram of IM and DC motor .....	75
Figure 6.4: Schematic diagram of the system implemented for speed control .....	77
Figure 6.5: 3 Phase - 3 Level Voltage source Inverter.....	78
Figure 6.6: Snubber circuit for MOSFET protection and its hardware implementation in laboratory .....	79
Figure 6.7: AC current sensor circuit.....	80
Figure 6.8: AC voltage sensing circuit .....	80
Figure 6.9: Pulse Amplification and Isolation Circuit .....	81
Figure 6.10: FPGA used in hardware and the control switches .....	82
Figure 6.11: Connection diagram for power supplies $-12,0,+12\text{v}$ .....	82
Figure 6.12: Image showing the overall setup of the hardware evaluation.....	83

# LIST OF ACRONYMS

---

AC	Alternating Current
AI	Artificial Intelligence
ANN	Artificial Neural Network
ASIC	Application Specific Integrated Circuit
CSI	Current Source Inverter
DC	Direct Current
DSP	Digital Signal Processor
IGBT	Insulated Gate Bipolar Transistor
MOSFET	Metal Oxide Semiconductor Field Effect Transistor
PWM	Pulse Width Modulation
SHE	Selective Harmonics Elimination
SVM	Space Vector Modulation
TF	Transfer Function
THD	Total Harmonic Distortion
VSI	Voltage Source Inverter

# Chapter 1: Introduction

---

In this chapter we explore a brief discussion about the motive of this dissertation, its objectives and how much progress has been done in these areas as depicted by a literature review. Further we will discuss and interpret the reach and robustness of intelligent control techniques through a brief technical introduction, its various methods and applications in real life.

## 1.1 Research Motivation

Artificial Intelligence is a nascent topic in today's world which has acquired a rapid pace since last few decades. We interact with computer devices throughout the day and every work of a normal person involves interaction with these devices in some sort or another. Emergence of Artificial Intelligence research in contemporary period has had a major impact on how these devices work. We are now able to create computerized devices that tune to the necessities of its user. These machines tend to learn and correct itself for a better utility and robustness of its users. These are found in areas such as manufacturing, control, power generation, robotics, space travel and deep earth excavation as well.

It is evidently a great fascination to introduce such self-learning methodologies in Electrical Engineering applications. With an initial naïve analysis of applications we can realize that these methods have a vast utility in these fields. These find utility in every area such as power systems, protection, instrumentation, power generation, power quality management, power distribution and so on. Basically every place where a computer is used in the system for judging the working of it. These computing devices can be enhanced to introduce an intelligence and result in a further improvement in performance. This motivates a researcher, as the scope of development is massive, so is the application utility. This has been the prime reason for exploring the area. We explore and critically examine how these perform in applications of power electronics and review their utility.

## 1.2 Research Objective

Through this research, we answer critical questions about how we can use artificial intelligence techniques in power electronic applications. We answer if these really are a superior alternative to the conventional methods, and if yes what are the conditions of superiority, its

performance and the impact it can have on the present day applications. The prime motive of this research is to think out of the box ideas to modify and enhance conventional methods. This is a fair attempt to achieve it. We start with a brief literature review to analyze the reach and background. Later we study a brief introduction of the technical background of these areas and later on jump start into the actual applications of intelligent control techniques for improved performance in converters.

### **1.3 Literature Review**

Through this section, we see a review of research works that have already been held so far in the fields of intelligent control and the applications of Artificial Intelligence techniques in power electronics, especially converters. The presented review is divided into broadly two topics, selective harmonics elimination based pulse width modulation and inverter fed induction machine control.

An approach is made by Bimal Kumar Bose (1997) to present an overall review to show the various applications of intelligent control techniques in power electronics and drives, which discusses in vast detail, fuzzy controlled induction machine drive, neural network controlled feedback signal generation for drives and many similar implementations [13].

Another attempt was made by Bimal Kumar Bose (2002) to compile applications of Expert Systems, Fuzzy Logic and Neural Network applications in Power Electronics to diagnose faults in voltage source inverter fed ac drives, slip gain tuning of Induction Motor drive and other DC motor applications [14].

#### **1.3.1 Review based on Selective Harmonics Elimination**

Xin Yao (1999) presented how artificial neural networks are advancing in the current research and how these find application and utility in various fields of technology [1].

Hasmukh and Richard (1973) conducted extensive research in techniques to eliminate harmonics and voltage control in thyristor inverters. This led to the clear outlay of the problem needed to be solved in achieving output waveforms of superior quality. It further clearly stated the degree of difficulty in solving the mathematical model of the same [15].

Arvindan, Sharma and Subbiah (2006) made attempts to solve the mathematical model of selective harmonics elimination in voltage source inverters using microprocessor based controllers. This presented an offline solution finding technique in operating at this method. Further Sun.J and Grotstollen (1994) had earlier made advances to find real time solutions for Selective Harmonics Elimination at operating time using online solving controller. [16] [17]

Attempt by Bimal Kumar Bose (2007) to use the concept of Neural Networks to Selective Harmonics Elimination based Pulse Width Modulation technique. With this, it was introduced how intelligent control has application in generating inverter output waveforms that are devoid of targeted harmonics [18].

Helder (2013) made successful attempt in using Artificial Neural Networks to perform adaptive selective harmonics minimization for cascaded multi level inverters over a wide range of modulation index without having to analytically solve the mathematical model for every value of the modulation index. This presented a newer perspective and robust application of ANN in easy utility and solving of complicated mathematical models in Power Electronics. [19]. Further Basil Saied (2009) had implemented the same using an FPGA to realize satisfactory results. [20]

### **1.3.2 Review based on Inverter fed Induction Machine control**

Holmes and Kotsopoulos (1993) explain in broad terms, the various methods of speed control of a 3 phase induction motor fed by a voltage sourced inverter. [21].

Sayed and Donald (1994) discuss about how we can utilize robust and superior methods such as Fuzzy Logic to achieve speed control of a three phase induction machine which is fed using a voltage source inverter. This work further opens scope about different intelligent control techniques usage in achieving similar control. [22]

Kazmierkowski (2000) discusses on how different PWM techniques are used in such applications in conjunction with intelligent control techniques. Further, we can see works of Eltamaly (2010) and Marcelo Suetake (2011) that give a further insight of these methods which have been successfully implemented using hardware such as Digital Signal Processor, FPGA and other similar controllers. [23] [24] [25]

## 1.4 Introduction to Intelligent Control Techniques

Intelligent Control which essentially implies the involvement of Artificial Intelligence approach in the method. It is evidently one of the latest and most important areas in which computers are being utilized for simulation of human intelligence. Intelligent control techniques stand for the future of automatic control and is the new frontier for advancing developments in the science of automatic control. These techniques include the following:-

- Expert Systems (ES)
- Artificial Neural Network (ANN)
- Fuzzy Logic Algorithms (FL)
- Neuro Fuzzy Algorithms(NF)

These fields have emerged as a prime areas of research throughout the world. As aptly explained through literature by pioneers in the field [1], this field has enormous scope which can be abstracted and implemented in any other field and could readily produce better results than existing main stream methodologies. Further these have been recently applied widely in power electronics and motor drives. Systems with built in computational intelligence is often explained to be an Intelligent System which has capabilities such as self-learning, self-organizing and self-adaptability.

Computational intelligence has been a topic of debate since a long time. It will possibly be discussed forever. However we cannot deny the fact that computers have acceptable intelligence to supplement the solutions to our problems that cannot be solved by traditional methods easily. Therefore it is a fact that Artificial Intelligence techniques are now being widely used in areas such as process control, image recognition, medicine and even space study.

Expert System and Fuzzy Logic techniques are rule based and tend to aptly emulate the behavior of human nature. Artificial Neural Network techniques are generic in nature and tend to emulate the biological neural networks. The history of ANN goes back to the 1940s but recent advancements have happened mostly from 1990. Genetic algorithms were proposed during 1970s and tend to solve optimization problems through principles of Genetics and Evolution.

## 1.5 Artificial Neural Networks

A vital component of the human brain is the cerebral cortex which consists of several billions of biological neurons or nerve cells, which interconnect and form the biological nervous system. This neural network is responsible for human learning, intelligence and the corresponding thinking progression. The structure of biological neuron is known to humanity but the way these neural systems are interconnected are not known. An artificial neuron and thus an artificial neural network tends to emulate a biological nervous system in a limited manner utilizing electronic circuits and computer programming. This biological neuron is the processing element of human brain that receives such signals through several thousands of input paths called dendrites that pass through a synaptic junction called synapse as shown in Figure 1.1. These signals are combined at nucleus of the neuron and the output signal flows through the axon after adhering to a logic decided in the nucleus related to the input signals.

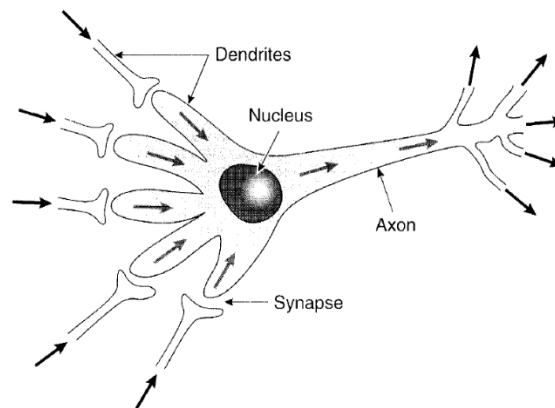


Figure 1.1: Structure of a biological neuron

Biological neurons are closely modelled into artificial neuron. Such an artificial neuron called as neurode, node or a cell has a summing operational amplifier like structure. It is also called a processing element (PE). Each input signal flows through a gain or weight as shown in Figure 1.2. The signal can be continuous or discrete pulses. Weights can be positive or negative or zero.



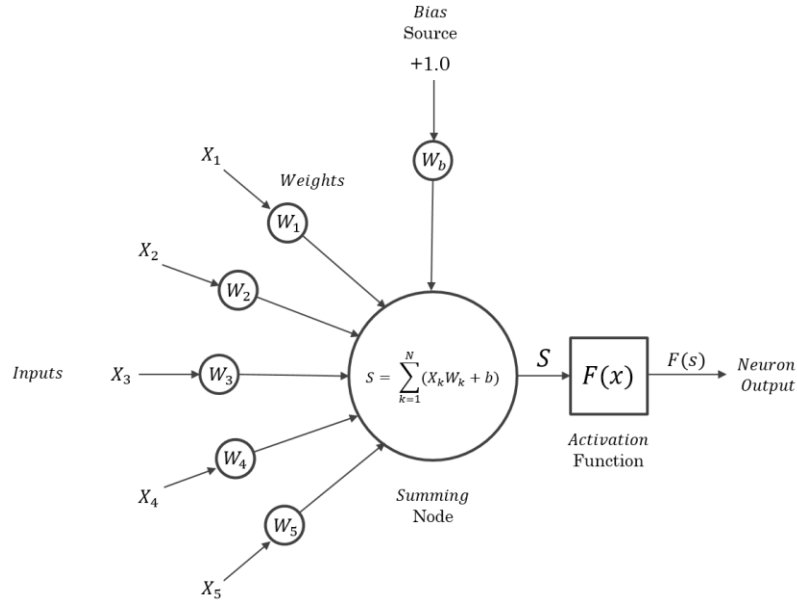


Figure 1.2: Model of Artificial Neuron

The summing node accumulates all the input-weighted signals, adds to the weighted bias signal  $b$ , and then passes to the output through the nonlinear or linear activation or transfer function (TF) as depicted in Figure 1.2. The output expression can be mathematically given as

$$Y = F(S) = F \left[ \sum_{K=1}^N X_k W_k + b \right]$$

Where  $X_k$  denotes the value of  $k^{th}$  input signal,  $W_k$  denotes the weight of  $k^{th}$  signal,  $F$  denotes the activation function and  $b$  denotes the bias applied at the current node.

### 1.5.1 Activation Functions

Several common activation functions are used in Artificial Neural Networks. To name a few, linear (bipolar), threshold, signum, sigmoidal, hyperbolic-tan. There have been examples in the literature in which Gaussian functions have been as well used. The function values of these vary between -1 to +1 or 0 to 1. These linear functions can be unipolar and bipolar. Further, the sigmoidal and hyperbolic-tan functions are the most commonly used activation functions. They are accompanied by gains or coefficients that adjust its slope or sensitivity. Both the functions are continuous and differentiable. Shown below are some of the activation functions graphs

Figure 1.3

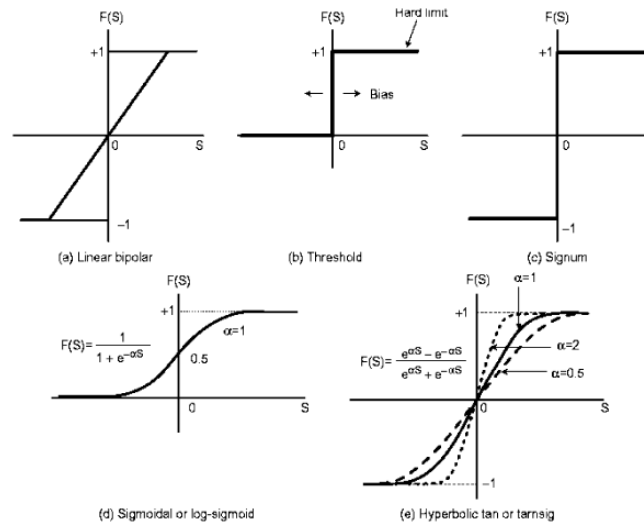


Figure 1.3: Various Activation Functions

## 1.5.2 Network Models

Interconnection of such artificial neurons result in a Neural Network. Its motive is to emulate the function of a brain in certain domain to solve specific, engineering and other real life problems. The structure of a biological neural network is not well-understood, and so, many Artificial Neural Network models have been devised. A few models are listed and briefed as follows:-

### 1. Perceptron

Simple single-layer feedforward neural network used in clear patterns that can be linearly separable. The general structure of such a perceptron network uses unipolar hard-limit activation function.

### 2. Adaline and Madaline

These neural network models have the structure same as that of perceptron networks exception being that the activation function is linear bipolar. These linear neural networks are capable of giving a linear input-output mapping. These can be used extensively to linearize a non-linear relationship.

### 3. Backpropagation Network (BP)

It is a feed-forward multilayer backpropagation topology and is the most commonly used topology in power electronics. The name backpropagation originates from the supervised

training method used to train such a network. It is also often called as a multi-layered perceptron network, as it has an input layer, hidden layers and an output layer.

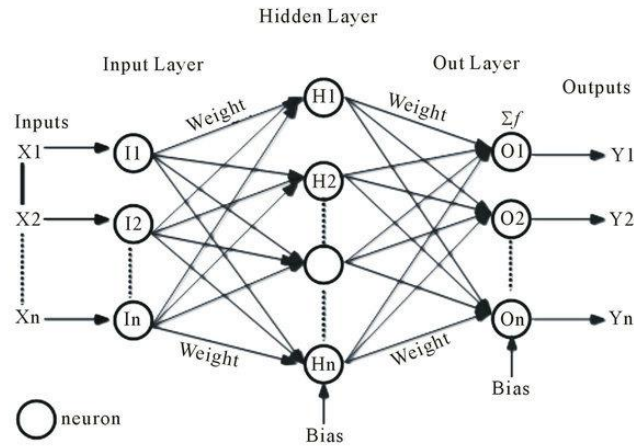


Figure 1.4: General Backpropagation Network

4. Other common Network models including :-

- a. Radial Basis Function Network
- b. Learning Vector Quantization Network
- c. Fuzzy Neural Networks
- d. Self-Organizing Feature Maps
- e. Adaptive Resonance Theory based Networks
- f. Real-Time Recurrent Network
- g. Boltzmann Machine

## 1.5.3 Training a Backpropagation Network

### 1.5.3.1 Offline Training

In simple words, the network is initialized by random weights and tested on the given known data. Each of the neuron weight is penalized by an amount governed by the backpropagation algorithm after each test. Eventually the training fine tunes the weights so that at the end of the training, such a network would fit for the given classification or relationship. The weight adjustment for the minimization of error uses the standard gradient descent technique, where the weights are iterated one at a time starting backward from the output layer.

If we consider input pattern number  $p$ , and the squared output error for all the output layer neurons of the network is given by equation 1, then the corresponding total sum of squared error for the set of  $P$  patterns is then given by equation 2. And the weight adjusted for the  $i+1$  th iteration is given by equation 3. Correspondingly.

$$E_p = (d^p - y^p)^2 = \sum_{j=1}^Q (d_j^p - y_j^p)^2 \quad (1)$$

$$SSE = E = \sum_{p=1}^P E_p = \sum_{p=1}^P \sum_{j=1}^Q (d_j^p - y_j^p)^2 \quad (2)$$

$$W_{ij}(k + 1) = W_{ij}(k) - \eta \left( \frac{\delta E_p}{\delta W_{ij}(k)} \right) \quad (3)$$

Where,  $d_j^p$  = desired output of the  $j$ th neuron in the output layer,

$y_j^p$  = corresponding actual output,  $Q$  = dimension of the output vector,

$y^p$  = actual network output vector,  $d^p$  = corresponding desired output vector,

$\eta$  = learning rate,  $W_{ij}(k + 1)$  = new weight between  $i$ th and  $j$ th neuron.

The weight adjustment done for reducing of error is usually done using gradient descent technique. Such a process is called a reverse pass, which is the reason for naming this as ‘backpropagation’. A round-trip is a pair of forward pass and a reverse pass, called as an epoch. Such a propagation learning algorithm is known as Levenberg-Marquardt algorithm, which is perhaps the most widely used process in modern AI techniques. This technique is known for its fast convergence.

### 1.5.3.2 Online Training

In the above offline training method, Neural Network weights are fixed while in operation. In many applications of Power Electronic Systems we encounter utilities that involve nonlinear and time variable functions where the mathematical model of the plant gets altered depending upon the operating conditions and variation in parameters. Such a cases require the neural networks to train online and called as adaptive, credited to the online variation of weights and structure. Various improved versions of Levenberg-Marquardt algorithm have been proposed using high-speed Microprocessors.

Extended Kalman filter based training methods and Random Weight Change (RWC) based training methods are also widely used in online training of neural networks.

### 1.5.4 Other Neural Network Models

#### Radial Basis Function Network

It is a feed forward network whose output layer neurons have characteristics of linear nature, whereas the hidden neurons use a radial basis function as its activation function.

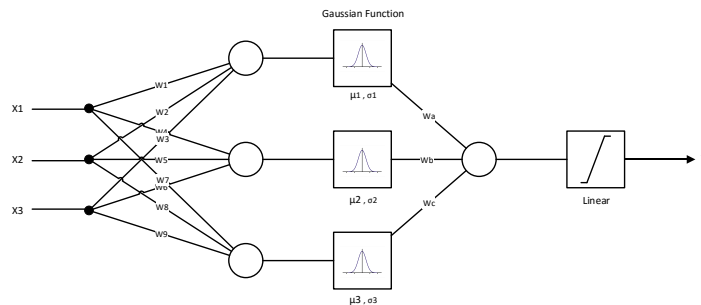


Figure 1.5: Radial basis function based network topology

#### Self-Organizing Feature Map Network

This network is trained using competitive learning where the neurons compete among themselves to be activated or fired since the result has only one neuron active per group at any time.

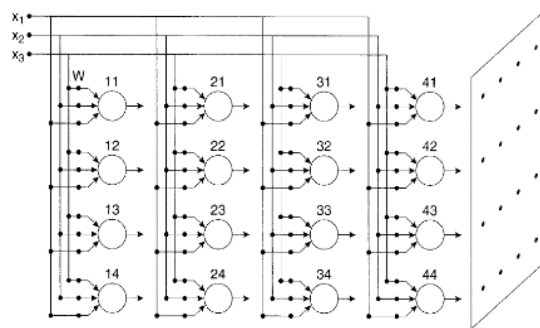


Figure 1.6: Self Organizing Map based Network

#### Recurrent Neural Network

Recurrent networks use feedback from output layers to an earlier layer through a delay and is defined as feedback network. Figure 1.7 is an example recurrent neural network .The output of the  $j^{\text{th}}$  neuron at instant  $k$  is given as

$$Q_j(k) = \sum_{i=1}^5 W_{ij}(k)U_i(k)$$

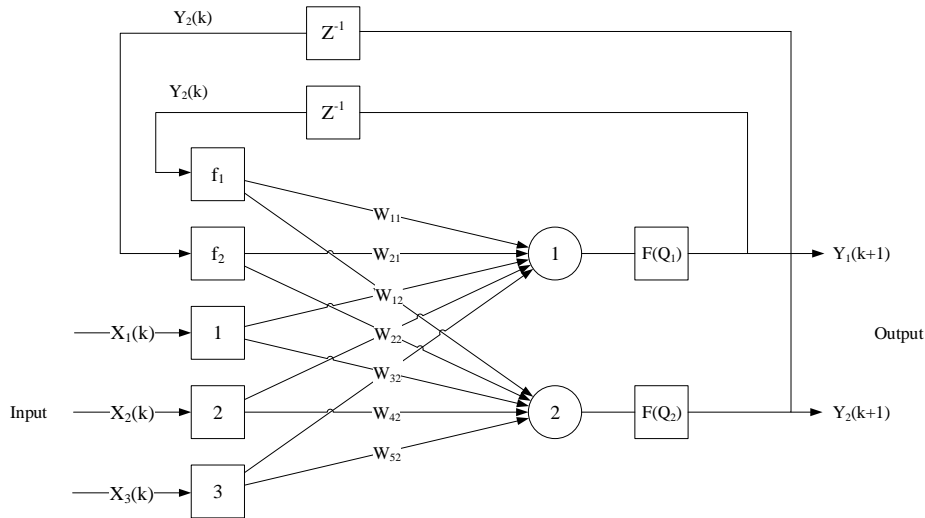


Figure 1.7: Recurrent Neural Network example model

## 1.5.5 Neural Networks in Control Systems

### Time-Delayed Neural Network

Identification and control of nonlinear dynamic systems can be done by dynamic neural networks that have recurrent networks based topology or time-delay network based topology. The present and the past time sequence signals are used through the network and the output is given by the expression

$$y(k) = F \left[ \sum_{n=0}^N W_{nk} x(k-n) \right]$$

Where  $W_{nk} = [W_{0k}, W_{1k}, W_{2k} \dots W_{nk}]$  denotes the network weight vector and F denotes the activation function. Such a network is often trained using backpropagation and this method constitutes a vital part in identification and control of dynamic systems.

### 1.5.6 Neural Network Based Control

Neural Networks are efficiently used in closed loop and open loop control. Neural network controllers are trained to replace traditional controllers in a system as depicted in Figure 1.8(a). The neural network controller can replace the P-I controller thus simplifying the control implementation. It should be noted that output shall vary from the input in an unpredicted way if the parameters of the plant are changed and there is no feedback. Figure 1.8(b) depicts an inverse dynamic model based control of plant.

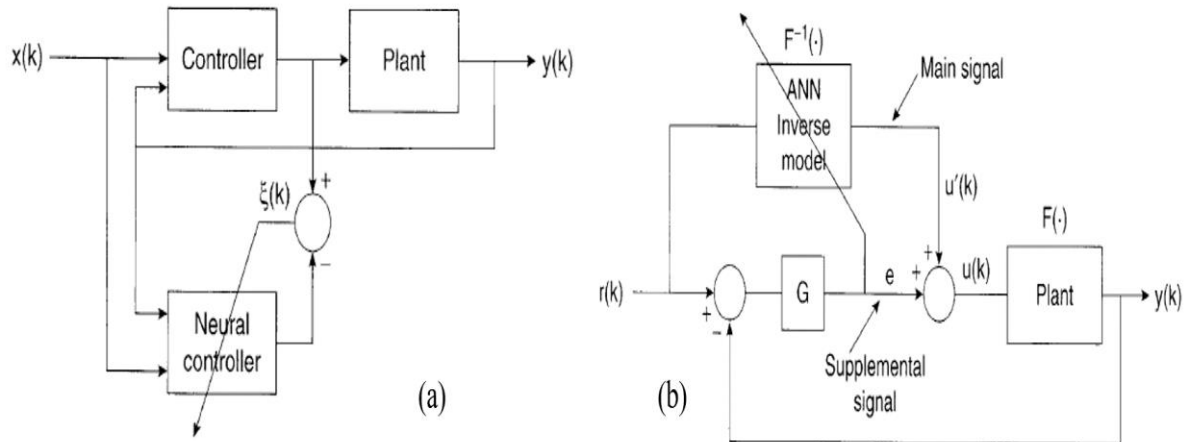


Figure 1.8: (a) Training a neural controller to emulate actual controller, (b) Inverse dynamic model based adaptive control of plant using neural control

### 1.5.7 Applications of Neural Network Based Control

Neural networks have been applied for various control, identification and estimation applications in power electronics and drives. Few of them are:

- Selective Harmonics Elimination based PWM
- Instantaneous current control based PWM
- Space Vector PWM based control
- Vector controlled drive feedback signal estimation
- Distorted waves estimation applications
- Drive control using Model Identification and Adaptive Drive control
- Recurrent Neural Networks based speed estimation
- Recurrent Neural Networks based adaptive Flux estimation
- Delay less filtering applications

## 1.6 Fuzzy Logic

Fuzzy logic was first introduced in 1965 by Lofti A. Zadeh[3]. It embodies human-similar thinking into control systems.

### 1.6.1 Classical Set and Fuzzy Set Comparison

Let  $Y$  be a space of objects, called as universe of discourse or the universal set and  $y$  be a generic element of  $Y$ . A classical set  $S$ , which is a subset of  $Y$  is defined as a collection of elements or objects  $y \in Y$  such that each  $y$  can belong or not belong to the set  $S$ . By defining a function for each element  $y$  in  $Y$ , called characteristic function, we can represent the classical set  $S$  by a set of ordered pairs  $(y, 0)$  or  $(y, 1)$  which indicates  $y \notin S$  or  $y \in S$ , respectively.

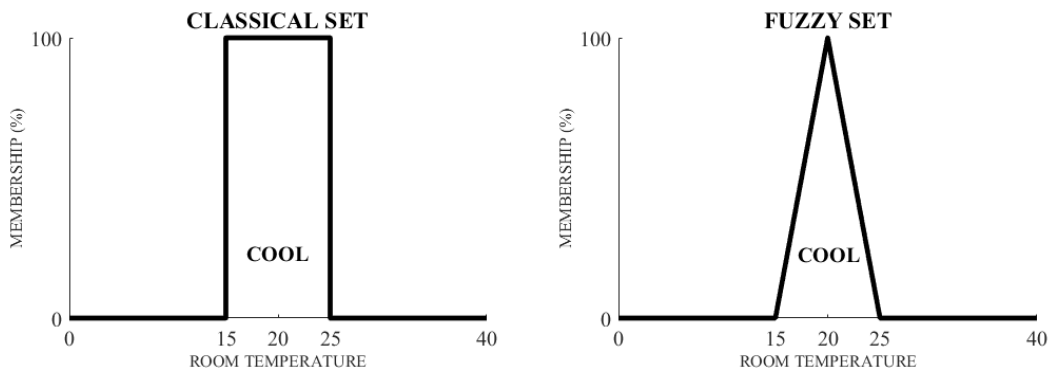


Figure 1.9: Example for a Classical Set and Fuzzy Set

Example application for fuzzy set is shown in Figure 1.9. Different classes of parameterized membership functions[4] commonly used are :-

1. Triangular Function
2. Trapezoidal Function
3. Gaussian Function
4. Generalized Bell Curve
5. Sigmoidal Curve
6. Polynomial Curve



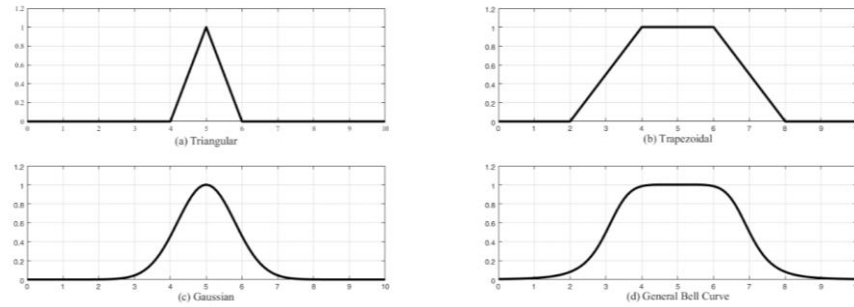


Figure 1.10: Graphs of (a) Triangular (b) Trapezoidal (c) Gaussian and (d) General Bell Curves

## 1.6.2 Fuzzy Systems

A fuzzy inference system, or simply a fuzzy system consists of a construction of the mapping from a given input set to an output set using Fuzzy Logic and this mapping provides the basis from which inferences or conclusions can be made. Such a fuzzy inference system consists of five steps as given:-

1. Fuzzification of the input variables
2. Application of fuzzy operators like AND, OR in the IF part of the rule
3. Implication deduction from the antecedent to the consequent, i.e. the THEN part of the rule
4. Aggregation of the consequents across the rules
5. Defuzzification process

There are a number of implication methods explained in literature. Few of them are:-

1. Mamdani Type
2. Lusing Larson Type
3. Sugeno Type

### Mamdani Type

This is the most common implication method which involves truncation of graph in a fuzzy statement. In this implication, degree of fulfilment of each rule is calculated for a given set of inputs using the minimum operator. The rule output is then given by the truncated membership function as shown in Figure 1.11.

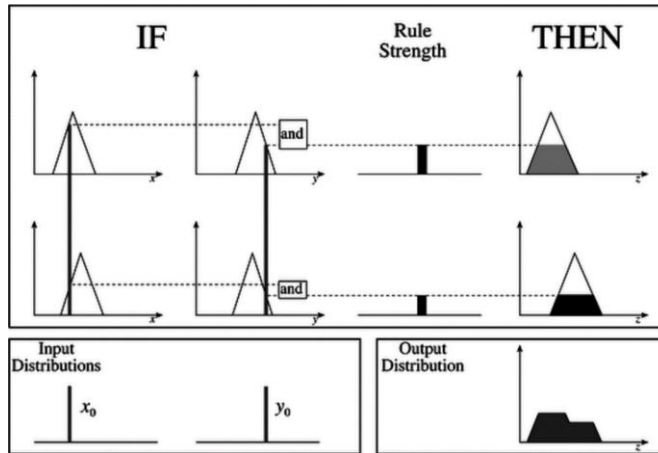


Figure 1.11: Mamdani type of inference method

### Larsen Type

In this method, output membership function is scaled instead of being truncated as done in Mamdani method. Figure 1.12 shows the process of scaling for each rule output.

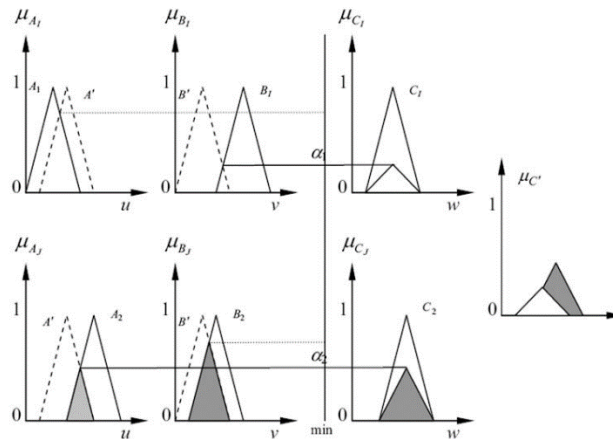


Figure 1.12: Larsen type of inference method

### Sugeno Type

The Sugeno method of implication was first introduced in 1985. The difference is that unlike the previous two methods of implication i.e. Mamdani and Larsen type, the output membership functions are only constants or have linear relations with the inputs. With a constant output membership function, it is defined as the zero-order Sugeno method whereas it is called first-order-Sugeno with linear relation. Figure 1.13 shows the Sugeno implication method.

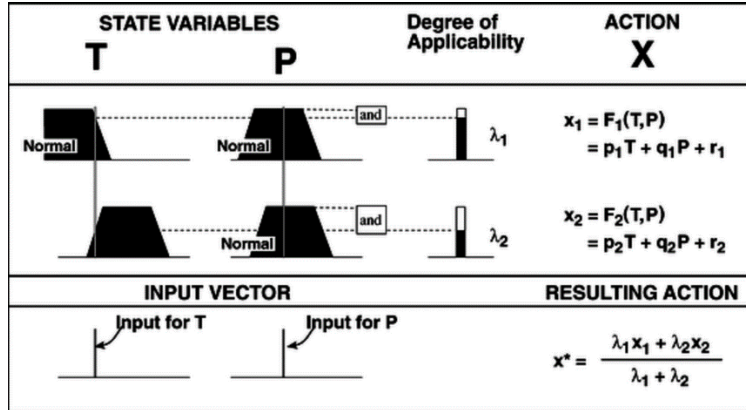


Figure 1.13: Sugeno type of implication method

The output membership function in each rule is a singleton spike which is multiplied by the respective degree of fulfilment to contribute to the fuzzy output of each rule.

### 1.6.3 Defuzzification Methods

The implication and aggregation steps result in a fuzzy output which is the union of all outputs of individual rules that were validated. The conversion of such a fuzzy output to a crisp output value is called as Defuzzification process. Few Defuzzification methods include :

- Center of area method
- Height method
- Mean of Maxima method
- Sugeno method

The Center of Area method, or often called center of gravity method involves calculation of the geometric center of the output fuzzy value aggregated from previous steps. The general expression for calculating the center is

$$Z_0 = \frac{\int Z \mu_{out}(Z) dZ}{\int \mu_{out}(Z) dZ}$$

The height method of Defuzzification is simplified to consider only the height of each contributing member function at the mid-point of the base, whereas mean of maxima method of Defuzzification is further simplified to include only the highest membership function component in the output. Sugeno method is a weighted average of the discrete output values obtained for each rule evaluation

## 1.6.4 Fuzzy Control

The general structure of a fuzzy feedback control system is shown in Figure 1.14. The loop error  $E$  and change in error  $CE$  signals are converted to the respective per unit signals  $e$  and  $ce$  by dividing the respective scalar factors, that is,  $e = E/GE$  and  $ce = CE/GC$ . Further the output plant control signal  $U$  is derived from multiplying the per-unit output by the scale factor  $GU$  and then summed up to generate the  $U$  signal.

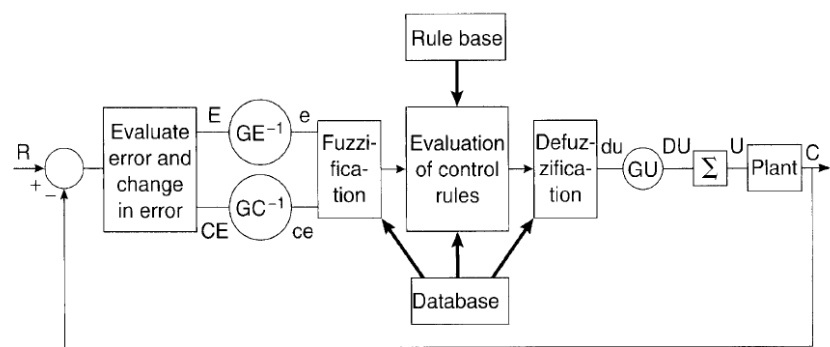


Figure 1.14: Structure of a fuzzy control in feedback system

## 1.6.6 Applications

Fuzzy logic based control has been widely applied in power electronic systems. Applications range from speed control of drives, online tuning of controllers to parameter estimation and performance optimization.

Few of the popular applications include:

1. Speed control of Induction Motor
2. Flux programming efficiency improvement for Induction Motor Drive
3. Wind generation systems
4. Slip gain tuning of Indirect Vector Control
5. Stator resistance Estimation in drives
6. Estimation of Distorted waves

## 1.8 Objective of the Thesis

Although there are numerous applications of intelligent control techniques in power electronics to attempt for a performance improvement, through this thesis we explore the possibilities in converters.

Converters is in itself a very broad topic to critically examine. Thus we reduce our area of study to inverters and inverter applications. Power electronics inverters are devices used in the conversion of direct current to alternating current. They are employed in areas such as renewable energy utilization, universal power supply and control of motor drives to name a few. Inverters have switching devices such as MOSFETs or IGBTs that turn on and off based upon the gate signals given to it by a signal generator fed by a controller. The duty of a controller is to generate signals in such a manner that output signals of an inverter looks near sinusoidal, i.e. be void of as many harmonics as possible. Here we can ponder over one of the discussed application. We examine how such a controller can be designed using neural networks to eliminate particular harmonics from the output wave forms.

Next application that is critically reviewed is the performance of such an inverter in association with an induction machine and how controllers can be used to control the speed of motor in simple terms. Here we choose a fairly performing pulse width modulating technique and concentrate upon the intelligent control techniques being used for improved performance in inverter fed induction machine. Fairly working PWM strategies include Sinusoidal PWM, Hysteresis control based PWM and Space Vector based PWM. We must note here that, the scope of this thesis has been limited to the utility and performance using sinusoidal PWM technique considering factors such as the short span of completing the dissertation, ease of implementation in hardware and other parameters.

Thus following chapters, we build a background and critically examine these 2 applications:

- Application in eliminating harmonics based on Modulation Index.
- Application as a controller for inverter fed induction machine.

## 1.9 Thesis Organization

This thesis comprises of six chapters. Each of the six chapters discusses various possibilities of utilizing Artificial Intelligence based control techniques to attempt an improved performance in power electronic converters, precisely inverters.

**Chapter 1** explains a brief literature review, the motive and force behind attempting this dissertation and further gives a brief introduction to the techniques used in following chapters.

**Chapter 2** gives an insight of how intelligent control techniques such as neural networks can be applied for varying the modulation index in working of a 3 phase inverter powered by a selective harmonic elimination based PWM scheme.

**Chapter 3** delves into finding better Pulse Width Modulation schemes such as Sine PWM, which can be made use of with the Artificial Intelligence techniques in applications involving computerized devices as control scheme blocks.

**Chapter 4** involves discussions related to a generalized application of control schemes discussed earlier on a Three phase Inverter fed Induction Machine to analyze the performance of intelligent control application.

**Chapter 5** gives exhaustive analysis and deductions of performance achieved in implementing and simulating a three phase inverter fed Induction Machine of different levels with various types of artificial intelligence controllers and with conventional controllers. Further we visualize comparisons between different techniques for the same application.

**Chapter 6** discusses about how the described application has been been developed in laboratory as a hardware prototype. It concludes with recommendations for further work in the field and conclusion.

# Chapter 2: Selective Harmonics Elimination based PWM Inverter

## 2.1 Introduction

For sinusoidal ac outputs, the magnitude, frequency and phase should be controllable. According to type of output, these are considered as Voltage Source Inverters (VSI) and Current Source Inverters (CSI). The inverter output waveform may not be sinusoidal as expected, but its fundamental component behaves as sinusoidal. This can be ensured by a modulating technique that controls the time and the sequences used to switch the power valves. This is called PWM technique. Most common used PWM techniques are Sine-PWM and Selective-Harmonic-Elimination Technique. The discrete shapes of output waveform lays restriction on the applications of inverters. The Voltage Source Inverter generates output of high  $\left(\frac{dv}{dt}\right)$ , therefore load should be inductive and similarly capacitive in case of Current Source Inverter.

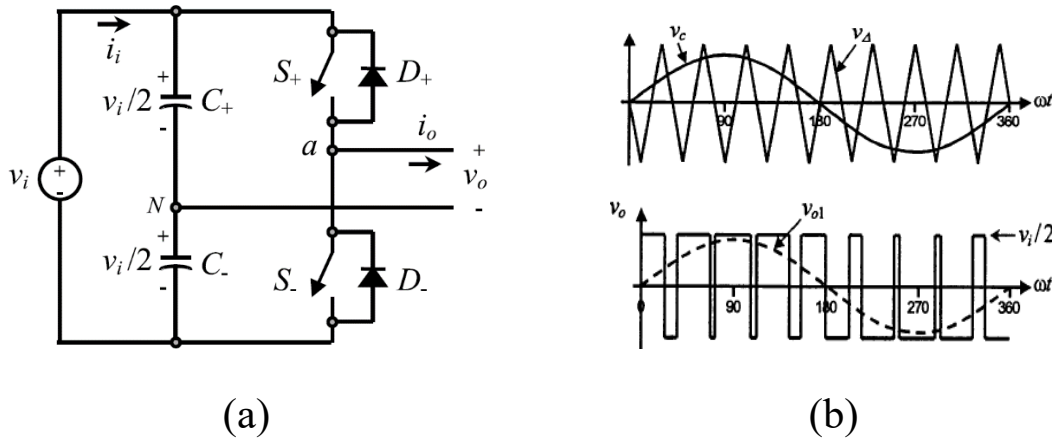


Figure 2.1: (a) General Inverter leg. (b) PWM generation using sine comparison. (Reference [4])

PWM fed to an inverter is usually generated using a carrier wave having greater frequency than the frequency of the required sinusoidal waveform. We should note that this higher frequency is the one at which each switch of the inverter operates at. It is called Switching Frequency ( $f_{sw}$ ). Selective Harmonic elimination is one such inverter PWM generation scheme that primarily focuses on removal of required harmonics in the output waveform. It is briefly discussed next.

## 2.2 Harmonics in Inverter Output

As stated before, the output voltage of an inverter is not really a sinusoidal waveform, but a series pulses which collectively represent a sine waveform as shown in Figure 2.1(b). The fundamental component of the output waveform is sinusoidal and is the component of voltage which is utilized by load. That said, the waveform still contains harmonic components of non-fundamental value which are harmful for the load, say Induction Motor. Effects include:-

1. Forced current flow to outer rims of conductor, known as skin effect. Present in rotor bars of Induction Motors and called as “deep bar effect”.
2. Reduced active surface area due to deep bar effect which results in increased resistance of rotor bar.
3. Harmonics result in electro-magnetic power and consequently mechanical torque. In motoring operation they result in breaking torques.

Given a periodic function  $f(x)$  of period  $2\pi$ , its Fourier Representation is given as :-

$$f(x) = \sum_{n=1}^{\infty} [a_n \sin(nx) + b_n \cos(nx)]$$

Where,

$$a_n = \frac{1}{\pi} \int_0^{2\pi} f(x) \sin(nx) dx, \quad b_n = \frac{1}{\pi} \int_0^{2\pi} f(x) \cos(nx) dx$$

In situations where the period is  $2\pi$ , the value of  $b_n$  shall be 0. Further in all waveforms with half wave symmetry, the even harmonics become zero, called cancellation of even harmonics. Triplen harmonics are nulled and flow through the neutral. The remaining harmonics which need to be explicitly eliminated for a good waveform are 5<sup>th</sup>, 7<sup>th</sup>, 11<sup>th</sup>, 13<sup>th</sup>, 17<sup>th</sup>, 19<sup>th</sup>, 23<sup>rd</sup>... Harmonics.  $V_n$  is the amplitude of the  $n^{th}$  harmonic component. The Total Harmonic Distortion is given by:-

$$THD = \frac{\sqrt{V_2^2 + V_3^2 + V_4^2 + \dots}}{V_1}$$



## 2.3 Switching Angles

For the sake of Selective Harmonics Elimination, we consider switching angles in a particular pattern as follows:-

- Number of switching angles in a cycle is at least 4
- Switching angles have quarter wave mirror symmetry
- Switching angles have half wave inverse symmetry
- Number of switching angles in a quarter wave are odd.

$$f_{sw} = 4 \times (\text{Number of Switching angles in quarter wave}) \times f_w$$

Thus if we desire to generate an output waveform from the inverter, whose fundamental frequency is 50Hz utilizing 5 switching angles per quarter wave, we should be generating and feeding a PWM scheme that has a switching frequency of  $4 \times 5 \times 50 = 1000\text{Hz}$

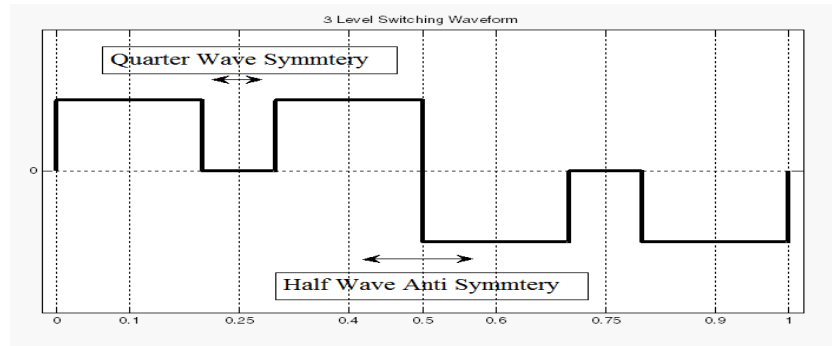


Figure 2.2: Quarter and Half wave symmetry

## 2.4 Fourier Analysis for 2 Level PWM based Inverter Scheme

Let  $f(\omega t)$  represent the output waveform. It is a two state periodic function with  $M$  chops per half cycle. 1 chop = 2 switching angles. Let  $\alpha_1, \alpha_2, \dots, \alpha_{2M}$  define the  $M$  chops, i.e. they represent each of the switching angle, then the Fourier series can be realized as follows:-

$f(\omega t) = \sum_{n=1}^{\infty} [a_n \sin(n\omega t) + b_n \cos(n\omega t)]$ . Where,

$$a_n = \frac{1}{\pi} \int_0^{2\pi} f(\omega t) \cos(n\omega t) d(\omega t)$$

$$b_n = \frac{1}{\pi} \int_0^{2\pi} f(\omega t) \cos(n\omega t) d(\omega t)$$

Because of half wave symmetry,  $b_n = 0$  and  $a_n = 0$  for all even values of  $n$ . Further substituting  $f(\omega t)$  and the value of  $a_0 = 0$  and  $a_{2M+1} = \pi$ , the relation reduces to

$$a_n = \frac{4}{n\pi} \left[ 1 + \sum_{k=1}^{2M} (-1)^k \cos(n\alpha_k) \right]$$

$$b_n = \frac{4}{n\pi} \left[ - \sum_{k=1}^{2M} (-1)^k \sin(n\alpha_k) \right]$$

Further, substituting relation  $f(\omega t) = f(\pi - \omega t)$  quarter wave symmetry  $\alpha_k = \pi - \alpha_{2M-k+1}$

$$b_n = \frac{4}{n\pi} \left[ - \sum_{k=1}^M (\sin n\alpha_k - \sin n\alpha_{2M-k+1}) \right] = 0$$

$$a_n = \frac{4}{n\pi} \left[ 1 + 2 \sum_{k=1}^M (-1)^k \cos(n\alpha_k) \right]$$

These  $M$  equations are non-linear as well as transcendental in nature. There is no general method that can be applied to solve this kind of system of equations and only Numerical Methods based solutions are feasible such as Newton-Raphson's method and better squared error optimization techniques such as Sequential Quadratic Programming (SQP optimization).

$$f_1(\alpha) = 1 + 2 \sum_{k=1}^M (-1)^k \cos n_1 \alpha_k = 0$$

$$f_2(\alpha) = 1 + 2 \sum_{k=1}^M (-1)^k \cos n_2 \alpha_k = 0$$

..

$$f_M(\alpha) = 1 + 2 \sum_{k=1}^M (-1)^k \cos n_M \alpha_k = 0$$

These are the transcendental equations required to be solved. First equation is non zero for operation.

## 2.5 Implementations from Literature

Exploring literature made in past in this field of harmonics elimination, one finds vast number of attempts to implement this scheme such as:-

1. Microprocessor based Online calculation

Robust and precise method, but is not feasible with increasing number of switching angles. Time to calculate angles for a single modulation index value using MATLAB:

No. of Switching Angles	Avg. Time
5	~ 1 second
7	~ 60 seconds
9	~ 600 – 1000 seconds
11	> 3600 seconds (verified)
13	?

Switching angles vs time of calculation at a given modulation index

2. Pre-calculated Lookup Table based implementations.

Fast for known values of modulation index. Fails for unknown values of  $m$ .

It is clear that there is a good scope for improvements in Selective Harmonics Elimination. Proposed solution should have an intelligent interpretation. At this point, we can introduce the utility of Neural Networks as an excellent trained retainer of experience as well as robust curve fitting and extrapolation provided by it together could be used to solve the problem. Literature shows good usage of ANN and Swarm Optimization algorithms to tackle this transcendental problem [7], [8], [9], [10]. [11] and [12].

## 2.6 ANN based Selective Harmonics Elimination in Inverters

Angles denoted by  $\theta_1, \theta_2, \theta_3, \theta_4, \dots, \theta_m$  none of which is zero and are numerically greater than one another.

$$\text{Required amplitude of First Harmonic} = a_1 \times E = m \times E$$

Where  $a_1$  is multiplication factor for 1st harmonic, E is DC voltage and m is modulation index.

$$\frac{4}{\pi} [1 + 2(-\cos \alpha_1 + \cos \alpha_2 - \cos \alpha_3 + \dots + \cos \alpha_8 - \cos \alpha_9)] = m$$

$$\frac{4}{\pi} [1 + 2(-\cos 3\alpha_1 + \cos 3\alpha_2 - \cos 3\alpha_3 + \dots + \cos 3\alpha_8 - \cos 3\alpha_9)] = 0$$

...

$$\frac{4}{\pi} [1 + 2(-\cos 17\alpha_1 + \cos 17\alpha_2 - \cos 17\alpha_3 + \dots + \cos 17\alpha_8 - \cos 17\alpha_9)] = 0$$

In the above set of equations, the harmonics eliminated from the output waveform are 3, 5, 7, 9, 11, 13, 15 and 17. Thus effectively in a three phase system the harmonics eliminated will be 5 and 7, 11, 13 and 17 since the triplen harmonics are automatically drained through neutral.

We calculate remaining angles in 2<sup>nd</sup>, 3<sup>rd</sup> and 4<sup>th</sup> quarter cycle using the following relations:-

$$\text{Angle in 2nd Quarter} = \pi - \text{Angle in 1st Quarter}$$

$$\text{Angle in 3rd Quarter} = \pi + \text{Angle in 1st Quarter}$$

$$\text{Angle in 4th Quarter} = 2\pi - \text{Angle in 1st Quarter}$$

## 2.7 Artificial Neural Network Block

This part of block diagram realizes a neural network with the following specification:-

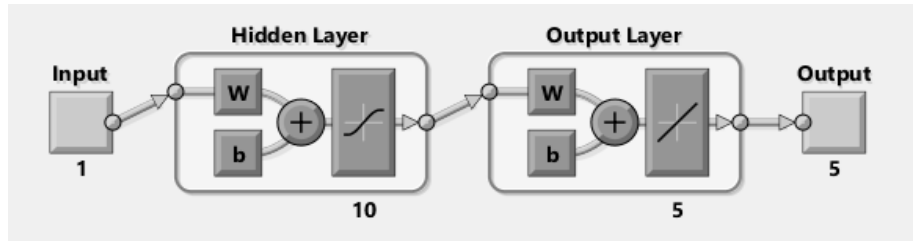


Figure 2.3: Block diagram for Neural Network used in the implementation

- **3 Layer Back propagation network** input layer receives modulation index (0 to 1) and output layer gives the required switching angles, say 5, 7 and 9.
- **Tan-Hyperbolic function** as the Activation function for the nodes in hidden layer.
- **Adaline perceptron function** for nodes in the output layer.

## 2.8 Block Diagram

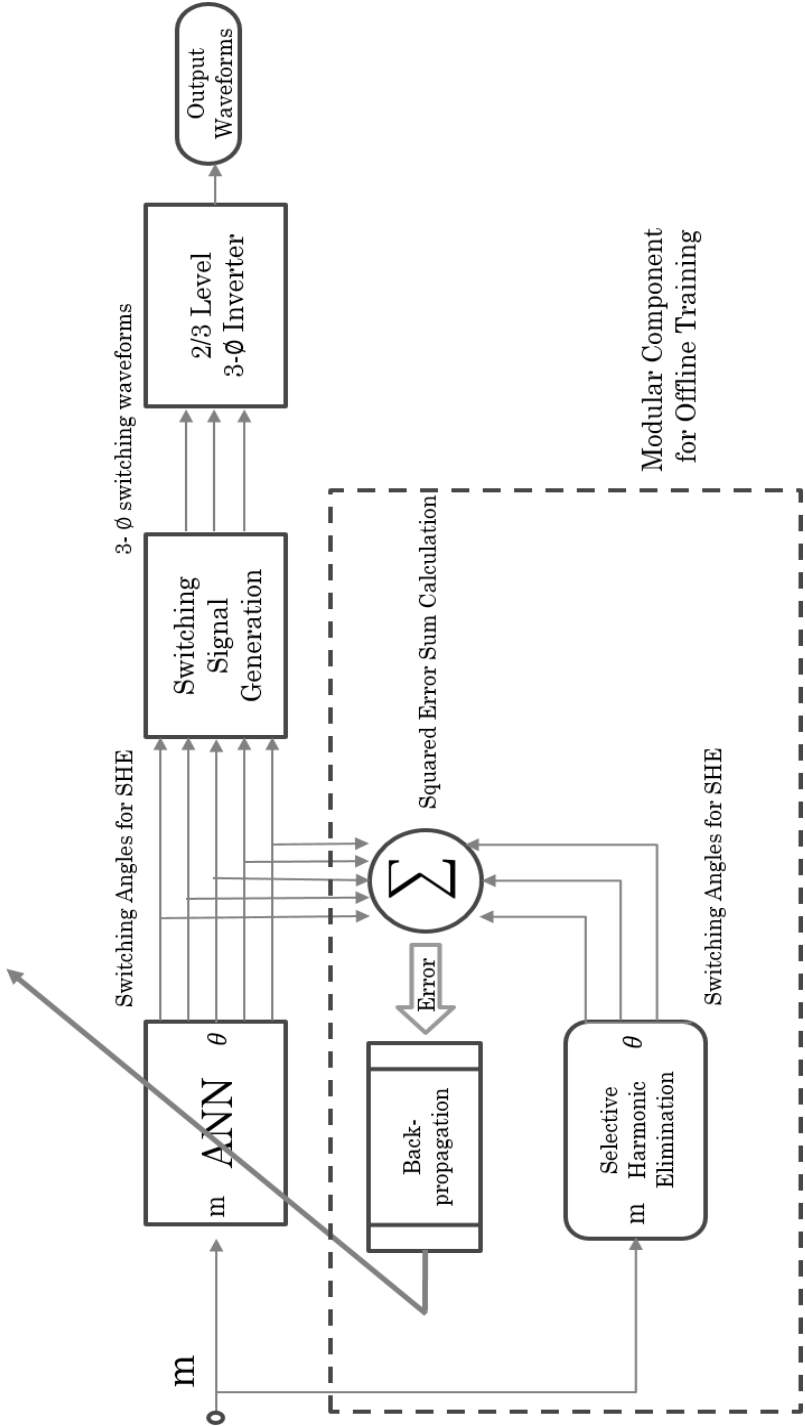


Figure 2.4: Block Diagram for Selective Harmonics Elimination using ANN

## 2.9 Selective Harmonics Block

This part of the block is essentially a microprocessor/computer based calculation of the switching angles, given modulation index as the input. This is utilized so as to generate a dataset that will be used to train Neural Network Block using Backpropagation algorithm. An implementation of dissected Newton-Raphson's method is used along with repeated optimization using random initial value is used. This ensures that the squared sum of errors is minimum. Also methods such as Genetic Algorithms and Bee Colony algorithm based optimization can be utilized to find solutions.

## 2.10 Neural Network Training (Offline)

We train the neural network using existing data obtained from the previous SHE block. This can be done in two ways, online operation for different values of modulation index or train it separately with the dataset for various values of modulation index and later replace the SHE block with the NN block called as offline method and is the preferred method

## 2.11 Switching Waveform Generation Block

This part corresponds to the process involved after receiving the output angles from the NN block. It implements multiple comparisons and products based operations over the angle signals to generate one phase PWM. Delay circuits for creating the remaining two PWM waveforms. Figure 2.5 Shows the SIMULINK realization for this scheme.

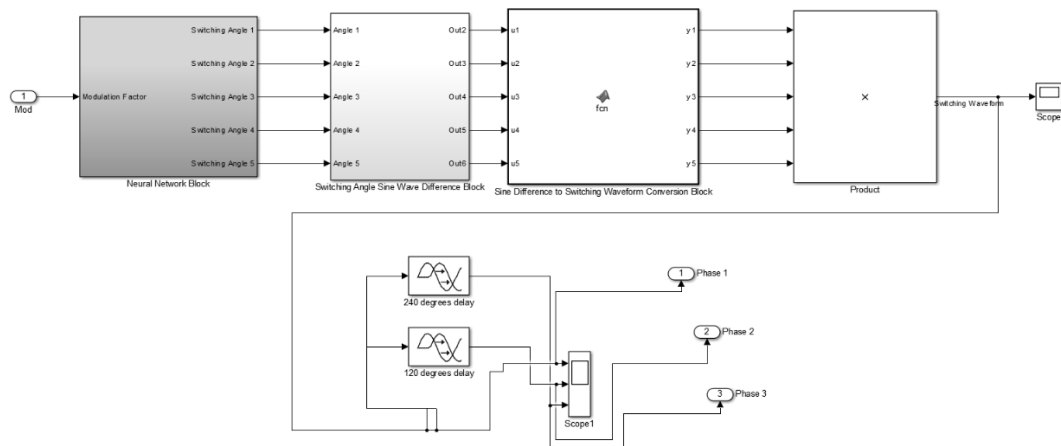


Figure 2.5: MATLAB Simulink model for generation of PWM waveform from Switching Angle values

## 2.12 Inverter Block

This is a general realization of a 3 phase inverter consisting of 3 legs with 2 switches. The inverter consists of MOSFETs/IGBTs as the switches. Constant DC source has been used for simulation.

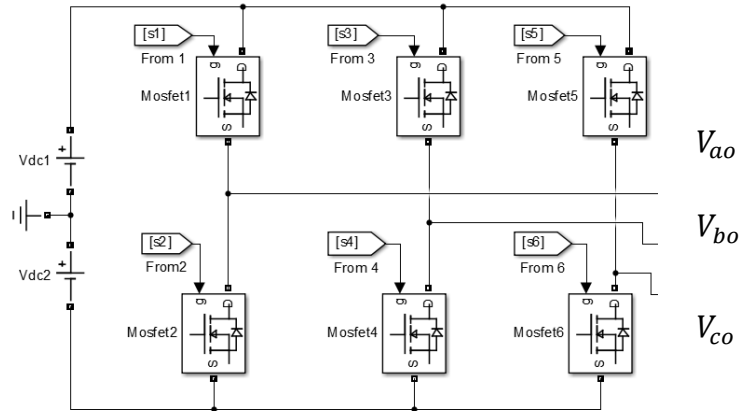


Figure 2.6: General 3 Phase Inverter Diagram in SIMULINK

Now we can measure the required voltages by trapping voltages across the terminals in load

## 2.13 Results of Simulation

### 2 Level PWM based Inverter – 9 Switching Angles ( $m = 0.9$ , $E=400$ )

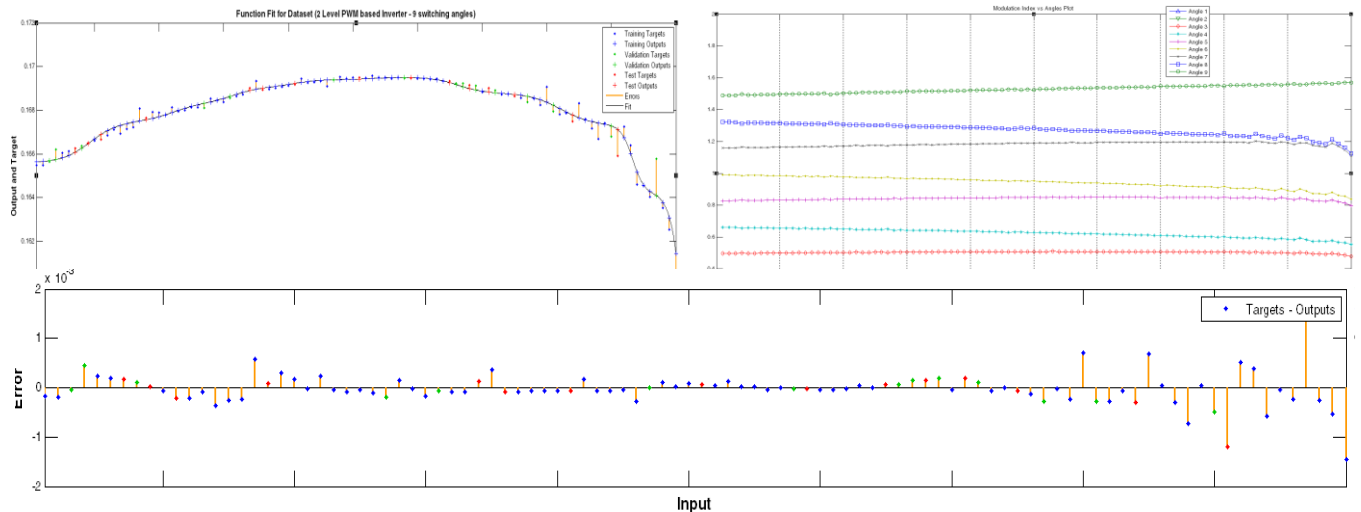
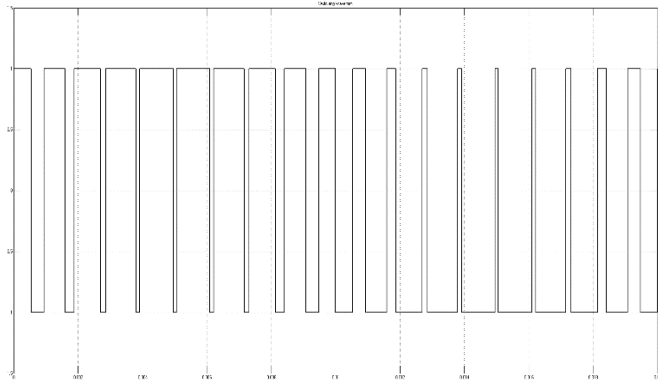
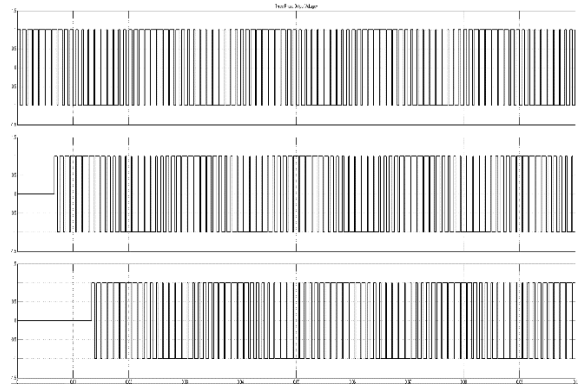


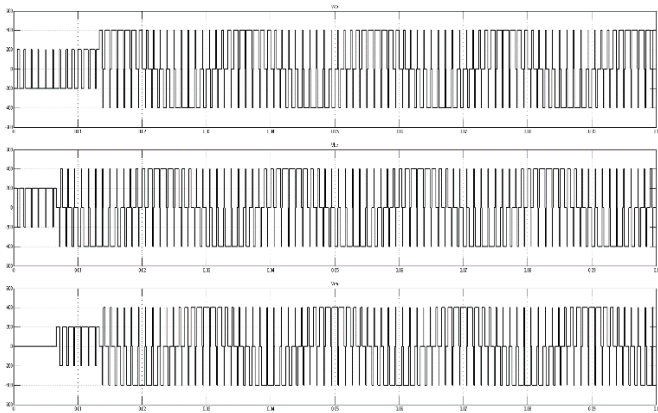
Figure 2.7: Plot fit graph, Modulation Index vs Angles graph and Training Error Plot for 2 Level PWM – 9 switching angles



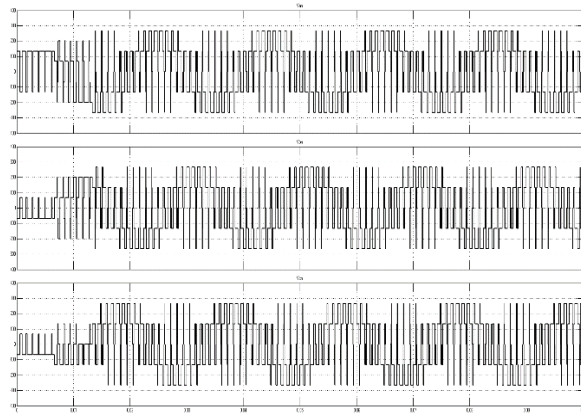
(a)



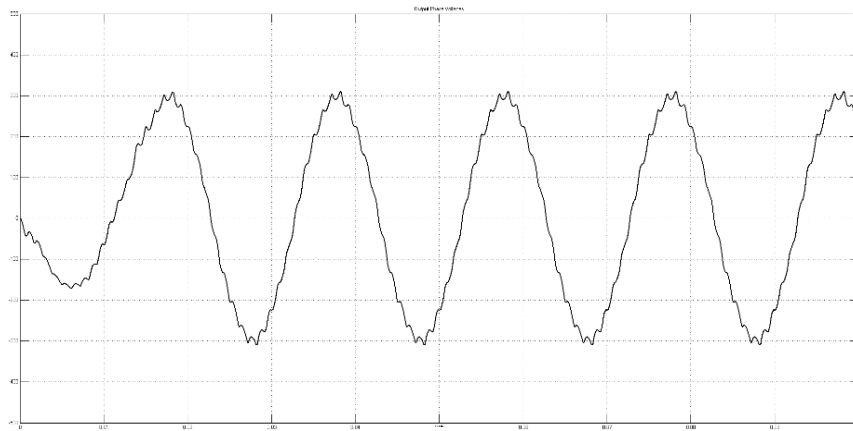
(b)



(c)



(d)



(e)

Figure 2.8: (a) PWM waveform showing switching angles in one cycle, (b) 3 Phase PWM, (c) 3 Phase Line to Neutral Voltage waveforms, (d) 3 Phase Line to Line Voltage waveforms, (e) Single phase Line Voltage waveform output passed through a Low pass filter



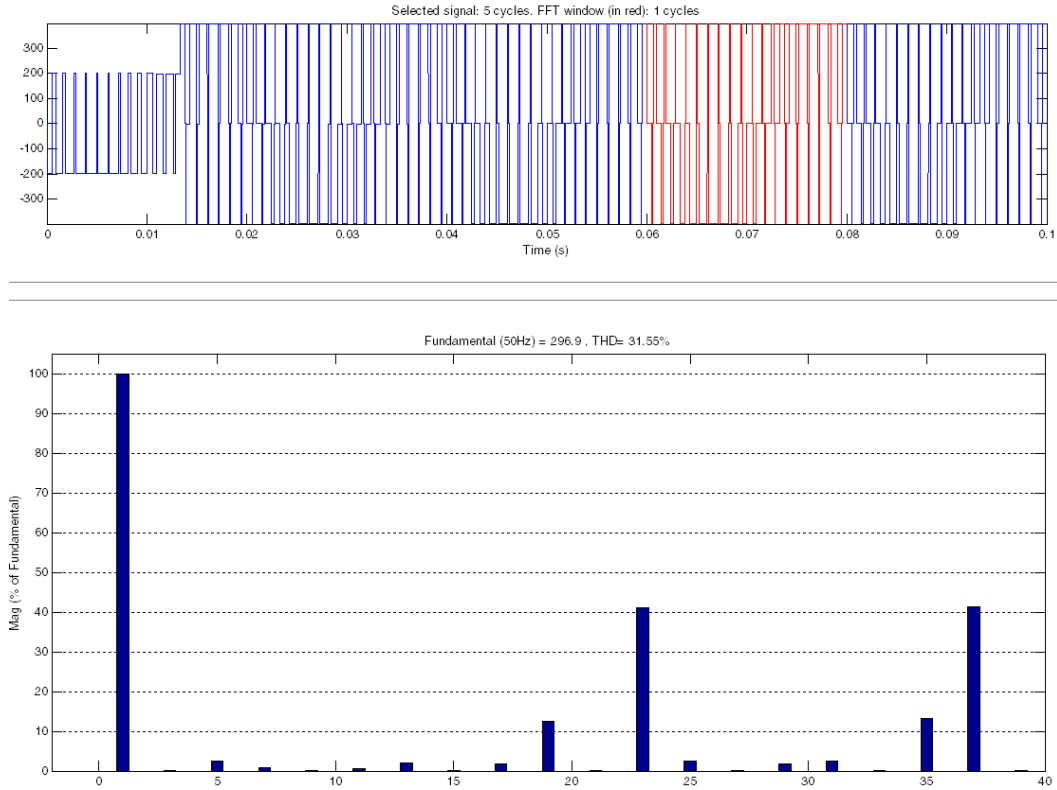


Figure 2.9: Line Voltage waveform Fourier Analysis for 2 Level PWM – 9 Angles at  $m = 0.9$

## 2.14 Observations

We can observe from the above set of results for SHE Inverter that the output waveforms are quite nearby to sine waveform. Advantages and Disadvantages in using this sort of PWM is given:

### Advantages

- Simple, robust and easy to implement.
- Can be used in low switching frequency applications

### Disadvantages

- Poor performance with respect to THD at output (31%) even after using Neural Network  
Cannot be used in high frequency applications since the degree of complexity in equations increases transcendentally. THD inversely related to operating frequency.

Thus we must examine applications of Intelligent Control Techniques in further strategies like sine based PWM and space vector based PWM that can offer utility at higher frequency ratings. Further we take one step ahead and use these PWM techniques with a load to analyze control.

# Chapter 3: Sinusoidal Pulse Width Modulation Based Inverter

## Sinusoidal Pulse Width Modulation (SPWM):

Sinusoidal pulse width modulation uses a sinusoidal signal of required frequency output and a carrier signal of high frequency (here triangular) to generate gate pulses. A comparator compares sinusoidal modulating signal and the triangular carrier signal.

The R-L load which is used in evaluating the performance of the multilevel inverters has specifications as below:

Resistance  $R = 10$  Ohms

Inductance  $L = 5$  mH to  $50$  mH and the input DC supply voltage is

$V_{dc} = 100$  Volts.

## 3.1 Two-Level Inverter

Figure 3.1 shows a model of a 2-level inverter with the three-phase R-L load built in Simulink.

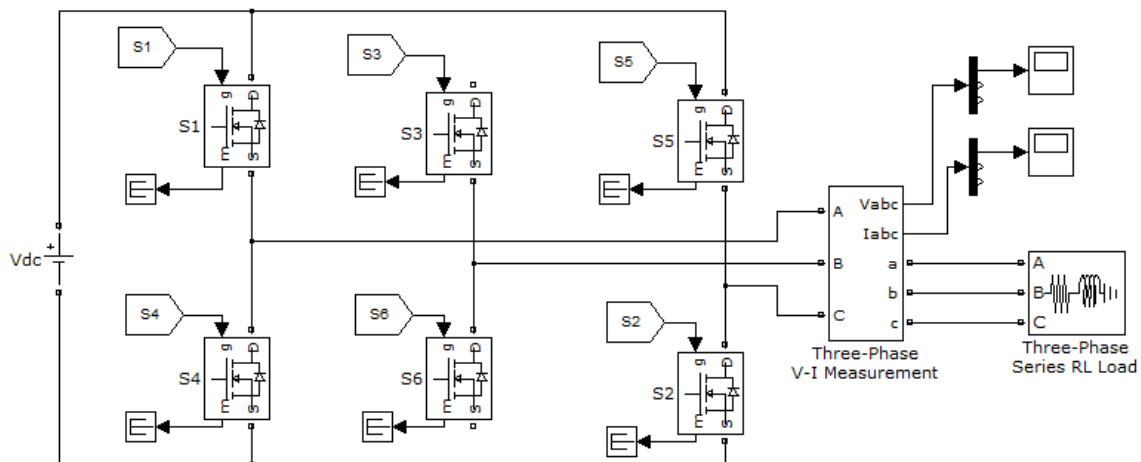


Figure 3.1: Simulink Model of 2-Level Inverter

Figure 3.2 shows the diagram to generate control signals of a 2-level inverter. One triangular carrier signal has been compared with three sinusoidal modulating signals as shown.

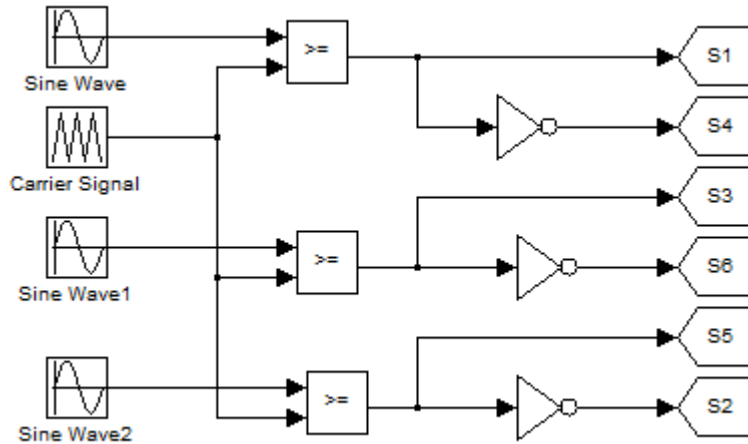


Figure 3.2: Control Signal Generation for 2-Level Inverter

The three sine waves are at a phase displacement of  $120^\circ$ . All the four signals developed are shown in Figure 3.3. Further, Figure 3.4 shows the firing pulses to the six MOSFETs of 2-level inverter.

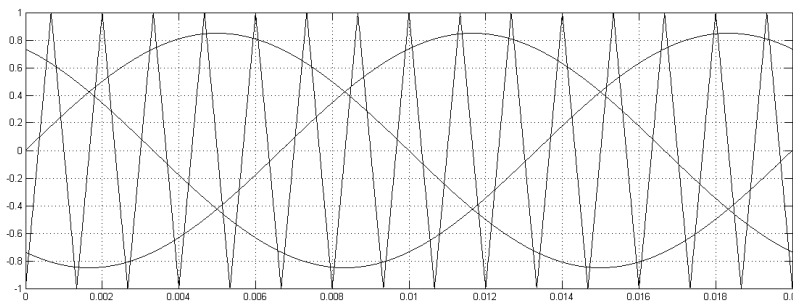


Figure 3.3: Carrier and modulating Signals for 2-Level Inverter

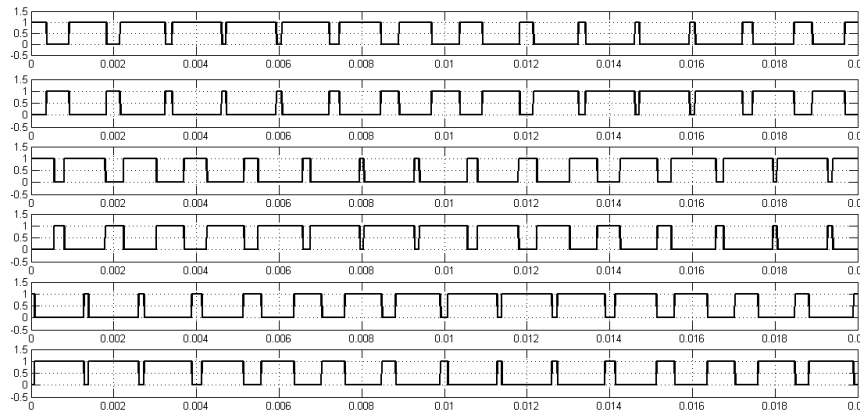


Figure 3.4: Firing Pulses to Six MOSFETS S1, S4, S3, S6, S5, S2 from Top to Bottom

Figure 3.5 to Figure 3.8 shows the phase voltage, line voltage and its harmonic spectrum, line current waveform and its harmonic spectrum for R-L load.

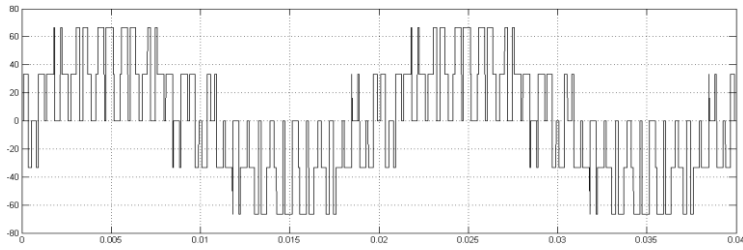


Figure 3.5: Phase Voltage at  $f = 50\text{Hz}$ ,  $MI = 0.85$ ,  $fr = 15$

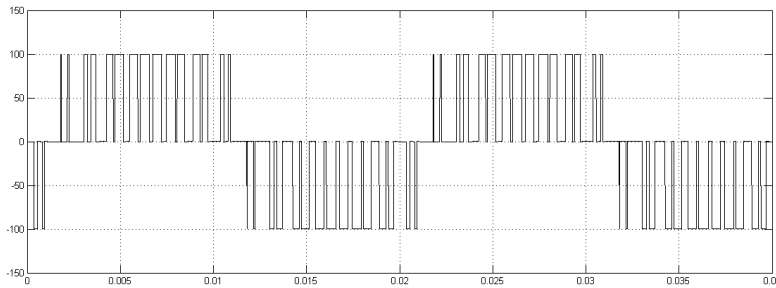


Figure 3.6: Line Voltage at  $f = 50\text{Hz}$ ,  $MI = 0.85$ ,  $fr = 15$

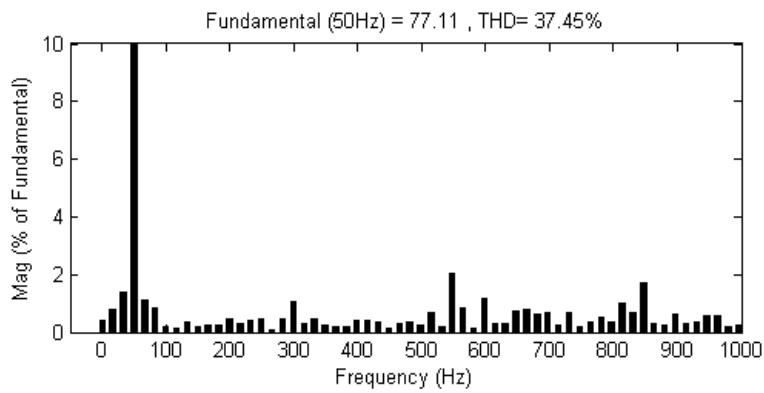


Figure 3.7: Line Voltage Harmonic Spectrum at  $f = 50\text{Hz}$

**Figure 29: (g)**

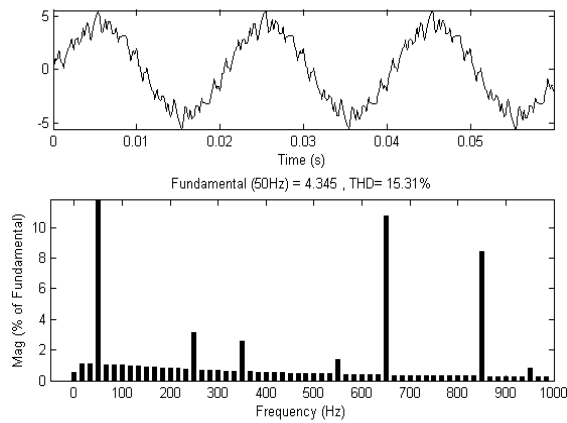


Figure 3.8: Line Current Waveform and its Harmonic Spectrum at  $f = 50\text{Hz}$  ( $P.F = 0.95$ )

### 3.1.1 THD Variation with Power Factor

Load power factor is varied while keeping frequency fixed and the effects on the harmonic spectrum and THD for the current waveform were observed. It shows for low values of inductance or power factor close to unity, steps are well defined and the THD is high. On increasing the inductance steps smoothen out, reducing the THD. This is accounted to the filtering action of the load inductance. The power factor is varied in the range of 0.537 to 1.0 and corresponding variations in THD is plotted in Figure 3.9.

### 3.1.2 THD Variation with Frequency

Load is kept constant while the frequency is varied over a range 20-90Hz. The effect on line current harmonic spectrum and on THD is seen. The variation of THD with frequency is plotted in Figure 3.9. It can be seen that there is substantial decrease in THD as frequency increases, because with increase in frequency the inductive reactance increases and provides filtering action for the current.

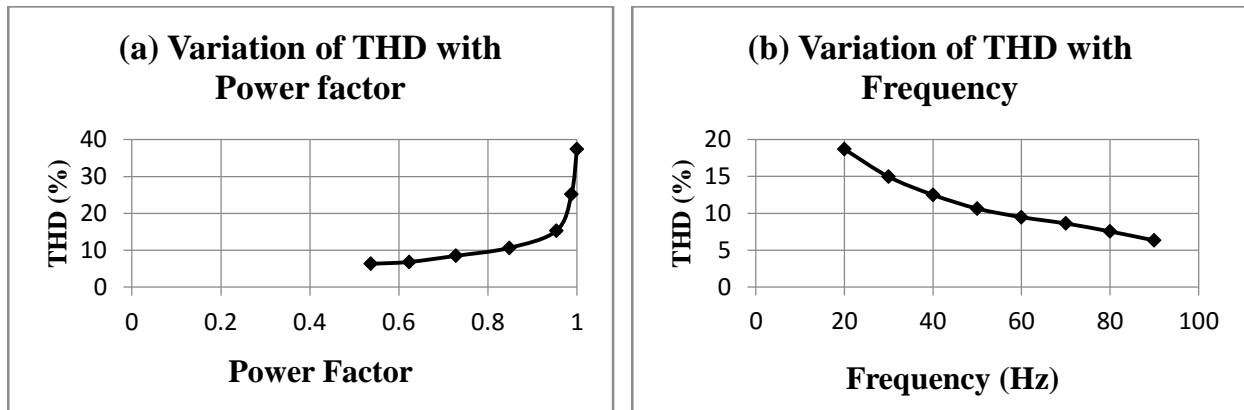


Figure 3.9: (a) Variation of THD with Power Factor and (b) Variation of THD with Frequency for Two-Level Inverter.

### 3.2 Diode-Clamped Three-Level Inverter

We evaluate the performance of a three level inverter using sinusoidal PWM scheme. Figure 3.10 shows the model of a 3-level Diode-clamped inverter along with the three-phase R-L load.

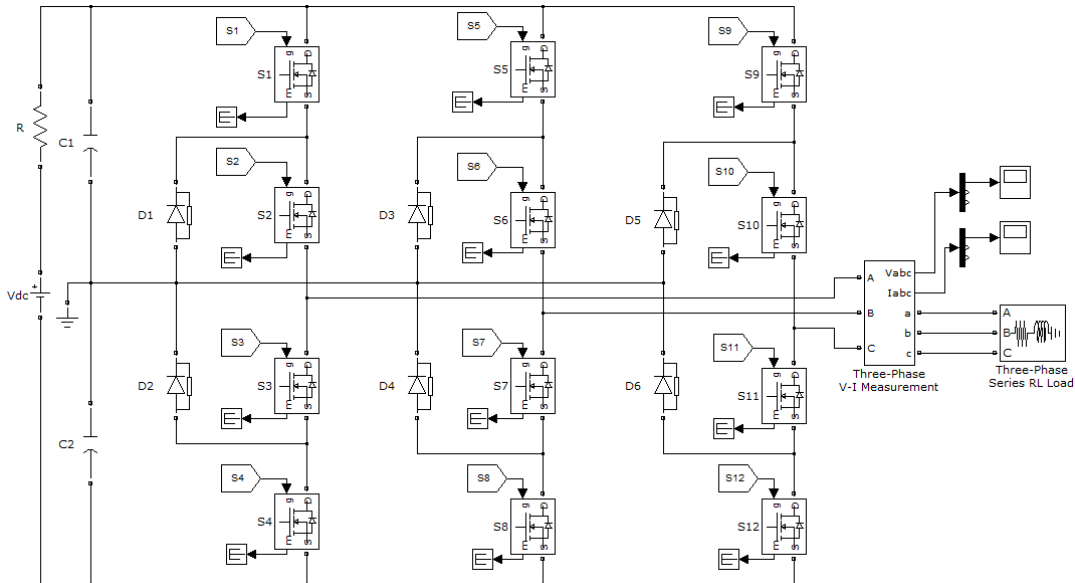


Figure 3.10: Simulink Model of 3-Level Diode-Clamped Inverter

Figure 3.11 shows diagram for control signal generation in a 3-level Diode-clamped inverter. Two triangular carrier signals are compared with three sinusoidal modulating signals as shown in Figure 3.11. The two carrier signals are shifted in their magnitude (Level-Shifted PWM). The three sinusoidal signals have a phase displacement of  $120^\circ$ .

The three signals developed in the simulation for the control signals generation of a phase are shown in Figure 3.12. Firing pulses are generated according to the logic similar to that of generation in two level inverter as described before. Firing pulses for the four MOSFETs in one phase leg of 3-level Diode-clamped inverter are shown in Figure 3.13.

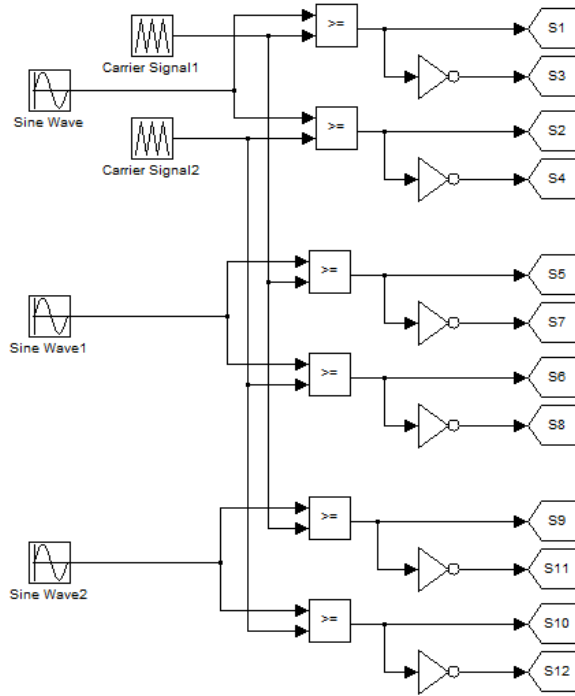


Figure 3.11: Control Signal Generation for 3-Level Diode-Clamped Inverter

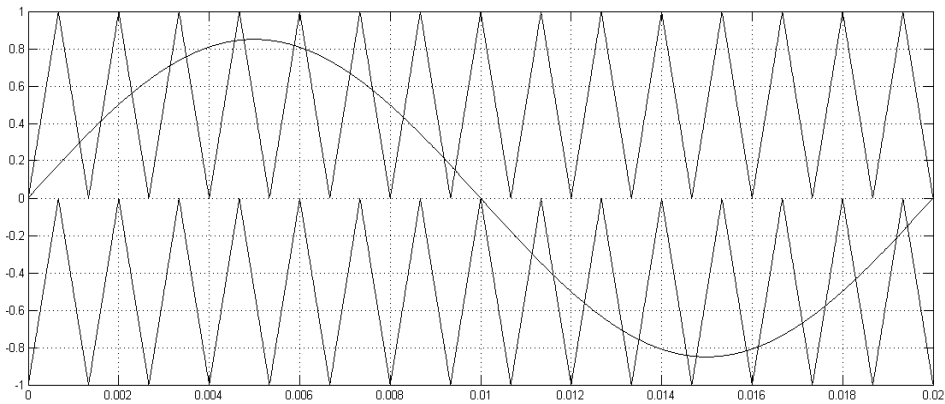


Figure 3.12: Carrier and modulating Signal for one Phase Leg of 3-Level Diode-Clamped Inverter

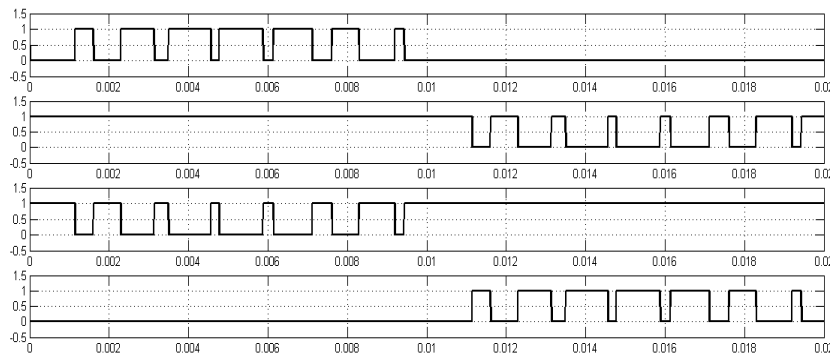


Figure 3.13: Firing Pulses to Four MOSFETS of a Phase Leg of 3-Level Diode-Clamped Inverter

The phase voltage, line voltage waveform and its harmonic spectrum, line current waveform and its harmonic spectrum respectively for R-L load are shown from Figure 3.14 to Figure 3.17.

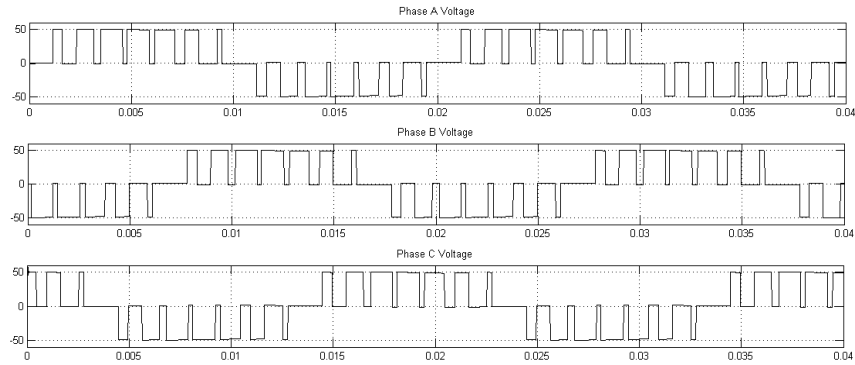


Figure 3.14: Phase Voltages at  $f = 50\text{Hz}$ ,  $MI = 0.85$ ,  $fr = 15$

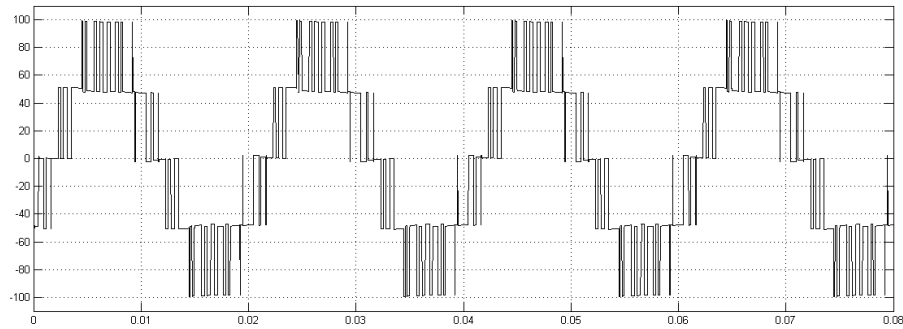


Figure 3.15: Line Voltage at  $f = 50\text{Hz}$ ,  $MI = 0.85$ ,  $fr = 15$

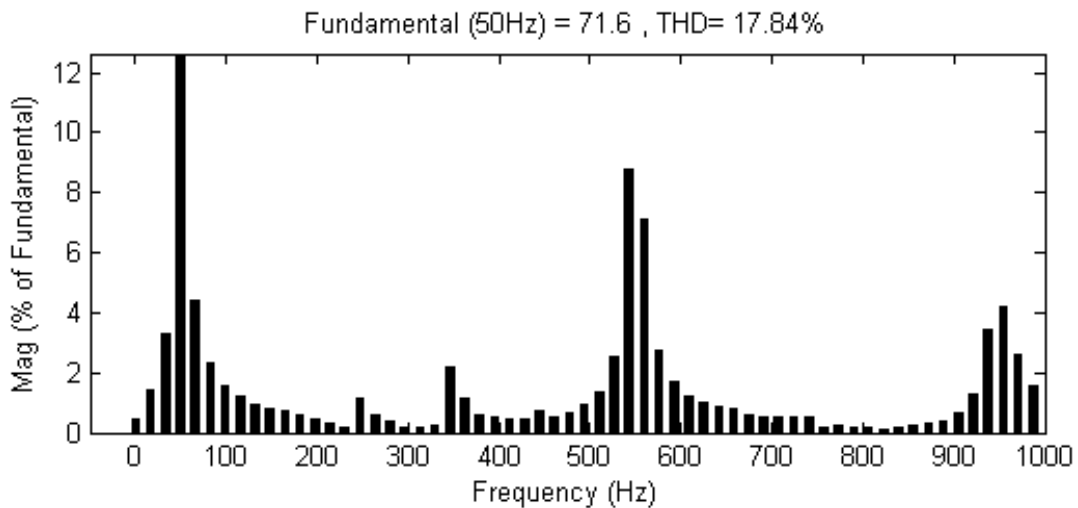


Figure 3.16: Line Voltage Harmonic Spectrum at  $f = 50\text{Hz}$



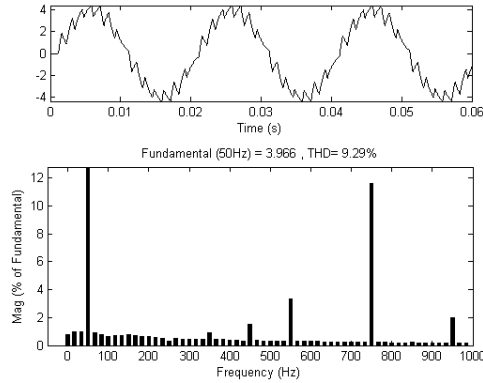


Figure 3.17: Line Current Waveform and its Harmonic Spectrum at  $f = 50\text{Hz}$  (P.F = 0.95)

### 3.2.1 THD Variation with Power Factor

The power factor is varied in the range of 0.537 to 1.0 and the corresponding variation in THD is shown graphically in Figure 3.18(a), which is given below.

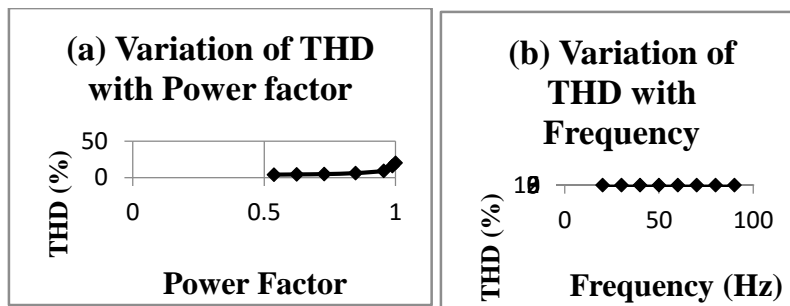


Figure 3.18: (a) Variation of THD with Power Factor and (b) Variation of THD with Frequency for a 3-Level Diode-Clamped Inverter

### 3.2.2 THD Variation with Frequency

The effect on THD and the line current harmonic spectrum have been observed. The variation of THD with frequency plotted and shown in Figure 3.18(b).

## 3.3 Conclusion

In this chapter, we implemented and analyzed Sinusoidal PWM schemes for a two level and three level inverter with R-L Load. We observed that the performance is vastly better than that of Selective Harmonic Elimination based PWM. The THD falls in the range of 4%-20% for various variations in PF and frequency. This scheme is a better scheme to use in drives and analyze the utility of Intelligent Control Techniques in these schemes.

# Chapter 4: Multi Level Inverter Based Induction Motor Drive

AC asynchronous machine is also called as induction motor and is one of the most widespread motor in use today. The prime advantage of induction motors is that it does not require electrical connections between stator and rotor parts of motor. Thus the need of a mechanical commutator or brush is eliminated and leads to less maintenance of the motor. Also these motors have low weight and inertia along with high efficiency and good overload capabilities. So these are more cheap, robust and less prone to failure at high speeds. Also this motor can work in extreme environments such as explosive locations as the motor doesn't produce sparks like commutator clad machines do.

## 4.1 Scalar Control of Multilevel Inverter fed Induction Motor Drive

Control of an induction machine's output can be done in two ways, namely scalar and vector control. Scalar control of Induction Machines is a highly useful and simple technique of speed control. Here, the V/f ratio is maintained constant in order to get constant torque over the entire operating range. The expression of torque for a three phase inverter is given as follows:

$$T_e = 3 \left( \frac{P}{2} \right) \frac{R_r}{S \omega_e} \cdot \frac{V_s^2}{\left( R_s + R_r/S \right)^2 + \omega_e^2 (L_{ls} + L_{lr})^2}$$

Where

$R_r$  is the rotor resistance

$L_{lr}$  is the rotor inductance referred to stator

$R_s$  is the stator resistance

$L_{ls}$  is the stator inductance

$S$  is the slip

$\omega_e$  is the stator frequency

$V_s$  is the stator phase voltage

$P$  is the number of poles in stator

The relation above has been deduced considering approximate equivalent per phase circuit of an induction machine referred to the stator as shown:

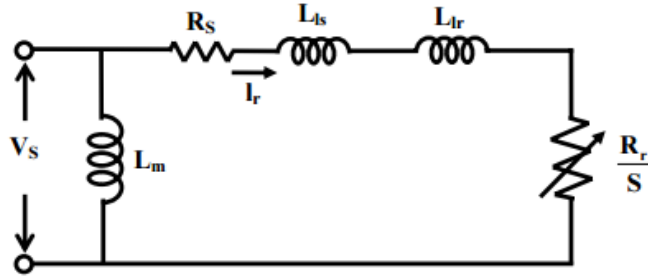


Figure 4.1: Approximate per phase equivalent circuit of an induction machine

In this chapter we analyze the schemes for multilevel inverter fed induction motor drive. Controlling techniques of such a drive are discussed. Control is usually done in two ways:

1. Open loop v/f Control
2. Closed loop v/f control

### 4.1.1 Open-Loop v/f Control

Figure 4.2 is a simple open-loop voltage/frequency control of an induction machine used commonly in the industry.

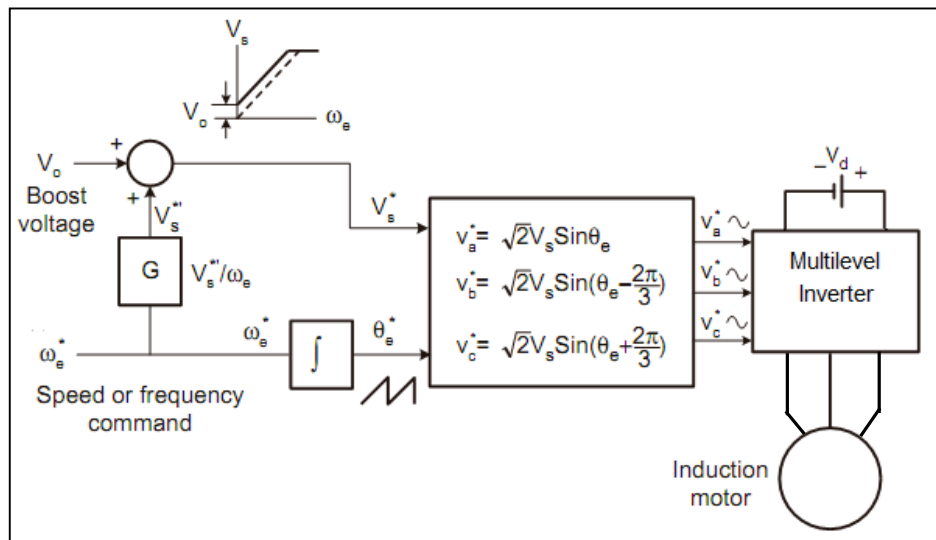


Figure 4.2: Open-Loop Speed Control of Induction Motor Using V/f principle

In the front side, the dc voltage  $V_d$  can be maintained by simple diode rectifier scheme or a battery. The speed or frequency is the command signal and the proportional voltage signal  $V_s^*$  is deduced from it so that airgap flux remains a constant. Boost voltage is added to this signal so that flux does not decrease at lower frequencies.

The command sinusoidal phase voltages are calculated using the voltage magnitude and angle command signal for the PWM based inverter, as shown in the Figure 34. The drive can be accelerated or decelerated by slowly increasing or decreasing the speed command signal. The motor speed is reversed by interchanging the phase sequence of inverter output. The advantages and disadvantages of open-loop scalar control technique for induction motor drive can be described as follows:

**Advantages:**

1. Open loop scalar voltage/frequency control is simple, inexpensive, and very extensively used in industry.
2. The complexity of processing the feedback signals is avoided.
3. Control of multiple machines operating in parallel can be easily done.

**Disadvantages:**

1. Performance of the drive is poor.
2. A reduction in the supply voltage decreases the airgap flux and reduces torque and speed. Similarly, higher load torque reduces the speed.

**4.1.2 Closed-Loop v/f Control**

Closed-loop speed control with slip regulation adds further improvement in performance for open-loop voltage/frequency control. The closed-loop scalar control is as explained below in Figure 4.3.

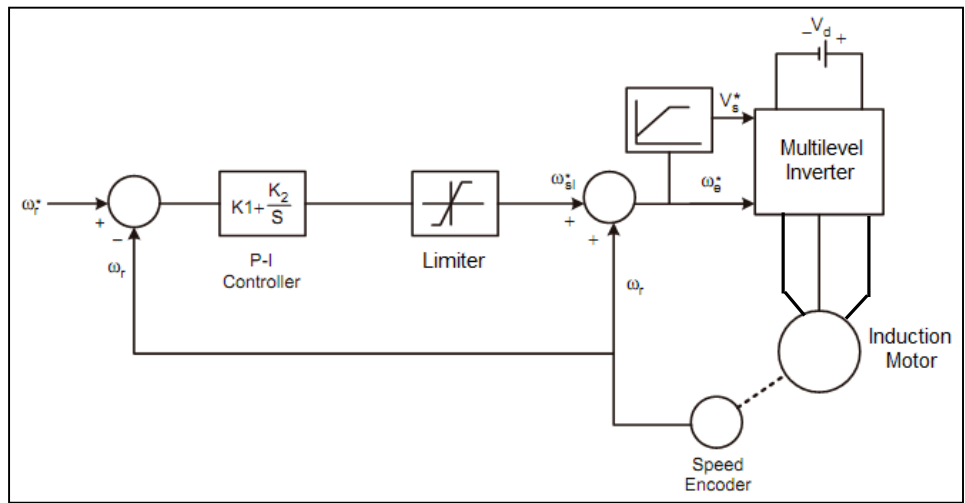


Figure 4.3: Closed-Loop Speed Control of Induction Motor Using V/f principle

In this, the speed of machine is compared with the command speed and error generates the slip frequency ( $\omega_{sl}^*$ ) command through a P-I compensator and limiter. This scheme compensates speed drift for supply voltage and load torque variation as explained in Figure 4.4(a) and Figure 4.4(b). As  $T_L$  increases from point 1 to 2 on curve a (in Figure 4.4(a)),  $\omega_r$  will tend to decrease, but it will be compensated by increasing the frequency as shown by curve b.

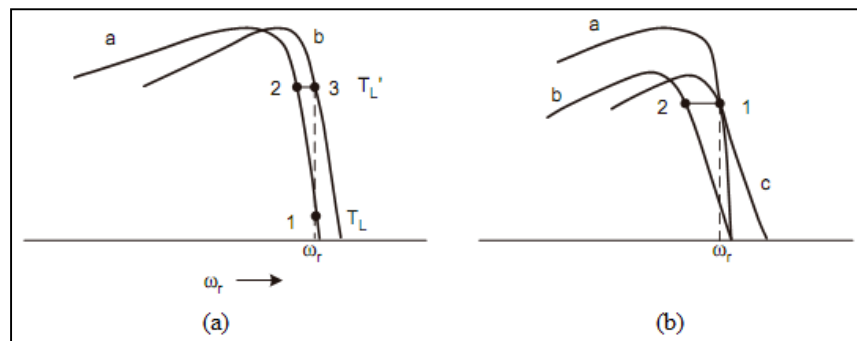


Figure 4.4: Speed Drift for (a) Supply Voltage (b) Load Torque Variation

Further, if supply voltage drops at constant torque  $T_L$  (shown in Figure 4.4(b)), the operating point 1 on curve *a* tends to drift to point 2 on curve *b*, so speed tends to decrease. Advantages and disadvantages of closed-loop scalar control technique for induction motor drive can be described as follows:

#### Advantages:

1. Improved performance of the drive.
2. Speed drift due to supply voltage and load torque variation is avoided.

#### Disadvantages:

1. Closed-loop voltage/frequency control is complex and expensive.
2. The feedback signals vary throughout a wide frequency range, and the processing of harmonics in these signals often is complex.

## 4.2 Salient Feature of Scalar Control

The salient features of Scalar control can be described as follows.

#### Advantages:

1. Simple and easy to interpret the operating principle. Inexpensive in comparison to other control techniques and easy to implement.

2. It is often possible to get reference signals from the slip in simple method. Whereas in other control techniques complex computational algorithms are required for generating the reference signal.

**Disadvantages:**

1. Due to dependence of speed upon the external load torque, it results in reduced dynamic performance. Because of this, electric motors using scalar control must be oversized so as to deliver required torque during load transients.
2. Further scalar techniques can result in an inefficient system, power factor degradation in the utility's network and noisy operation.
3. In this control approach the energy efficiency might degrade down to the 50 percent range from the theoretical maximum.

**Conclusion:**

In this chapter the scalar control techniques to control a multilevel inverter fed induction motor drive has been discussed. Open-loop and closed-loop scalar control techniques of the multilevel inverter fed induction motor drive have been analyzed along with their advantages and disadvantages.

# Chapter 5: Performance Evaluation of Inverter Fed Induction Motor Drive

In this chapter, we analyze and evaluate the performance of a 2 level PWM inverter and a 3 level Diode Clamped Inverter fed induction motor drive. Firstly, the control is accomplished utilizing conventional PI based controllers. Further, performance evaluation is done using intelligent control techniques based control schemes namely, Neural Network based control and Fuzzy Logic based control. The steady state performance and dynamic performance of the drive is discussed while varying conditions such as speed and load for voltage/frequency control in all the control schemes. Further, evaluation based on different control technique is also presented.

## 5.1 General Model using PI based controller

The basic operation of a multilevel inverter fed induction motor drive in scalar control (v/f control) has been explained previously. The induction motor drive was controlled in closed-loop manner. In this we utilize sinusoidal pulse width modulation (SPWM) for generating control signals for the inverters. Figure 5.1 shows the generalized Simulink model for all types of inverter fed induction motor drive using PI based control scheme. This model has been used to evaluate all inverters fed induction motor drive with corresponding changes in the inverter subsystem block and in the switching control block for PI

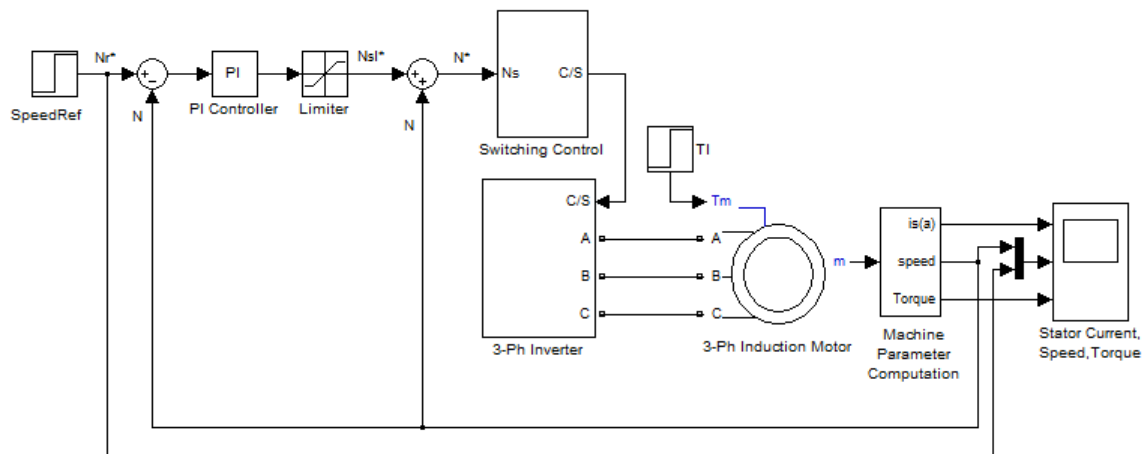


Figure 5.1: Generalized Simulink Model for Inverter fed Induction Motor Drive using PI based controller.

The Simulink model of types of inverters has been discussed previously. Here only the switching control block is discussed.

The 3-Phase Induction motor used in performance evaluation has the following rating:

Power	:	20 HP (15KW)
Voltage	:	400 Volts
Frequency	:	50 Hz
Speed	:	1460 RPM
Poles	:	4

## 5.2 Steady State Performance Using PI based controller

The steady-state performance of 2-level and 3-level Diode-clamped inverter fed induction motor drive across varying conditions such as load and speed are discussed here.

### 5.2.1 Two Level Inverter fed Induction Motor Drive using PI based controller

The inverter block for generalized Simulink model shown in Figure 5.1 is replaced with the 2 level inverter Simulink model that had been discussed in previous chapters. Figure 5.2 depicts the switching control block for 2-level inverter fed induction motor drive.

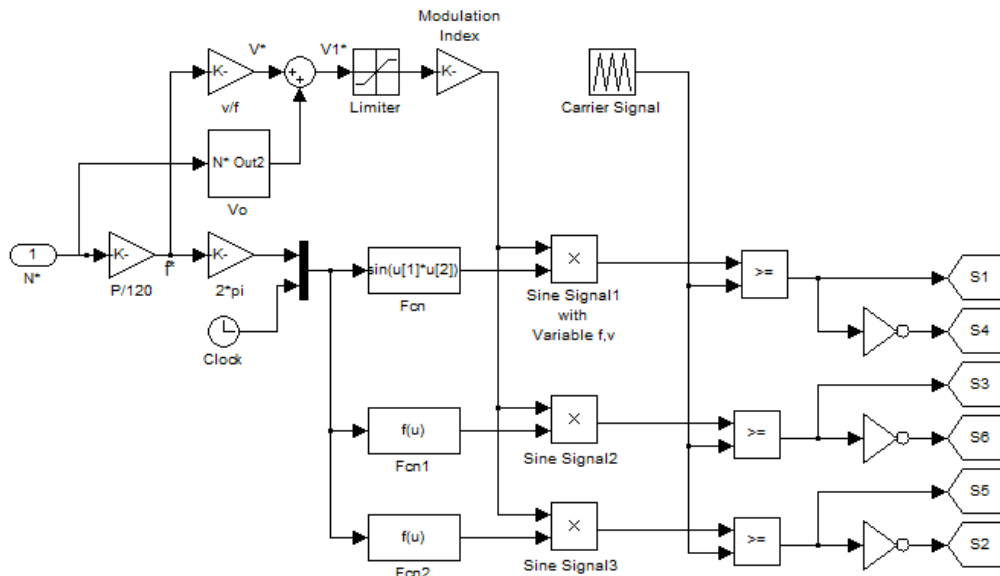


Figure 5.2: Switching Control Block for the 2-Level Inverter fed Induction Motor Drive



In the switching control block, the reference speed is obtained by processing the speed error through a PI-controller and limiter. It is then added to the measured speed, the frequency is calculated and converted to radians ( $\omega$ ). Using this, all the three sinusoidal modulating signals for Sine PWM are obtained by multiplying ' $\omega$ ' with time ' $t$ ' as follows.

$$\begin{aligned} & \text{Sin}(\omega * t) \\ & \text{Sin}(\omega * t - \frac{2 * \pi i}{3}) \\ & \text{Sin}(\omega * t + \frac{2 * \pi i}{3}) \end{aligned}$$

By multiplying the frequency obtained with a constant voltage/frequency ratio, adding boost voltage to it we get the required voltage. On dividing it with rated voltage, modulating index is obtained. These three sinusoidal modulating signals with variable frequency and voltage are ready for the Sine PWM. Rest part of generating control signals for the switches in inverter has been explained earlier.

The steady-state performance of the 2 level inverter fed induction motor drive for various speed and load conditions is shown in Figure 5.3 to Figure 5.7.

**Response for Starting with No Load:**

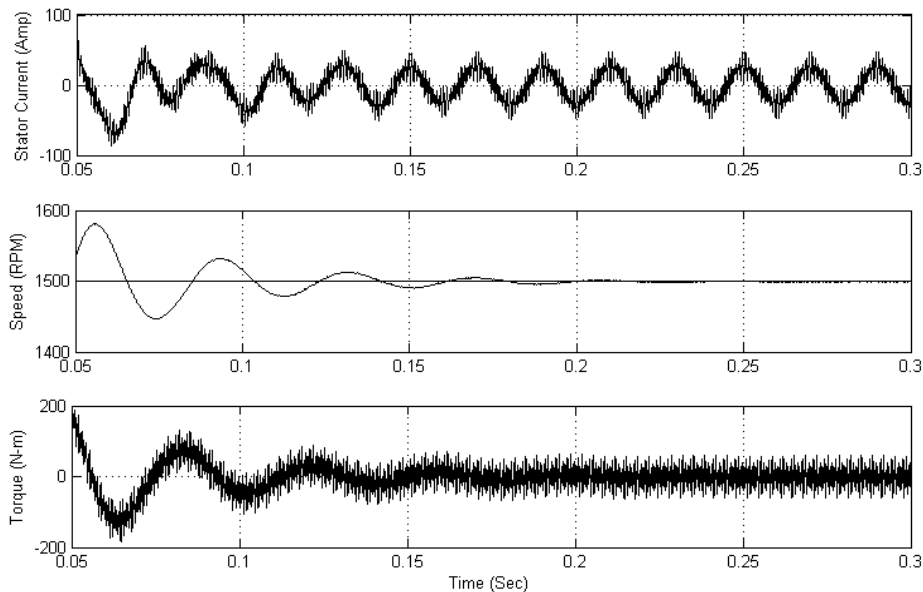


Figure 5.3: Steady-State Performance using PI when the Motor started with no load

In Figure 5.3, the motor started without any load and the reference speed has been set to 1460 RPM. As the speed error reaches nearly zero rpm, the winding current also reduces to no load value and the developed torque now become equals to zero.

**Response for Starting with Load:**

In this analysis, motor was started with a load ( $T_1 = 90\text{N-m}$ ) and reference speed was set to 1460 RPM. As the speed reaches steady state value, the winding current and developed torque becomes equal to the set value of load. The motor steady state response is shown in Figure 5.4

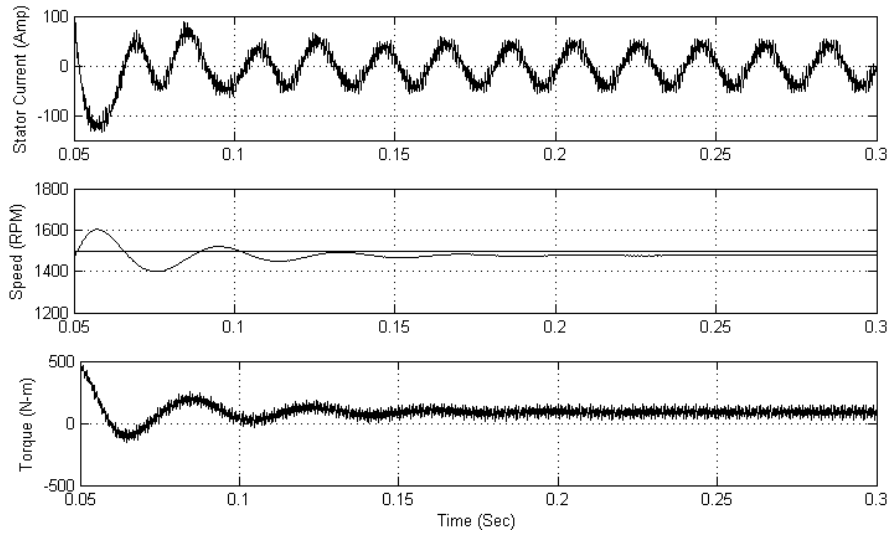


Figure 5.4: Steady-State Performance using PI when the Motor started with Load ( $T_l = 90\text{N-m}$ )

**Response for Step Change in Load:**

In this, the motor is started first on no load with reference speed of 1460 rpm. Starting torque is developed to accelerate the machine. As the speed reaches to reference speed torque developed is also set to zero, at 0.5sec a load torque of 90N-m is applied. Such a sudden application of load on rotor causes an instantaneous decline in speed of the motor. In reaction to this drop in speed, the output of controller responds by increasing the reference speed value. So the developed torque increases and motor speed settles at a steady value again, and winding currents will increase. The steady state response is shown in Figure 5.5(c).

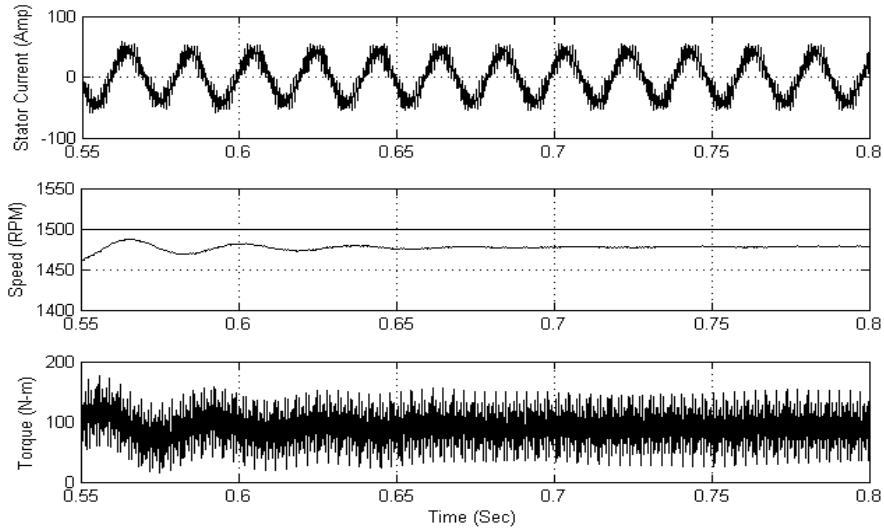


Figure 5.5: Steady-State Performance using PI for Step change in Load ( $T_l = 90\text{N-m}$ )

### Response for Step Change in Speed:

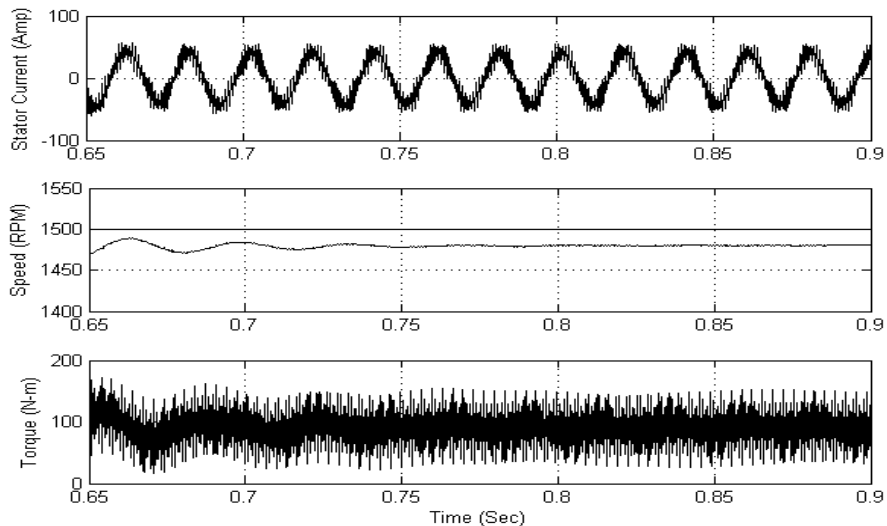


Figure 5.6: Steady-State Performance using PI for Step change in Speed ( $N = 1200$  to  $1460$  rpm)

Initially, the motor is started with a reference speed of  $1200$  RPM and the motor reaches its steady state speed and settles. At  $0.5$  seconds time, motor reference speed is increased to  $1460$  RPM. Due to controller action, the motor generates torque to reach its reference value. The response is depicted in Figure 5.5.

### Response for Speed Reversal:

If the reference speed is altered from  $1460$  RPM to  $-1460$  RPM, motor tends to rotate in the reverse direction. When the controller observes this change, it initially reduces the frequency of stator currents followed by phase reversal to start the motor in reverse direction. Since the drive is in same

dynamic state (on load) just before and just after the reversal of this phenomenon, the steady state values of inverter currents are observed to be same in either directions of the rotation for the motor. But the phase sequence of these currents in both directions will be different. This response is shown in Figure 5.6 shown below.

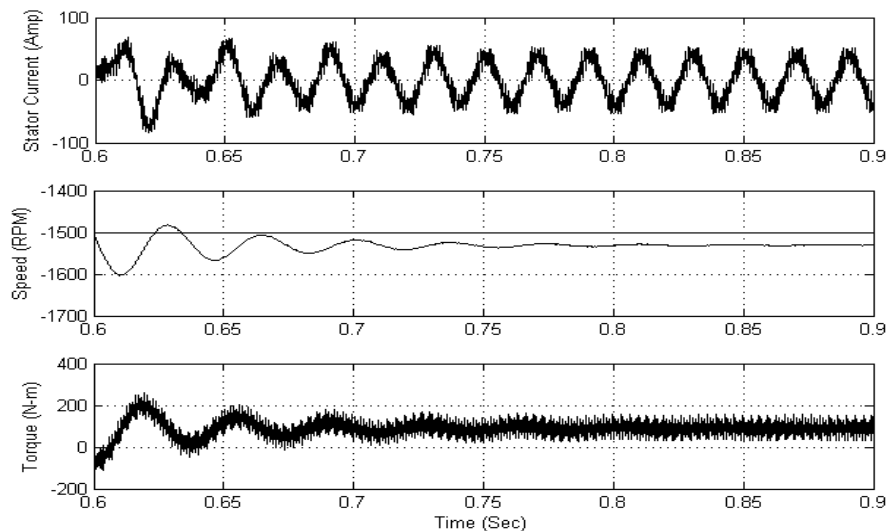


Figure 5.7: Steady-State Performance using PI for Speed Reversal (N = 1460 to -1460 rpm)

## 5.2.2 Three-Level Diode-clamped Inverter fed Induction Motor Drive using PI based controller

The model of a 3 level Diode clamped inverter fed induction motor drive has been simulated to evaluate the performance of drive. The steady state performance of the inverter fed drive under varying conditions such as load and speed are analyzed.

The inverter block from the generalized Simulink model discussed previously has been replaced with a 3 level Diode clamped inverter model which was discussed previously. Figure 5.8 depicts the switching control blocks for 3 level Diode clamped inverter fed induction motor drive.

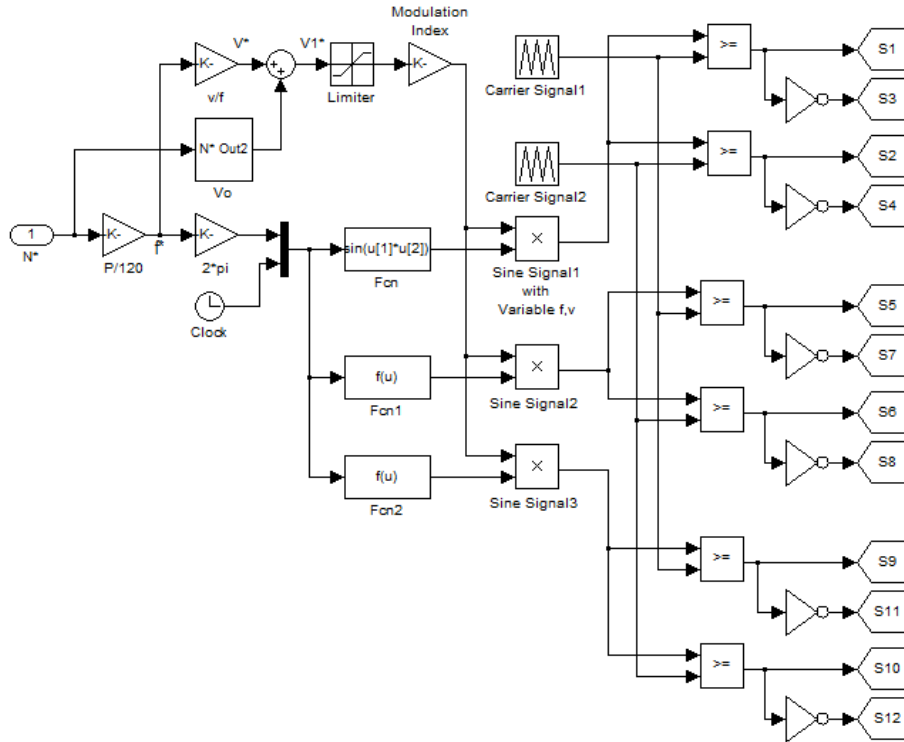


Figure 5.8: Switching Control Block for the 3 Level Diode Clamped Inverter fed Induction Motor Drive

In the above switching control block the process of procuring three sinusoidal modulating signals for Sine PWM scheme is same as described for 2 level inverter. The number of carrier signals used in this method is two and the process of generating control signals for the switches in the inverter has been discussed previously.

Steady state performance of the 3 level Diode clamped inverter fed induction motor drive for various speed and load conditions is depicted in Figures 5.9 to Figure 5.13.

**Response for Starting with No Load:**

In this, the motor is started without any load and the reference speed is set to 1460 RPM. When the speed error reaches nearly zero RPM, the winding current also reduces to no load value and the developed torque equals zero. The response is shown in Figure 5.9.

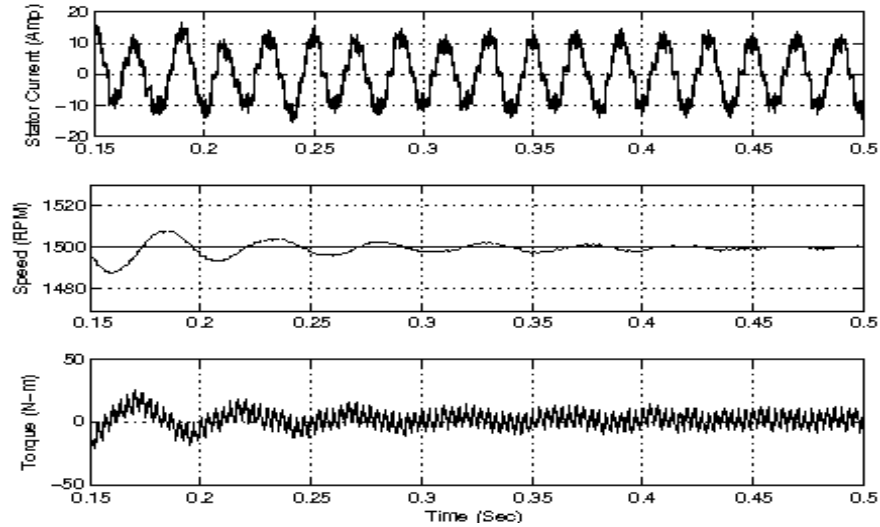


Figure 5.9: Steady-State Performance using PI when the Motor started with-out Load

**Response for Starting with Load:**

In this case, motor is started with load ( $T_l = 90\text{N-m}$ ) and the reference speed set to 1460 RPM. When the speed reaches steady state value, the winding current and the developed torque equals to the set value of load. The motor steady state response is shown in Figure 5.10.

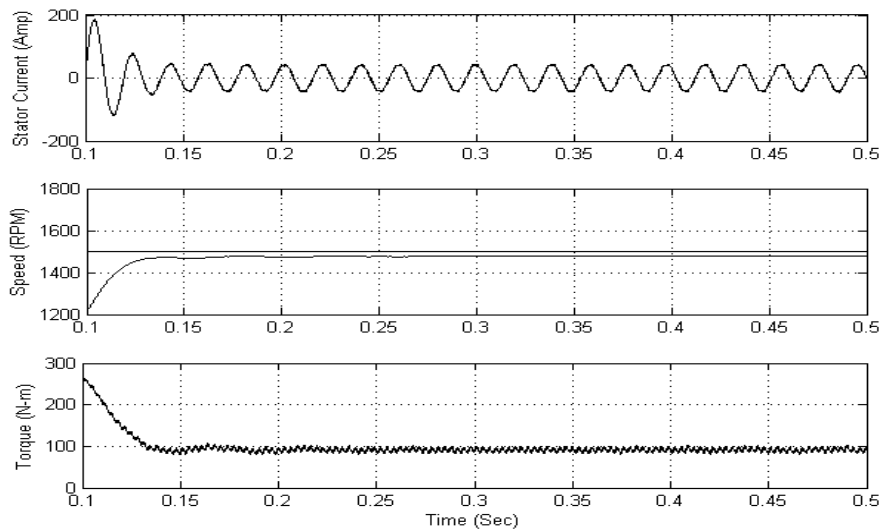


Figure 5.10: Steady-State Performance using PI when the Motor started with Load ( $T_l = 90\text{N-m}$ )

**Response for Step Change in Load:**

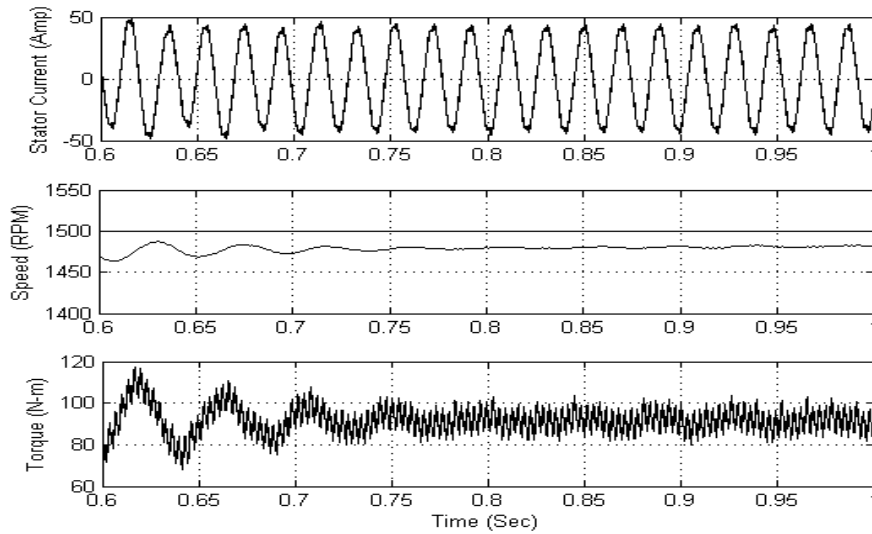


Figure 5.11: Steady-State Performance using PI for Step change in Load ( $T_l = 90\text{N-m}$ )

Motor is initially started with no load with a reference speed of 1460 RPM. Starting torque will be developed so as to accelerate the machine. As the speed reaches reference speed, torque developed is set to zero, at 0.5 seconds, a load torque of 90 N-m is applied. Due to controller action, the developed torque increases and the motor speed settles at steady state value again and winding currents increase. The steady state response is shown in Figure 5.11.

### Response for Step Change in Speed:

Initially motor is started with a reference speed of 1200 RPM. The motor reaches its steady state speed and settles there. At 0.5 seconds, the motor reference speed is increased to 1460 RPM. Due to the controller action, the motor develops torque to reach its reference value. The response is depicted in Figure 5.12

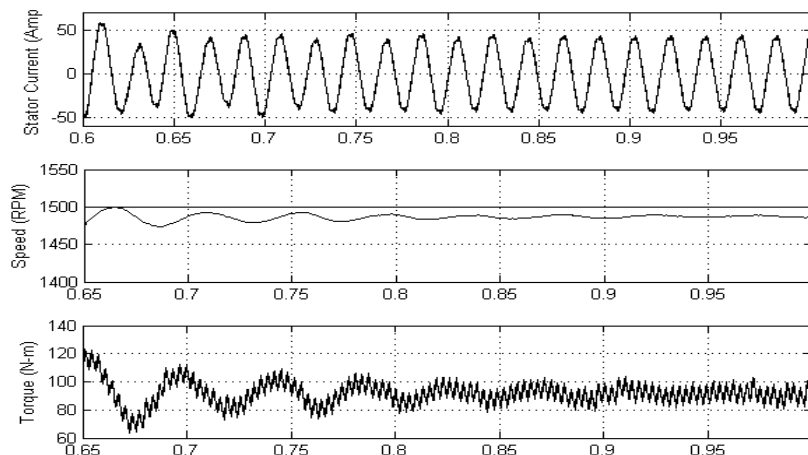


Figure 5.12: Steady-State Performance using PI for Step change in Speed ( $N = 1200$  to  $1460\text{rpm}$ )

### Response for Speed Reversal:

When the reference speed is altered from 1460 RPM to -1460 RPM, the controller observes this change and initially reduces the frequency of stator currents followed by phase reversal to star the motor in reverse direction. This response is shown in Figure 5.13 below.

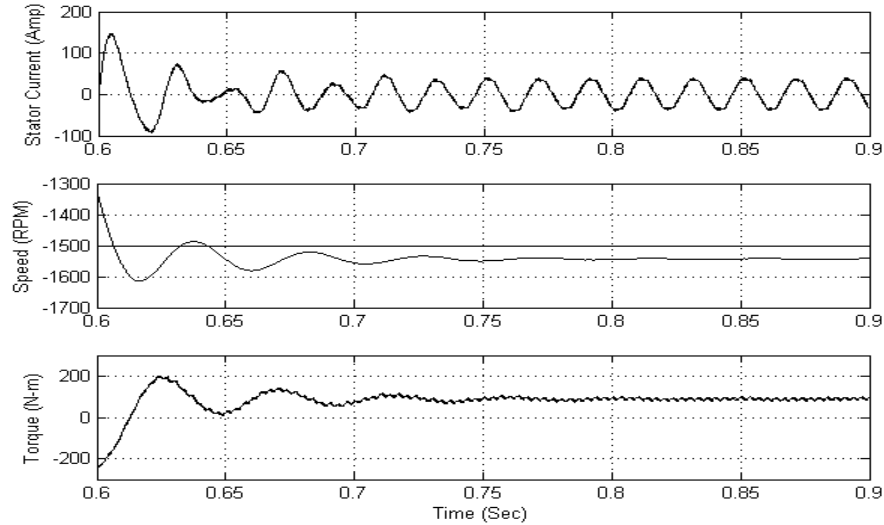


Figure 5.13: Steady-State Performance using PI for Speed Reversal (N = 1460 to -1460 rpm)

From the steady-state response characteristics of 3-level Diode-clamped inverter, it can be observed that the number of ripples and the magnitude of ripples in stator current, speed and torque are less compared to that of 2-level inverter. The performance of the drive has improved with 3-level Diode-clamped inverter compared to 2-level inverter while using PI based controller itself.

## 5.3 General Model using Neural Network based controller

The basic operation of a multilevel inverter fed induction motor drive in scalar control (v/f control) has been explained previously. The induction motor drive was controlled in closed-loop manner. In this we utilize sinusoidal pulse width modulation (SPWM) for generating control signals for the inverters. Figure 5.14 shows the generalized Simulink model for all types of inverter fed induction motor drive using Neural Network based control scheme. This model has been used to evaluate all inverters fed induction motor drive with corresponding changes in the inverter subsystem block and in the switching control block for Neural Network



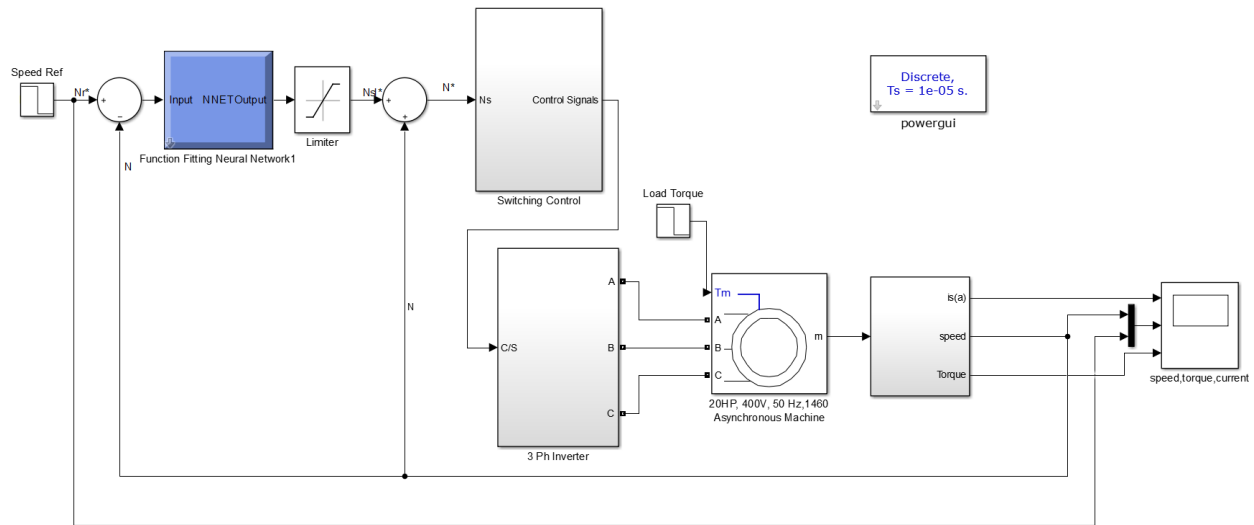


Figure 5.14: Generalized Simulink Model for Inverter fed Induction Motor Drive using Neural Network Based controller

The Simulink model of types of inverters has been discussed previously. Here only the switching control block is discussed.

## 5.4 Steady State Performance Using Neural Network based controller

The steady-state performance of 2-level and 3-level Diode-clamped inverter fed induction motor drive across varying conditions such as load and speed are discussed here.

### 5.4.1 Two Level Inverter fed Induction Motor Drive using Neural Network based controller

The steady-state performance of the 2 level inverter fed induction motor drive for various speed and load conditions is shown in Figure 5.15 to Figure 5.19.

#### Response for Starting with No Load:

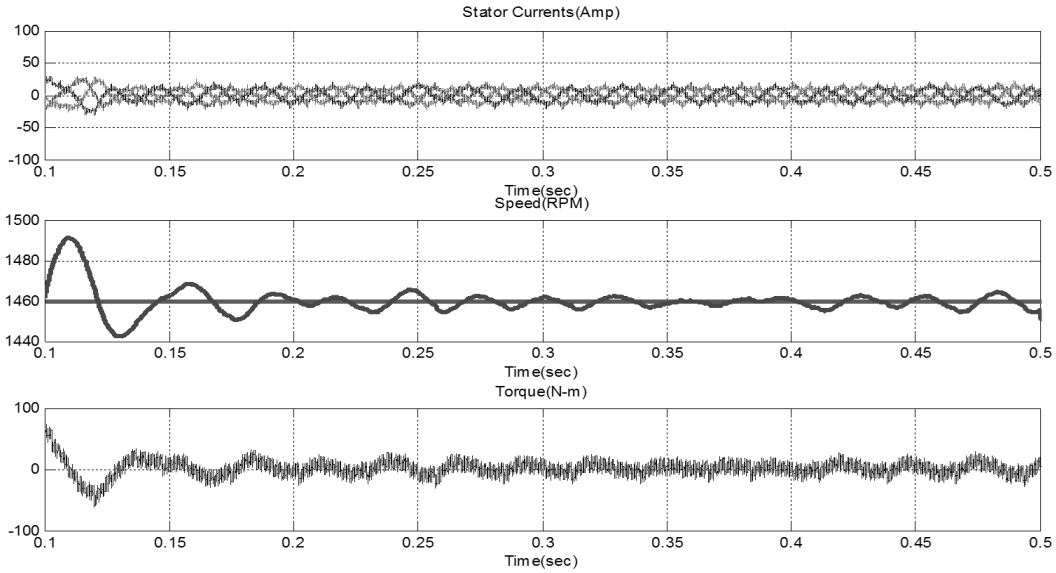


Figure 5.15: Steady-State Performance using NN when the Motor started with no load

In Figure 5.15, the motor started without any load and the reference speed has been set to 1460 RPM. As the speed error reaches nearly zero rpm, the winding current also reduces to no load value and the developed torque now become equals to zero.

**Response for Starting with Load:**

In this analysis, motor was started with a load ( $T_1 = 90\text{N-m}$ ) and reference speed was set to 1460 RPM. As the speed reaches steady state value, the winding current and developed torque becomes equal to the set value of load. The motor steady state response is shown in Figure 5.16

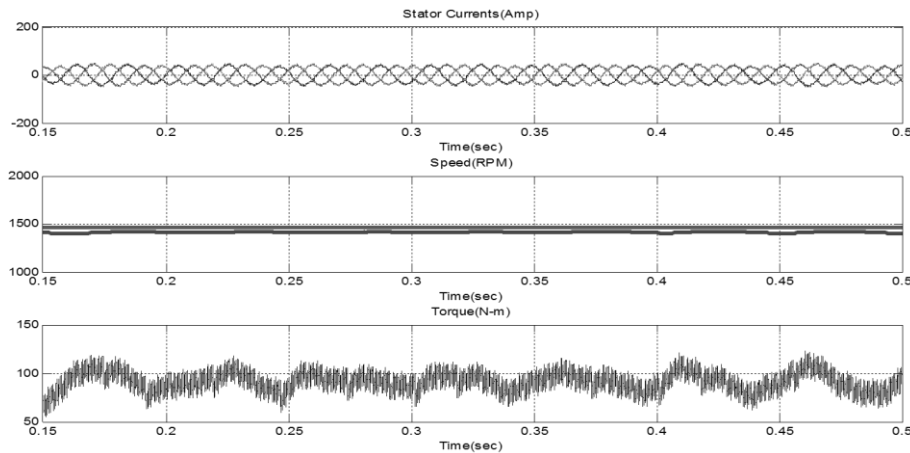


Figure 5.16: Steady-State Performance using NN when the Motor started with Load ( $T_l = 90\text{N-m}$ )

### Response for Step Change in Load:

In this, the motor is started first on no load with reference speed of 1460 rpm. Starting torque is developed to accelerate the machine. As the speed reaches to reference speed torque developed is also set to zero, at 0.5sec a load torque of 90N-m is applied. Such a sudden application of load on rotor causes an instantaneous decline in speed of the motor. In reaction to this drop in speed, the output of controller responds by increasing the reference speed value. So the developed torque increases and motor speed settles at a steady value again, and winding currents will increase. The steady state response is shown in Figure 5.17.

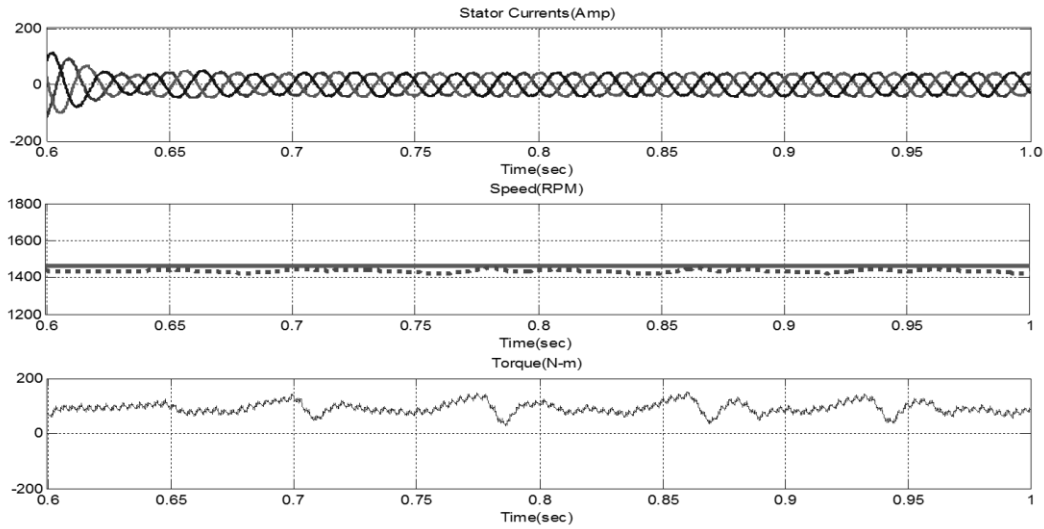


Figure 5.17: Steady-State Performance using NN for Step change in Load ( $T_l = 90\text{N-m}$ )

### Response for Step Change in Speed:

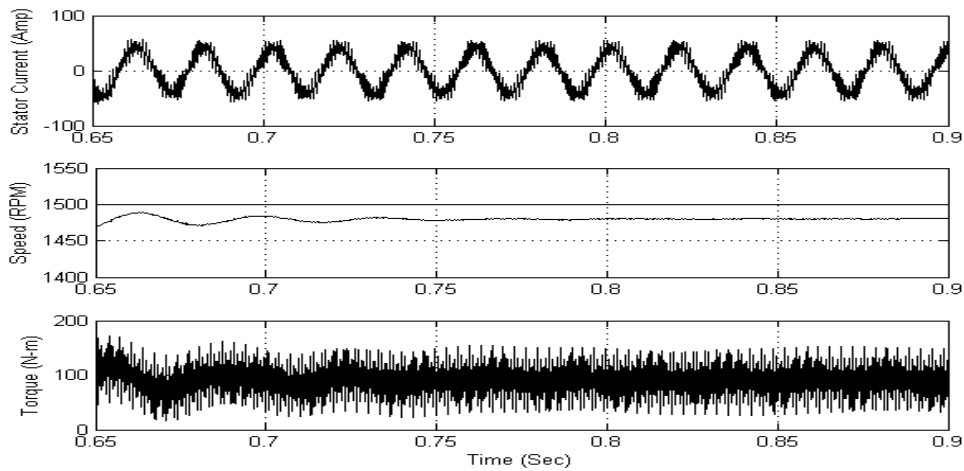


Figure 5.18: Steady-State Performance using NN for Step change in Speed ( $N = 1200$  to  $1460$  rpm)

Initially, the motor is started with a reference speed of 1200 RPM and the motor reaches its steady state speed and settles. At 0.5 seconds time, motor reference speed is increased to 1460 RPM. Due to controller action, the motor generates torque to reach its reference value. The response is depicted in Figure 5.18.

**Response for Speed Reversal:**

If the reference speed is altered from 1460 RPM to -1460 RPM, motor tends to rotate in the reverse direction. When the controller observes this change, it initially reduces the frequency of stator currents followed by phase reversal to start the motor in reverse direction. Since the drive is in same dynamic state (on load) just before and just after the reversal of this phenomenon, the steady state values of inverter currents are observed to be same in either directions of the rotation for the motor. But the phase sequence of these currents in both directions will be different. This response is shown in Figure 5.19 shown below.

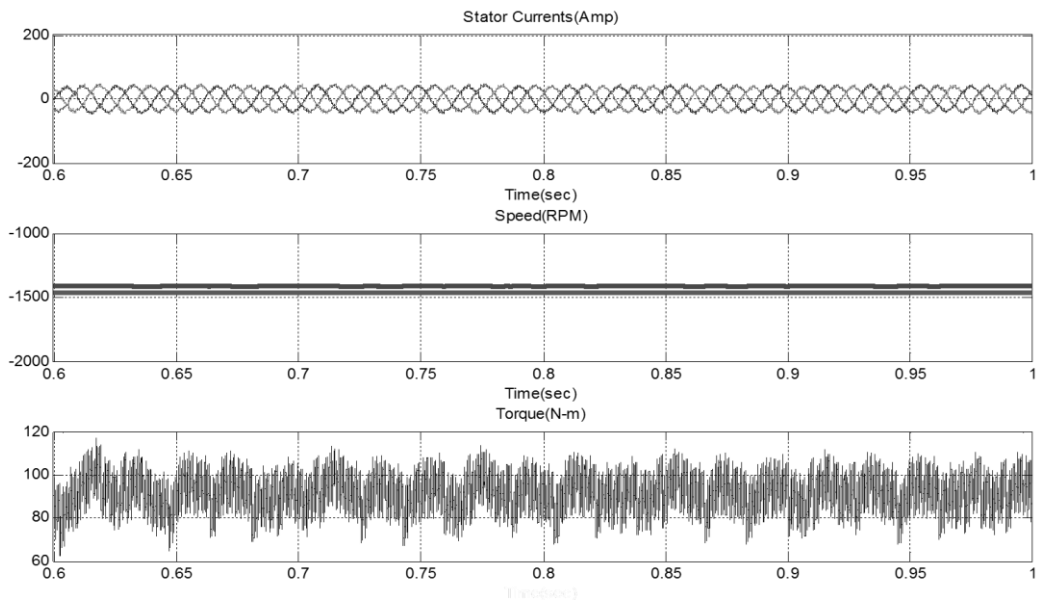


Figure 5.19: Steady-State Performance using NN for Speed Reversal (N = 1460 to -1460 rpm)

**5.4.2 Three-Level Diode-clamped Inverter fed Induction Motor Drive using Neural Network based controller**

Steady state performance of the 3 level Diode clamped inverter fed induction motor drive for various speed and load conditions is depicted in Figures 5.20 to Figure 5.24.

### Response for Starting with No Load:

In this, the motor is started without any load and the reference speed is set to 1460 RPM. When the speed error reaches nearly zero RPM, the winding current also reduces to no load value and the developed torque equals zero. The response is shown in Figure 5.20.

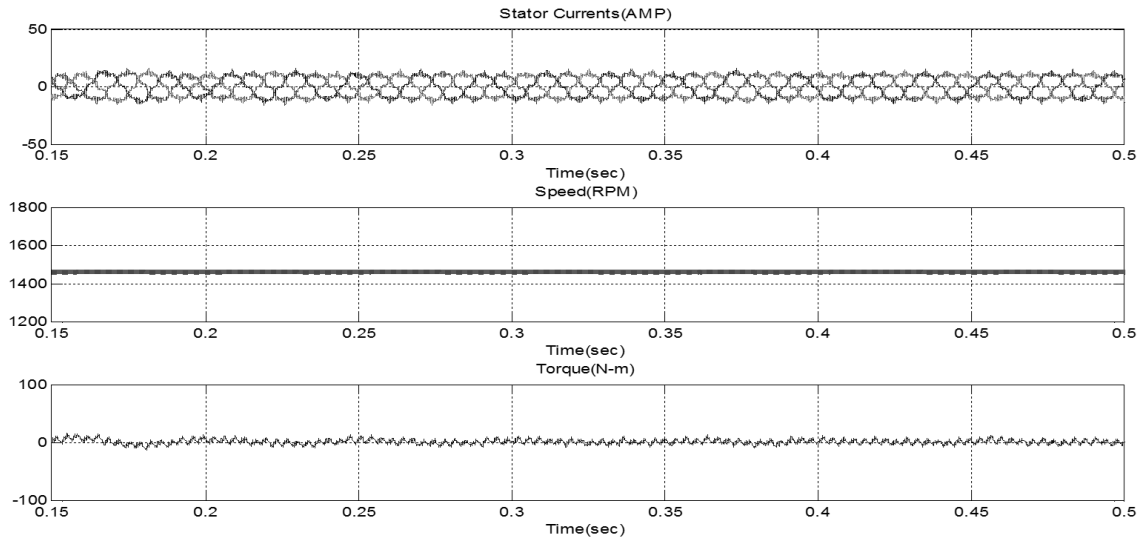


Figure 5.20: Steady-State Performance using NN when the Motor started with-out Load

### Response for Starting with Load:

In this case, motor is started with load ( $T_l = 90\text{N-m}$ ) and the reference speed set to 1460 RPM. When the speed reaches steady state value, the winding current and the developed torque equals to the set value of load. The motor steady state response is shown in Figure 5.21.

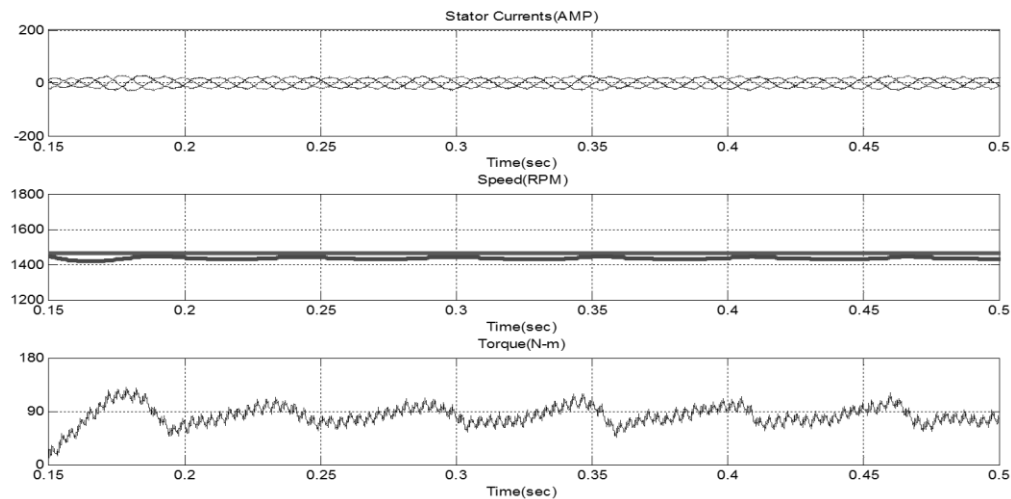


Figure 5.21: Steady-State Performance using NN when the Motor started with Load ( $T_l = 90\text{N-m}$ )

### Response for Step Change in Load:

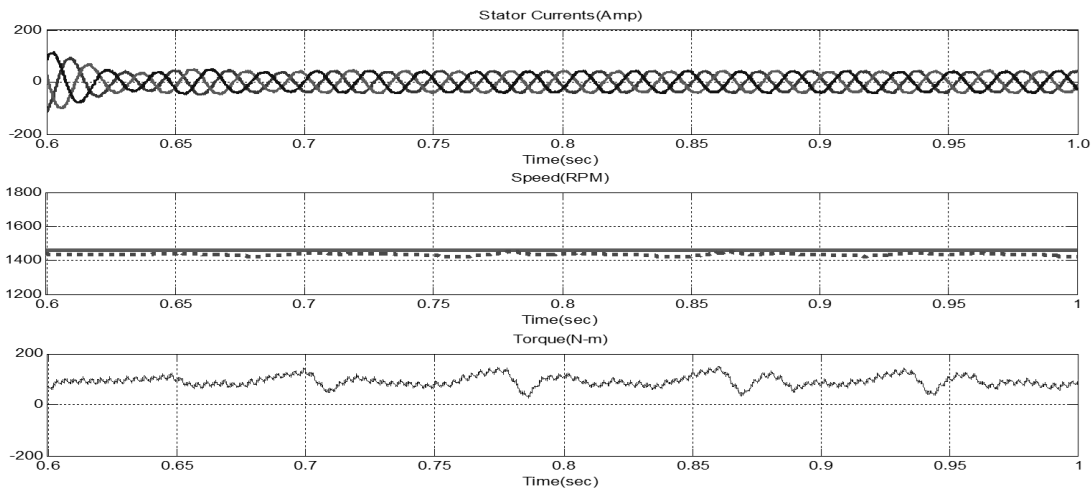


Figure 5.22: Steady-State Performance using NN for Step change in Load ( $T_l = 90\text{N-m}$ )

Motor is initially started with no load with a reference speed of 1460 RPM. Starting torque will be developed so as to accelerate the machine. As the speed reaches reference speed, torque developed is set to zero, at 0.5 seconds, a load torque of 90 N-m is applied. Due to controller action, the developed torque increases and the motor speed settles at steady state value again and winding currents increase. The steady state response is shown in Figure 5.22.

### Response for Step Change in Speed:

Initially motor is started with a reference speed of 1200 RPM. The motor reaches its steady state speed and settles there. At 0.5 seconds, the motor reference speed is increased to 1460 RPM. Due to the controller action, the motor develops torque to reach its reference value. The response is depicted in Figure 5.23

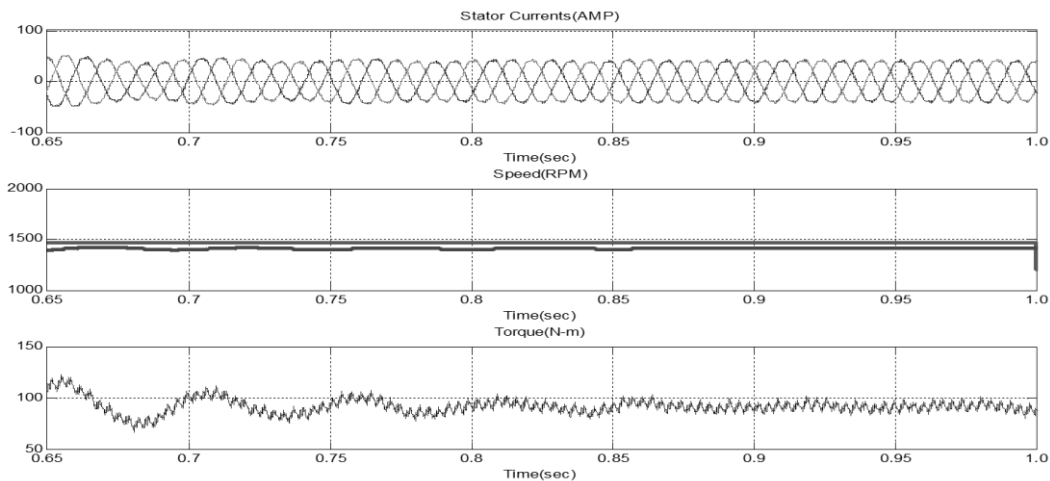


Figure 5.23: Steady-State Performance using NN for Step change in Speed (N = 1200 to 11460 rpm)

### Response for Speed Reversal:

When the reference speed is altered from 1460 RPM to -1460 RPM, the controller observes this change and initially reduces the frequency of stator currents followed by phase reversal to star the motor in reverse direction. This response is shown in Figure 5.24 below.

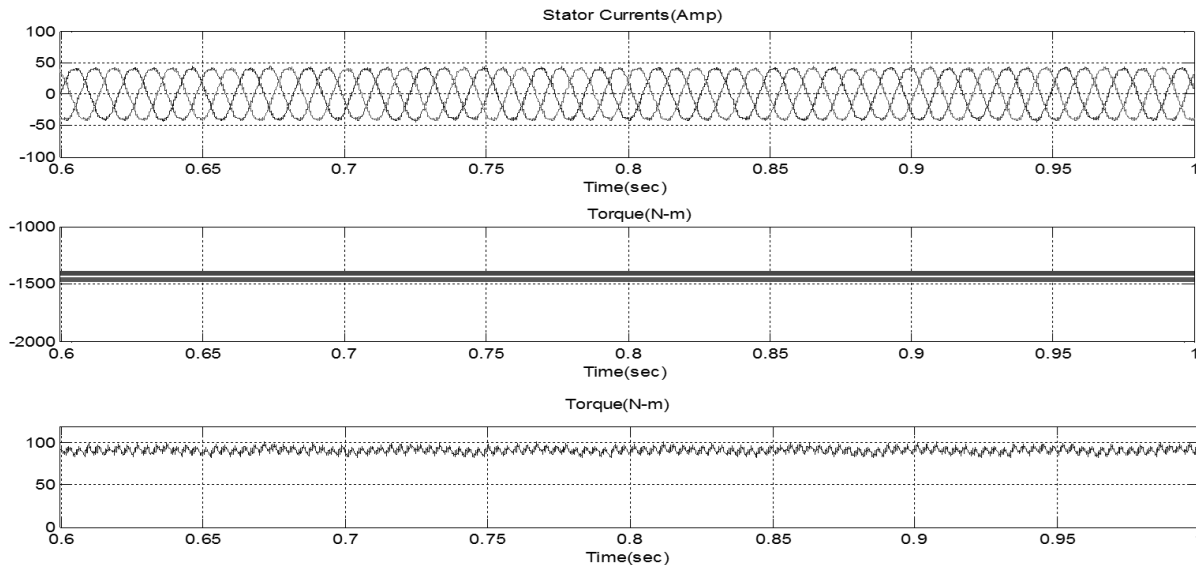


Figure 5.24: Steady-State Performance using NN for Speed Reversal (N = 1460 to -1460 rpm)

From the steady-state response characteristics of 3-level Diode-clamped inverter, it can be observed that the number of ripples and the magnitude of ripples in stator current, speed and torque are less compared to that of 2-level inverter. The performance of the drive has improved with 3-level Diode-clamped inverter compared to 2-level inverter while using Neural Network based controller itself.

## 5.5 General Model using Fuzzy Logic based controller

The basic operation of a multilevel inverter fed induction motor drive in scalar control (v/f control) has been explained previously. The induction motor drive was controlled in closed-loop manner. In this we utilize sinusoidal pulse width modulation (SPWM) for generating control signals for the inverters. Figure 5.25 shows the generalized Simulink model for all types of inverter fed induction motor drive using Fuzzy Logic based control scheme. This model has been used to evaluate all

inverters fed induction motor drive with corresponding changes in the inverter subsystem block and in the switching control block for Fuzzy Logic based control

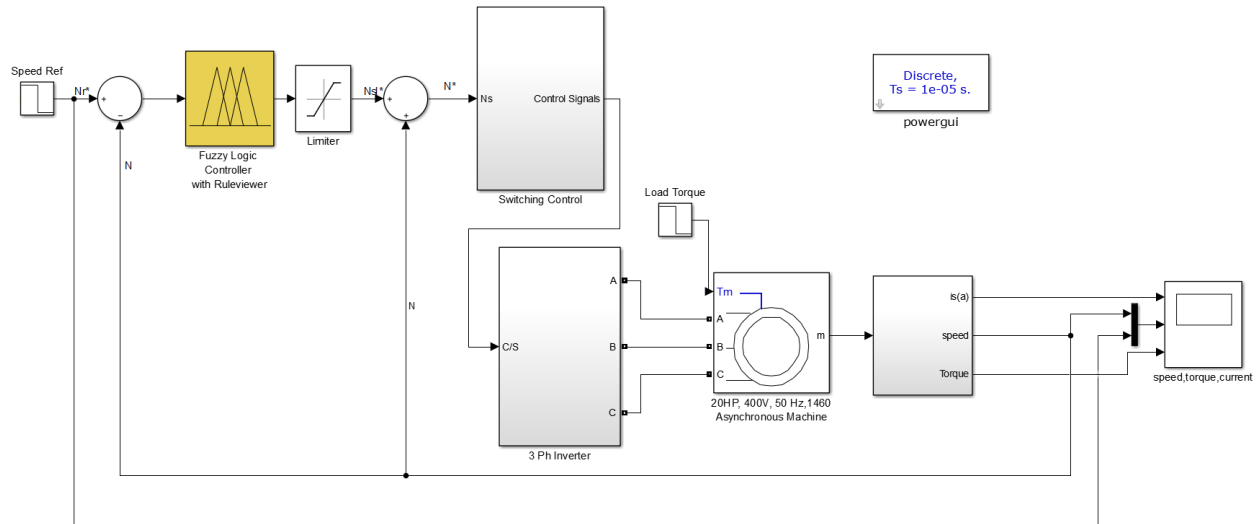


Figure 5.25: Generalized Simulink Model for Inverter fed Induction Motor Drive using Fuzzy Logic based controller

The Simulink model of types of inverters has been discussed previously. Here only the switching control block is discussed.

## 5.6 Steady State Performance Using Fuzzy Logic based controller

The steady-state performance of 2-level and 3-level Diode-clamped inverter fed induction motor drive across varying conditions such as load and speed are discussed here.

### 5.6.1 Two Level Inverter fed Induction Motor Drive using Fuzzy Logic based controller

The inverter block for generalized Simulink model shown in previous analysis is replaced with the 2 level inverter Simulink model that had been discussed in previous chapters. The steady-state performance of the 2 level inverter fed induction motor drive for various speed and load conditions is shown in Figure 5.26 to Figure 5.30.

**Response for Starting with No Load:**



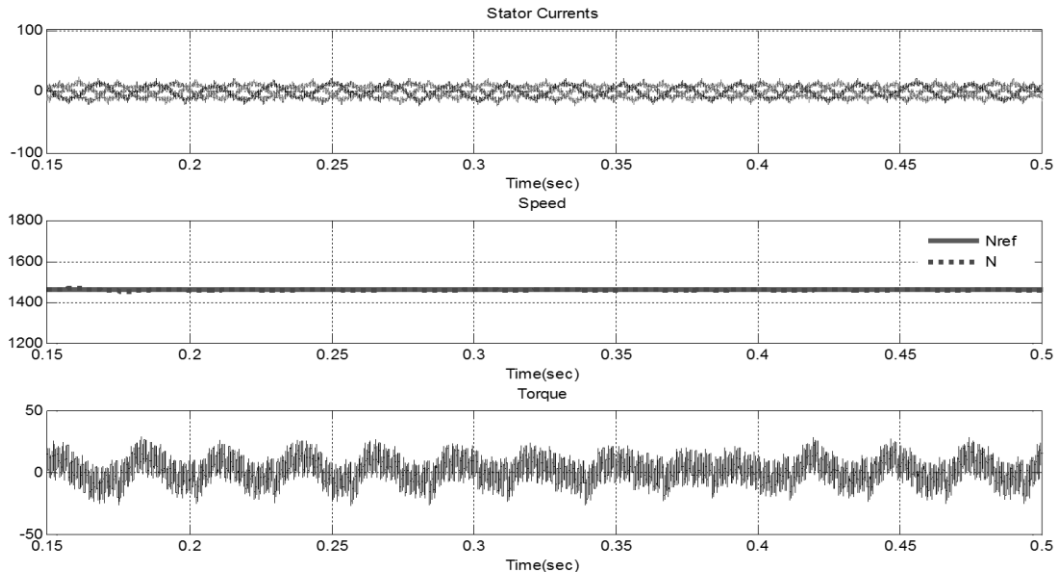


Figure 5.26: Steady-State Performance using Fuzzy Control when the Motor started with no load  
 In Figure 5.26, the motor started without any load and the reference speed has been set to 1460 RPM. As the speed error reaches nearly zero rpm, the winding current also reduces to no load value and the developed torque now become equals to zero.

**Response for Starting with Load:**

In this analysis, motor was started with a load ( $T_1 = 90\text{N-m}$ ) and reference speed was set to 1460 RPM. As the speed reaches steady state value, the winding current and developed torque becomes equal to the set value of load. The motor steady state response is shown in Figure 5.27

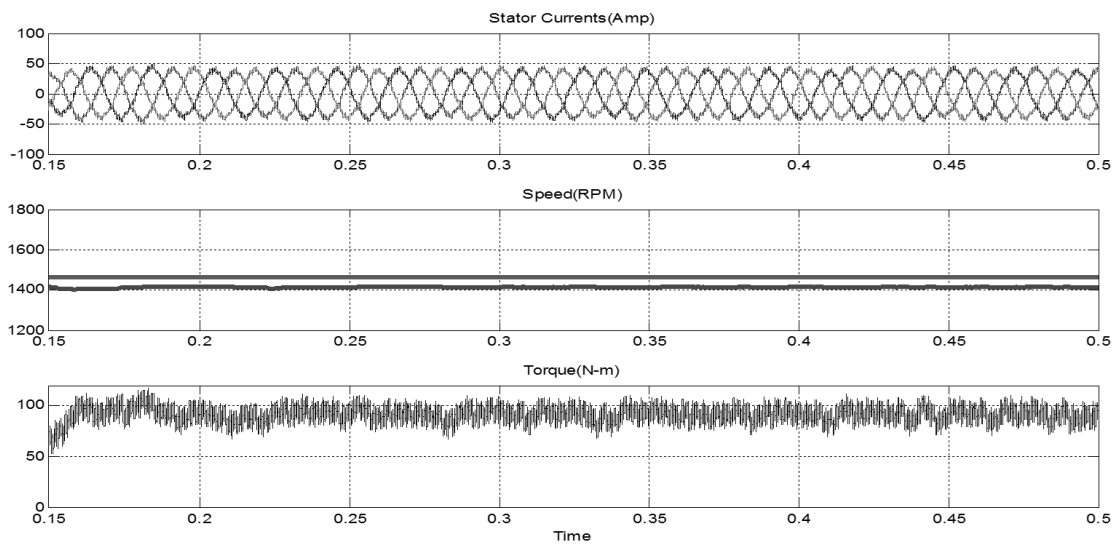


Figure 5.27: Steady-State Performance when using Fuzzy Control the Motor started with Load ( $T_1 = 90\text{N-m}$ )

### Response for Step Change in Load:

In this, the motor is started first on no load with reference speed of 1460 rpm. Starting torque is developed to accelerate the machine. As the speed reaches to reference speed torque developed is also set to zero, at 0.5sec a load torque of 90N-m is applied. Such a sudden application of load on rotor causes an instantaneous decline in speed of the motor. In reaction to this drop in speed, the output of controller responds by increasing the reference speed value. So the developed torque increases and motor speed settles at a steady value again, and winding currents will increase. The steady state response is shown in Figure 5.28.

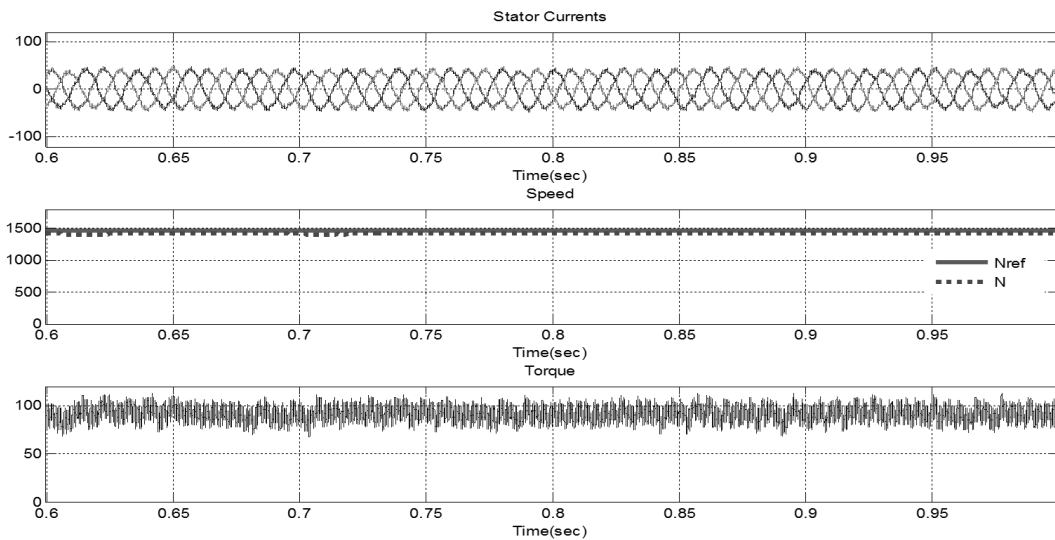


Figure 5.28: Steady-State Performance using Fuzzy Control for Step change in Load ( $T_l = 90\text{N-m}$ )

### Response for Step Change in Speed:

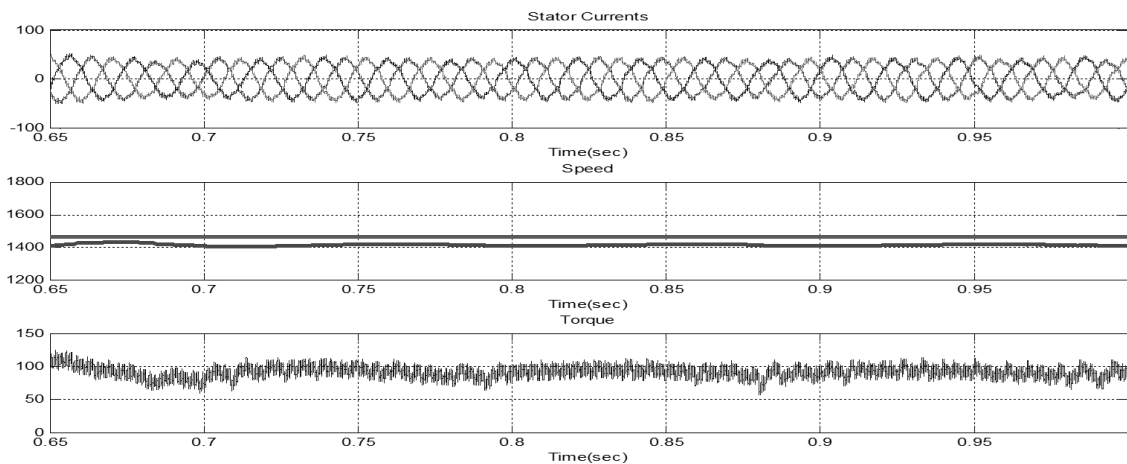


Figure 5.29: Steady-State Performance using Fuzzy Control for Step change in Speed ( $N = 1200$  to 1460 rpm)

Initially, the motor is started with a reference speed of 1200 RPM and the motor reaches its steady state speed and settles. At 0.5 seconds time, motor reference speed is increased to 1460 RPM. Due to controller action, the motor generates torque to reach its reference value. The response is depicted in Figure 5.29.

**Response for Speed Reversal:**

If the reference speed is altered from 1460 RPM to -1460 RPM, motor tends to rotate in the reverse direction. When the controller observes this change, it initially reduces the frequency of stator currents followed by phase reversal to start the motor in reverse direction. Since the drive is in same dynamic state (on load) just before and just after the reversal of this phenomenon, the steady state values of inverter currents are observed to be same in either directions of the rotation for the motor. But the phase sequence of these currents in both directions will be different. This response is shown in Figure 5.30 shown below.

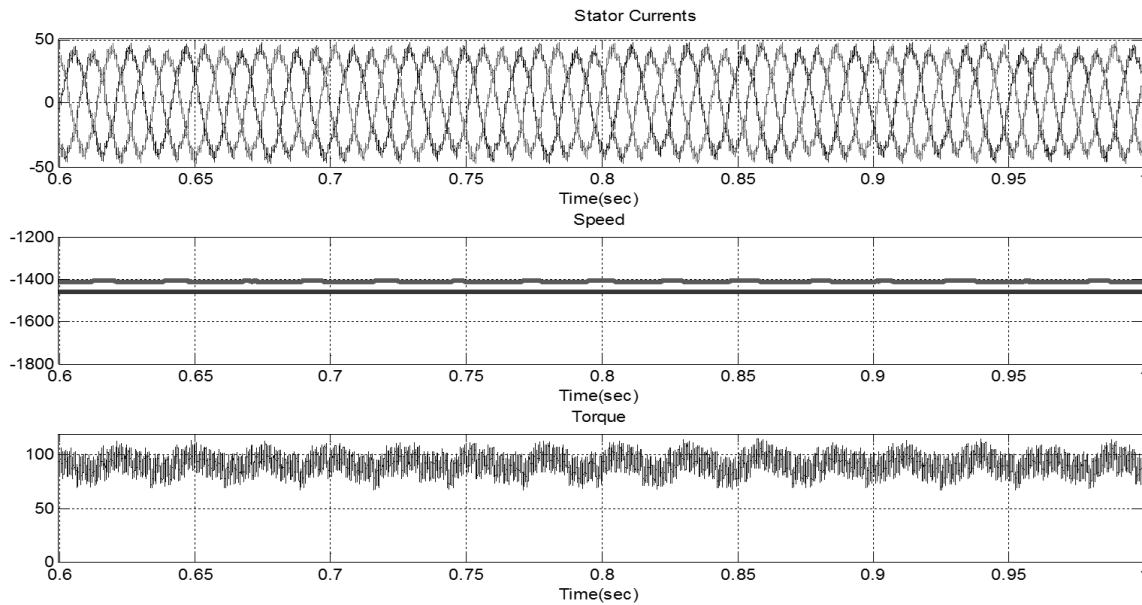


Figure 5.30: Steady-State Performance using Fuzzy Control for Speed Reversal (N = 1460 to -1460 rpm)

**5.6.2 Three-Level Diode-clamped Inverter fed Induction Motor Drive using Fuzzy Logic based controller**

Steady state performance of the 3 level Diode clamped inverter fed induction motor drive for various speed and load conditions is depicted in Figures 5.31 to Figure 5.35.

### Response for Starting with No Load:

In this, the motor is started without any load and the reference speed is set to 1460 RPM. When the speed error reaches nearly zero RPM, the winding current also reduces to no load value and the developed torque equals zero. The response is shown in Figure 5.31.

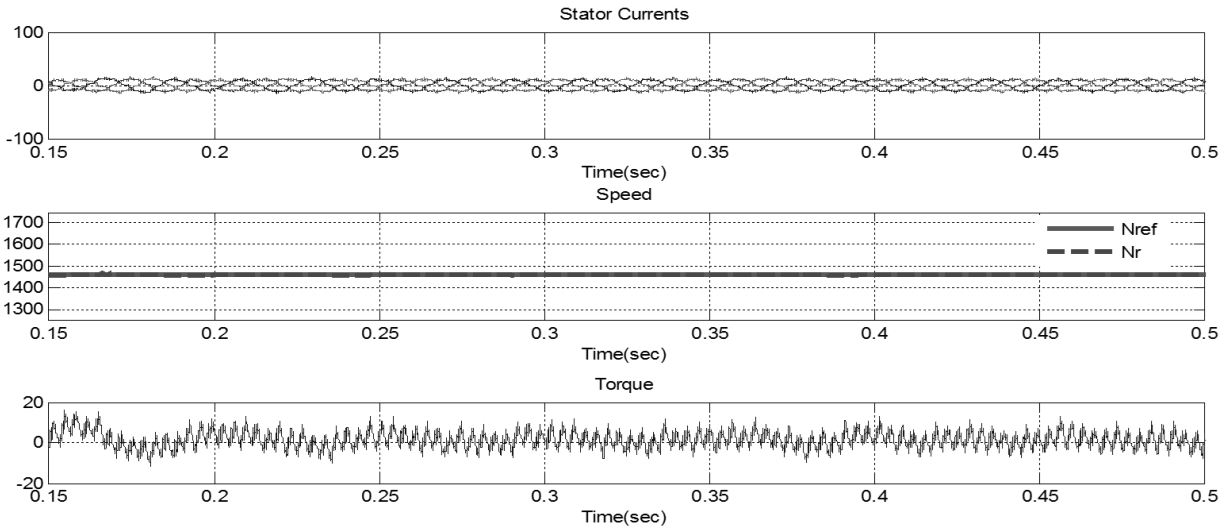


Figure 5.31: Steady-State Performance using Fuzzy Control when the Motor started with-out Load

### Response for Starting with Load:

In this case, motor is started with load ( $T_1 = 90\text{N-m}$ ) and the reference speed set to 1460 RPM. When the speed reaches steady state value, the winding current and the developed torque equals to the set value of load. The motor steady state response is shown in Figure 5.32.

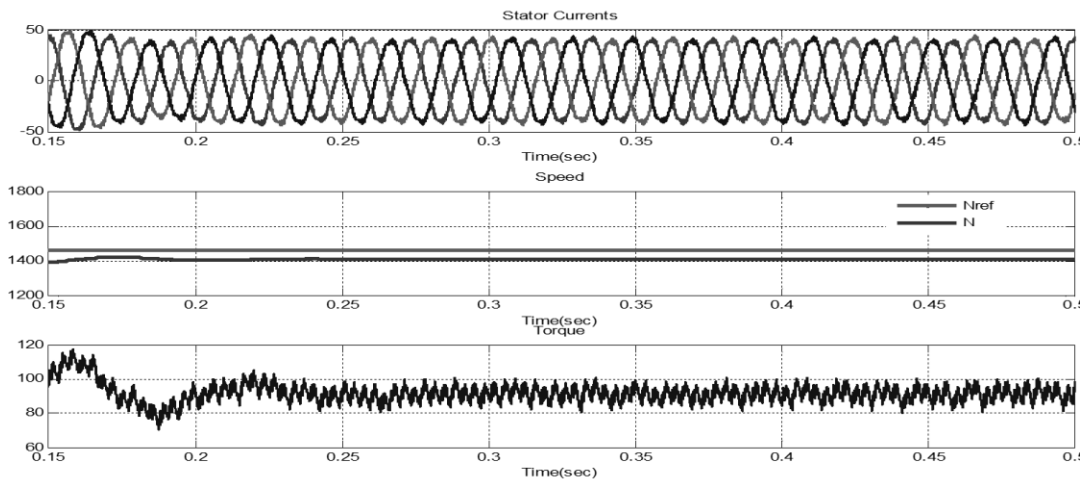


Figure 5.32: Steady-State Performance using Fuzzy Control when the Motor started with Load ( $T_1 = 90\text{N-m}$ )

### Response for Step Change in Load:

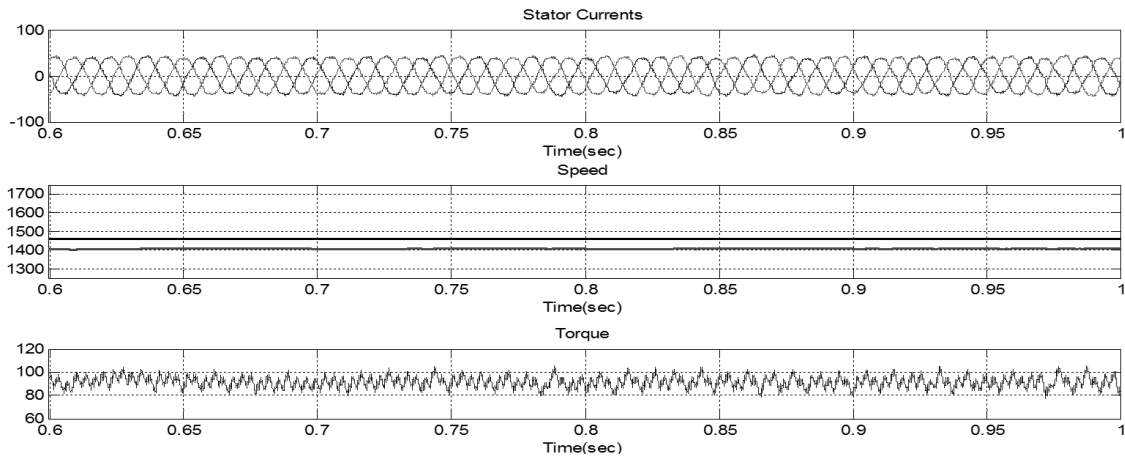


Figure 5.33: Steady-State Performance using Fuzzy Control for Step change in Load ( $T_l = 90\text{N-m}$ )

Motor is initially started with no load with a reference speed of 1460 RPM. Starting torque will be developed so as to accelerate the machine. As the speed reaches reference speed, torque developed is set to zero, at 0.5 seconds, a load torque of 90 N-m is applied. The steady state response is shown in Figure 5.33.

### Response for Step Change in Speed:

Initially motor is started with a reference speed of 1200 RPM. The motor reaches its steady state speed and settles there. At 0.5 seconds, the motor reference speed is increased to 1460 RPM. Due to the controller action, the motor develops torque to reach its reference value. The response is depicted in Figure 5.34

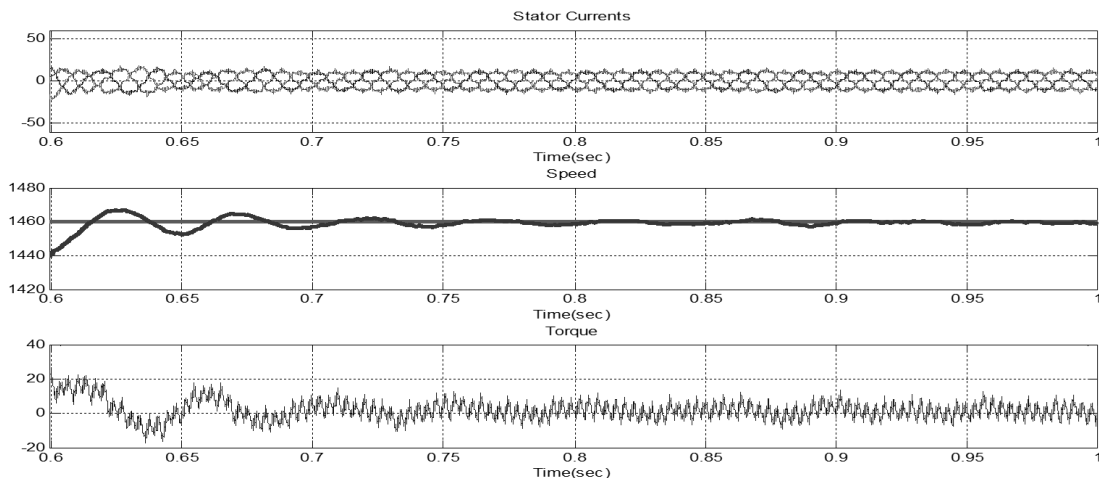


Figure 5.34: Steady-State Performance using Fuzzy Control for Step change in Speed ( $N = 1200$  to 1460 rpm)

### Response for Speed Reversal:

When the reference speed is altered from 1460 RPM to -1460 RPM, the controller observes this change and initially reduces the frequency of stator currents followed by phase reversal to star the motor in reverse direction. This response is shown in Figure 5.35 below.

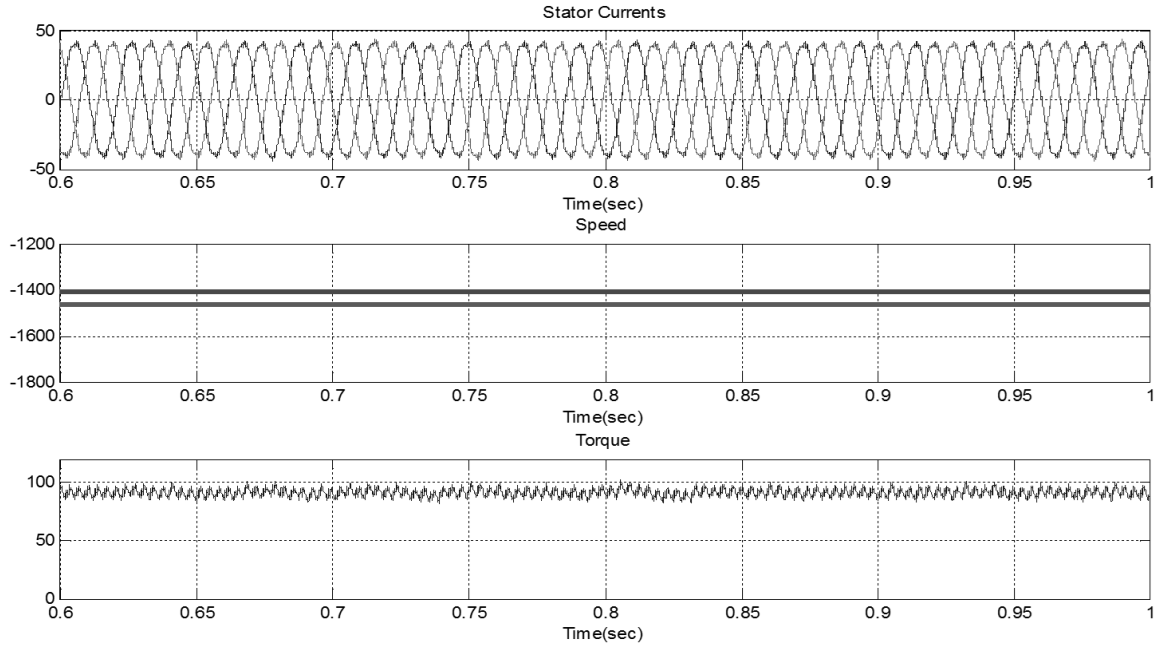


Figure 5.35: Steady-State Performance using Fuzzy Control for Speed Reversal (N = 1460 to -1460 rpm)

From the steady-state response characteristics of 3-level Diode-clamped inverter, it can be observed that the number of ripples and the magnitude of ripples in stator current, speed and torque are less compared to that of 2-level inverter. The performance of the drive has improved with 3-level Diode-clamped inverter compared to 2-level inverter while using Fuzzy Logic based controller itself.

## 5.7 Comparison of Performance

Using simulations obtained from section 5.1 to section 5.6, we broadly divide the simulation cases types into two scenarios of 5 cases each. They are listed below as follows for the inverter fed induction machine performance:

**Scenario 1:** 3 Phase – 2 Level Inverter fed Induction Machine with following cases:-

**Case 1:** Machine is started at No-load and reference speed set at rated speed (1460rpm)

**Case 2:** Machine is started at a load of 90 N-m with a reference speed of 1200rpm and at  $t=0.5s$  the reference speed set to 1460rpm. Analysis on the step change.

**Case 3:** Machine is started at a load of 90 N-m with a reference speed set at 1460rpm

**Case 4:** Machine is started at No-load and at  $t=0.5s$ , torque is stepped to 90 N-m

**Case 5:** Machine is started at a load of 90 N-m and reference speed of 1460rpm. At  $t=0.5s$  the reference speed is set to -1460rpm. Analysis on the step change.

**Scenario 2:** 3 Phase – 3 Level Inverter fed Induction Machine with following cases:-

**Case 1:** Machine is started at No-load and reference speed set at rated speed (1460rpm)

**Case 2:** Machine is started at a load of 90 N-m with a reference speed of 1200rpm and at  $t=0.5s$  the reference speed set to 1460rpm. Analysis on the step change.

**Case 3:** Machine is started at a load of 90 N-m with a reference speed set at 1460rpm

**Case 4:** Machine is started at No-load and at  $t=0.5s$ , torque is stepped to 90 N-m

**Case 5:** Machine is started at a load of 90 N-m and reference speed of 1460rpm. At  $t=0.5s$  the reference speed is set to -1460rpm. Analysis on the step change.

Both the scenarios above are applied to all of PI based control, Neural Network based control and Fuzzy Logic based control and the response graphs are shown in previous sections. Here we quantify the parameters of the response and analyze the performance with following parameters :-

1. Peak overshoot percentage (%)
2. Rise Time (s)
3. Ripple percentage in steady state torque (%)
4. Steady state error percentage (%)

Given below are the values of above parameters as found from graphs of the cases.

COMPARING PERFORMANCE OF CONTROL TECHNIQUES (2 Level Inverter)				
		PI	Neural	Fuzzy
		%	%	%
CASE 1	Peak Overshoot	1.80	1.58	1.50
	Steady State Error	1.40	1.32	1.28
	Torque Ripple	17.22	17.42	17.69
	Rise Time	0.15 sec	0.142 sec	0.135 sec
CASE 2	Peak Overshoot	1.44	1.39	1.22
	Steady State Error	3.82	3.73	3.69
	Torque Ripple	15.97	15.58	15.17
	Rise Time	0.18 sec	0.10 sec	0.10 sec
CASE 3	Peak Overshoot	1.57	1.67	1.67
	Steady State Error	3.88	3.68	3.52
	Torque Ripple	14.35	16.40	16.4
	Rise Time	0.18 sec	0.192 sec	0.177 sec
CASE 4	Peak Overshoot	2.70	2.60	2.52
	Steady State Error	3.66	3.53	3.44
	Torque Ripple	18.39	18.60	18.45
	Rise Time	NA	NA	NA
CASE 5	Peak Overshoot	2.72	2.60	2.40
	Steady State Error	3.07	2.92	2.82
	Torque Ripple	18.45	18.45	17.52
	Rise Time	0.11 sec	0.092 sec	0.09 sec

**Table 5.1:** Comparison table of different controllers for 2 level inverter fed induction machine speed control

COMPARING PERFORMANCE OF CONTROL TECHNIQUES (3 Level Inverter)				
		PI	Neural	Fuzzy
		%	%	%
CASE 1	Peak Overshoot	0.5491	0.41	0.38
	Steady State Error	0.205	0.0685	0.108
	Torque Ripple	17.8	17.93	18.4
	Rise Time	0.118 sec	0.112 sec	0.120 sec
CASE 2	Peak Overshoot	1.21	1.22	1.18
	Steady State Error	3.63	3.30	3.28
	Torque Ripple	16.4	12.30	12.3



	Rise Time	0.177 sec	0.108 sec	0.094
CASE 3	Peak Overshoot	1.49	1.38	1.32
	Steady State Error	3.63	3.18	2.96
	Torque Ripple	15.37	16.40	13.32
	Rise Time	0.12 sec	0.116 sec	0.102 sec
CASE 4	Peak Overshoot	2.48	2.20	2.12
	Steady State Error	3.42	3.20	3.08
	Torque Ripple	19.4	20.49	16.40
	Rise Time	NA	NA	NA
CASE 5	Peak Overshoot	2.40	2.20	2.08
	Steady State Error	2.88	2.60	2.32
	Torque Ripple	21.52	22.54	18.41
	Rise Time	0.11 sec	0.092 sec	0.072 sec

**Table 5.2:** Comparison table of different controllers for 3 level inverter fed induction machine speed control

We observe a quantification of the parameters specified above for all the cases of operation for PI, Neural and Fuzzy based control schemes of Inverter fed Induction Machine speed control. We get a better interpretation for the performance by plotting graphs for Peak Overshoot, Steady State Error, Torque Ripple and Rise time for all the cases and scenarios.

### Conclusion

Figure 5.36 and Figure 5.37 depict through clear graphs about how the performance of Fuzzy Logic based controller is superior to that of PI and Neural based control scheme performance. Also neural can be observed to perform better than PI based control, by a very small margin though.

Further we can see that these new control techniques fail to perform better than PI based control but instead perform equal to PI control in cases such as starting with load and no change. But it can be clearly observed that Fuzzy and Neural based controllers perform best in cases of step changes of speed or torque. This is a highly desired quality of any system. A system is better from another if it performs excellent even when there are sudden changes. This performance upgrade is attributed to the self-learning capabilities of these Intelligent control techniques. The complex practical model of a system is abstracted in the higher dimension curve fitting model of these techniques thus giving a better performance at sudden step changes/disturbances in the system.

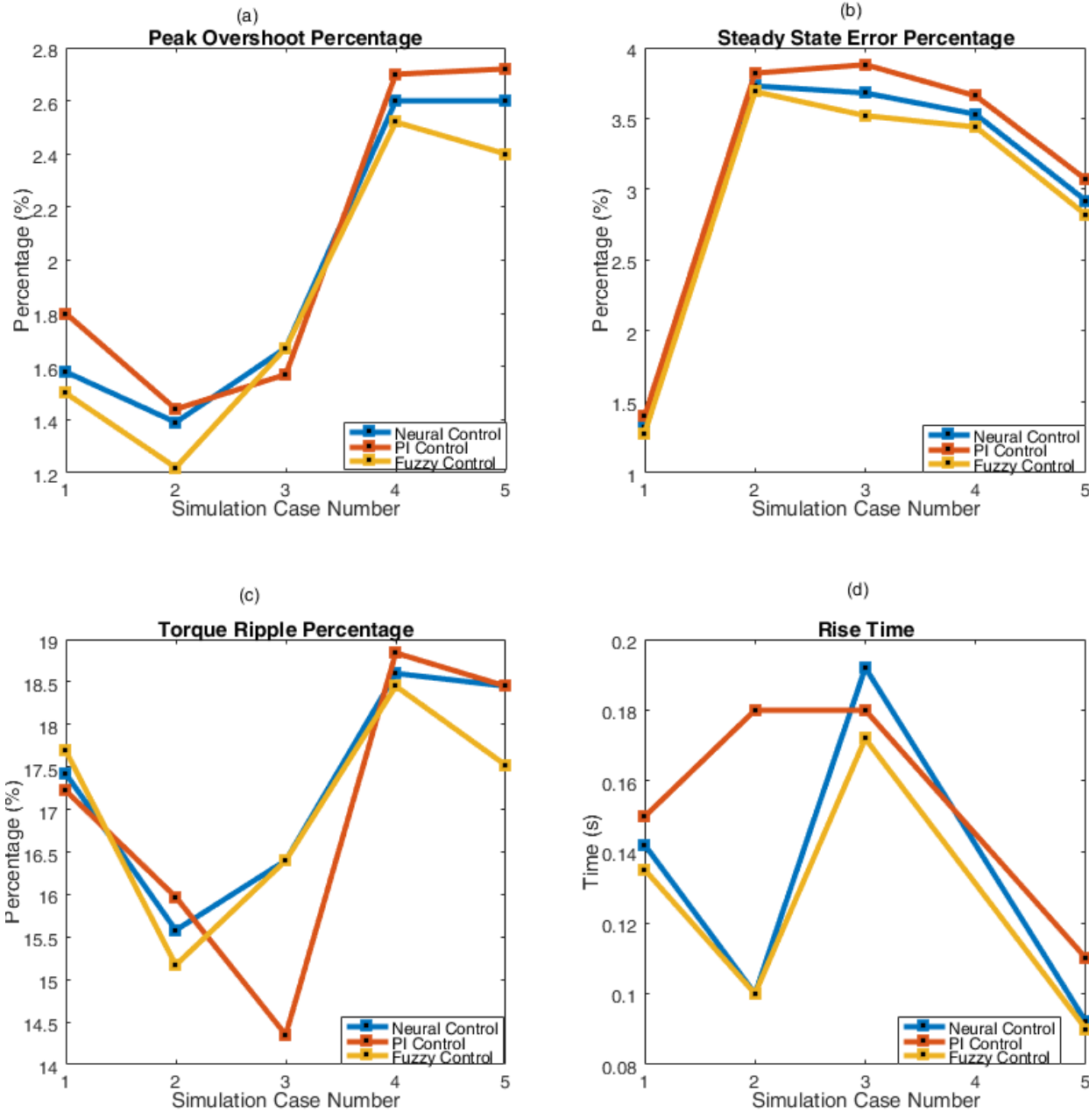


Figure 5.36: Graphs for (a) Peak overshoot (b) Steady state error (c) Torque ripple and (d) Rise time for 2 Level Inverter fed Induction Machine using different control techniques

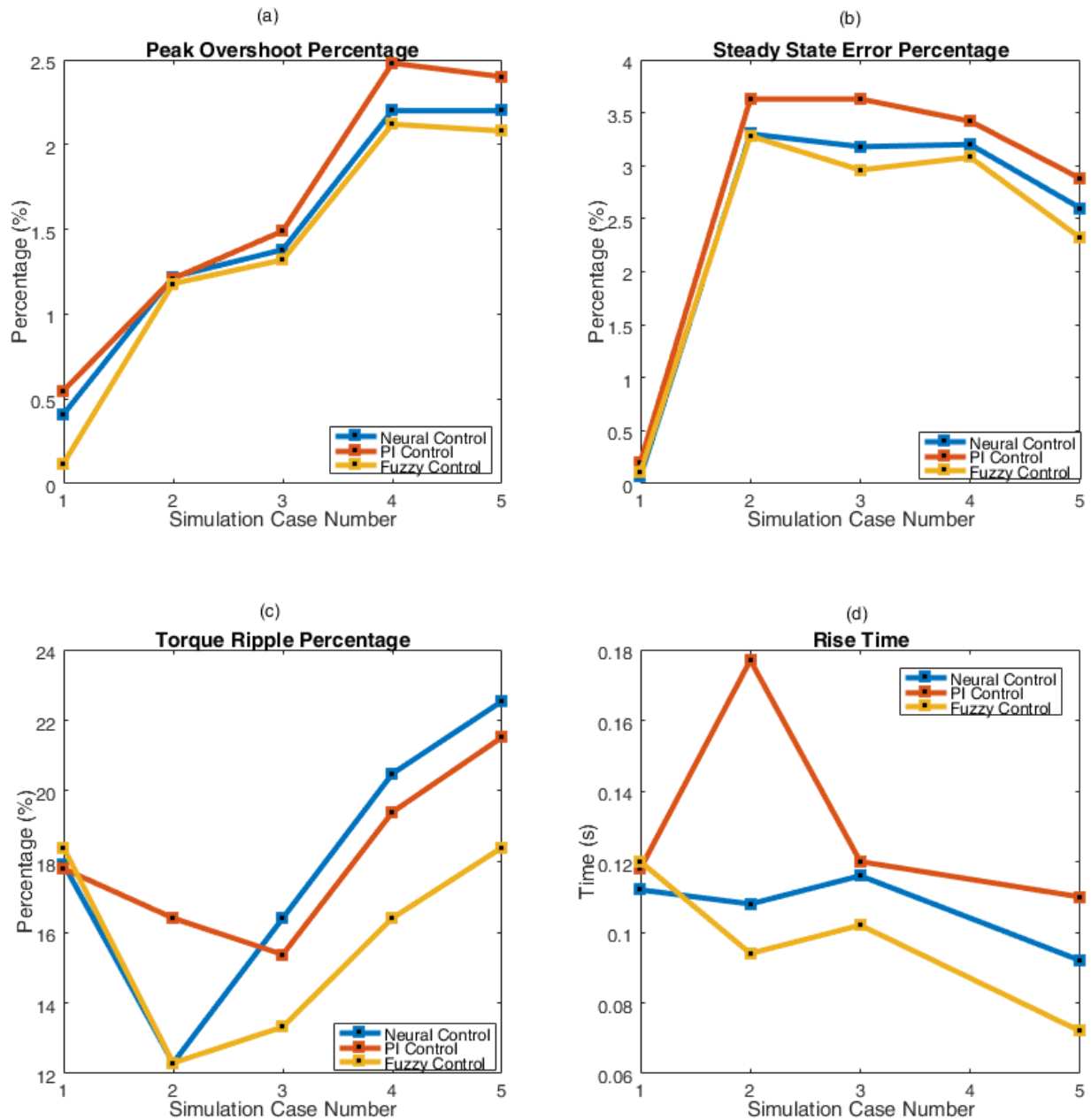


Figure 5.37: Graphs for (a) Peak overshoot (b) Steady state error (c) Torque ripple and (d) Rise time for 3 Level Inverter fed Induction Machine using different control techniques

## 5.8 Recommendation for Future Work

Further performance upgradation can be gained using better Pulse Width Modulation techniques such as Space Vector Modulation based PWM and further vector based control strategies. There is a very high utility of these Artificial Intelligence Techniques in these areas. Further, we can implement Adaptive Networks based Neuro Fuzzy techniques to improve the method.

# Chapter 6: System Hardware Development

## 6.1 Laboratory Tests

The dynamic performance of an inverter fed induction motor drive controlled by various intelligent control techniques has been discussed in earlier chapters. 3 phase induction machine of 2 HP rating is selected for hardware realization of the inverter fed drive. The parameters of the 2 HP machine has been calculated in the laboratory using Blocked Rotor Test, No Load Test and Retardation Test with and without DC Machine coupling.

The manufacturer stated nameplate has been shown in the image of Figure 6.1. Rated values of the Induction Machine are as follows:

Frequency	50 Hz	Mechanical Power	1.5 kW
Voltage	415 V	Efficiency	78.5 %
Current	3.3 A	Speed	1400 RPM

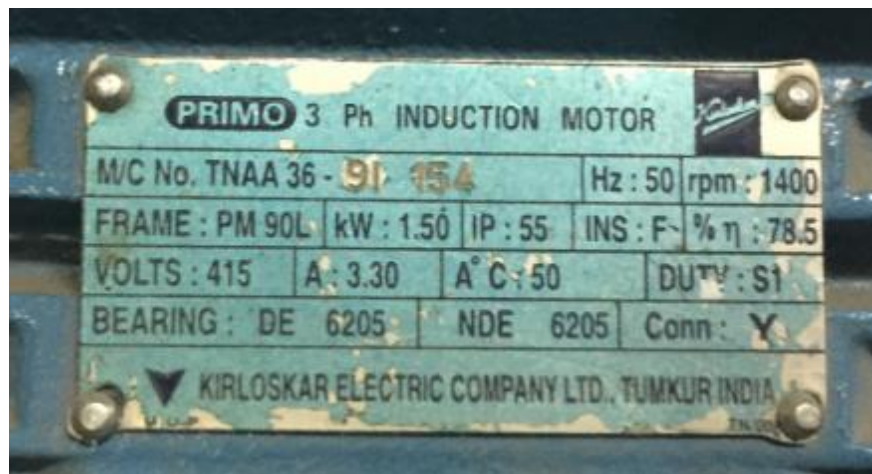


Figure 6.1: Nameplate showing the manufacturer stated ratings of Induction Machine

### 6.1.1 No Load and Blocked Rotor Test

Figure 6.2(a) and 6.2(b) illustrate the circuit diagram implemented for performing no load and blocked rotor tests on the given 2 HP Induction machine. The results of laboratory tests conducted are given below :

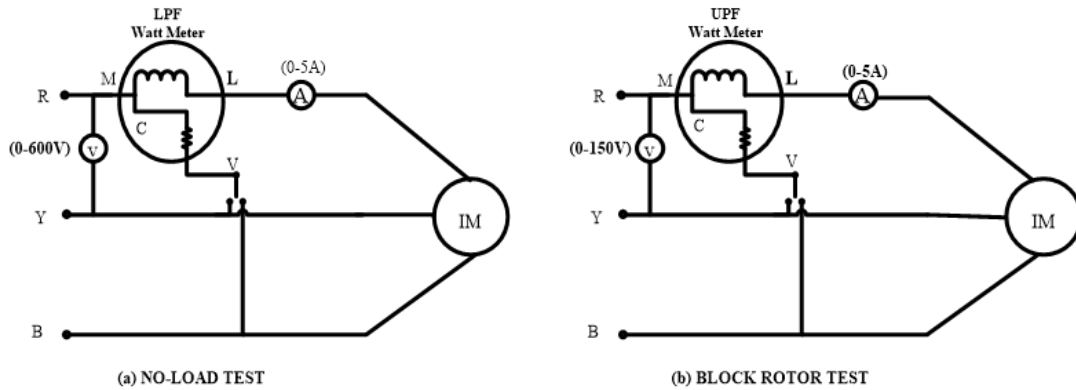


Figure 6.2: Circuit diagram of (a) No Load test (b) Blocked Rotor test

**No Load test data:**

$$V_{NL} = 415 \text{ V}, I_{NL} = 1.95 \text{ A}, N = 1491 \text{ RPM}$$

$$W_1 = 492 \text{ W}, W_2 = -284 \text{ W}, W_1 + W_2 = 208 \text{ W}$$

Per phase quantities:

$$P_1 = \frac{208}{3} = 69.33 \text{ W}, I_1 = 1.45 \text{ (Y - connected)}, V_1 = \frac{415}{\sqrt{3}} = 239.6 \text{ V}$$

$$P_1 = V_1 I_1 \cos \theta_1, \cos \theta_1 = 0.1483$$

$$I_M = I_1 \sin \theta_1 = 1.928$$

$$R_M = 825.97 \Omega$$

$$X_M = 124.27 \Omega$$

**Blocked Rotor test data:**

$$V_{BR} = 104 \text{ V}, I_{BR} = 3.3 \text{ A}, N = 0 \text{ RPM}$$

$$W_1 = 20 \text{ W}, W_2 = 280 \text{ W}, W_1 + W_2 = 300 \text{ W}$$

Per phase quantities:

$$P_1 = \frac{300}{3} = 100 \text{ W}, I_1 = 3.3 \text{ (Y - connected)}, V_1 = \frac{104}{\sqrt{3}} = 60.04 \text{ V}$$

$$P_2 = I_1^2 R_{eq}, \quad R_{eq} = 9.18 \Omega$$

$$R'_2 = R_{eq} - R_1 = 9.18 - 5.88 = 3.30 \Omega$$

$$R_1 = 5.88 \Omega$$

$$X_1 = 7.85 \Omega$$

$$X'_2 = 7.85 \Omega$$

### 6.1.2 Retardation Test

Retardation test is performed to calculate the Moment of Inertia  $J$  of the induction motor. The Induction machine is coupled with a DC machine and then the coupled MI is calculated. Next, moment of inertia of DC machine alone is found. MI of the induction machine is found by subtracting both the quantities. Figure 6.3(a) depicts the coupling diagram for DC and IM machines. Figure 6.3(b) shows the experimental setup for conducting the retardation test. Rated speed of DC Machine is 1500 RPM

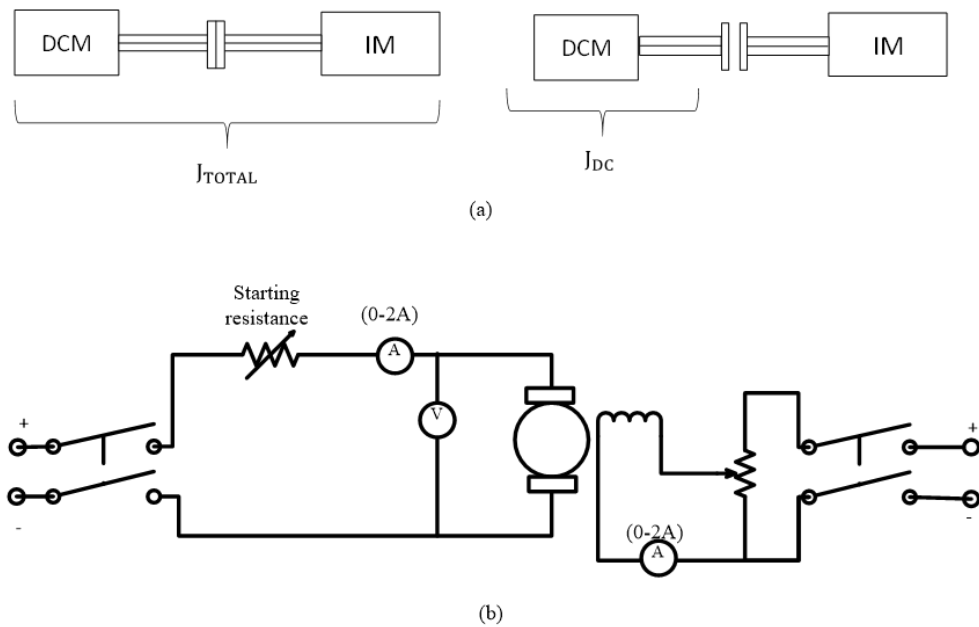


Figure 6.3: (a) coupling diagram of IM and DC motor (b) connection diagram of DC motor

Following is the results obtained from the retardation test:

<b>DC coupled with Induction Machine</b>				
$N$ (rpm)	$I_a$ (A)	$V_a$ (V)	$W$ (watt)	$T$ (s)
1500	0.85	146	124.1	2.75
1400	0.85	144	122.4	2.65

1116	0.8	108	86.4	2.15
800	0.75	80	60	1.45
568	0.65	56	36.4	0.75

**Table 8.1 :** Retardation test data on Induction motor coupled with DC motor

<b>DC motor</b>				
<b><i>N (rpm)</i></b>	<b><i>I<sub>a</sub>(A)</i></b>	<b><i>V<sub>a</sub>(V)</i></b>	<b><i>W(watt)</i></b>	<b><i>T(s)</i></b>
1500	0.35	132	46.2	2.73
1300	0.35	114	39.9	2.21
1100	0.33	96	31.68	2.15
933	0.32	84	26.88	1.50

**Table 8.2 :** Retardation test data on DC motor

For the coupled set  $\frac{dw}{dt} = \left( \frac{(146.6-83.77)}{2.65-1.45} \right) = 1.2$

$$W_{loss} = \frac{d(kE)}{dt} = J\omega \frac{d\omega}{dt}$$

$$122.4 = J_c \times 146.6 \times 1.2$$

$$J_c = 0.6958 \text{ kg} - \text{m}^2$$

For the standalone DC machine,

$$\frac{d\omega}{dt} = \left( \frac{(157.07-97.73)}{2.73-1.5} \right) = 1.23$$

$$W_{loss} = \frac{d(kE)}{dt} = J\omega \frac{d\omega}{dt}$$

$$46.2 = J \times 157.07 \times 1.23$$

$$J = 0.2391 \text{ kg} - \text{m}^2$$

Thus, the Moment of Inertia of Induction machine,  $J_{IM}$  is

$$J_{IM} = J_c - J = 0.6958 - 0.2391 = 0.4567 \text{ kg} - \text{m}^2$$

So the found parameters are as follows:

1.  $J_{IM} = 0.4567 \text{ kg} - \text{m}^2$
2.  $R_1 = 5.88 \Omega$

3.  $R'_2 = 3.30 \Omega$
4.  $X_1 = 7.85 \Omega$
5.  $X'_2 = 7.85 \Omega$
6.  $R_M = 825.97 \Omega$
7.  $X_M = 124.27 \Omega$

## 6.2 Hardware Development

A practical proof of concept of the intelligent control techniques based inverter fed induction machine setup has been designed with three phase system for verification of the dissertation. Diode Bridge based rectifier setup is prepared to procure the DC input part of the setup.

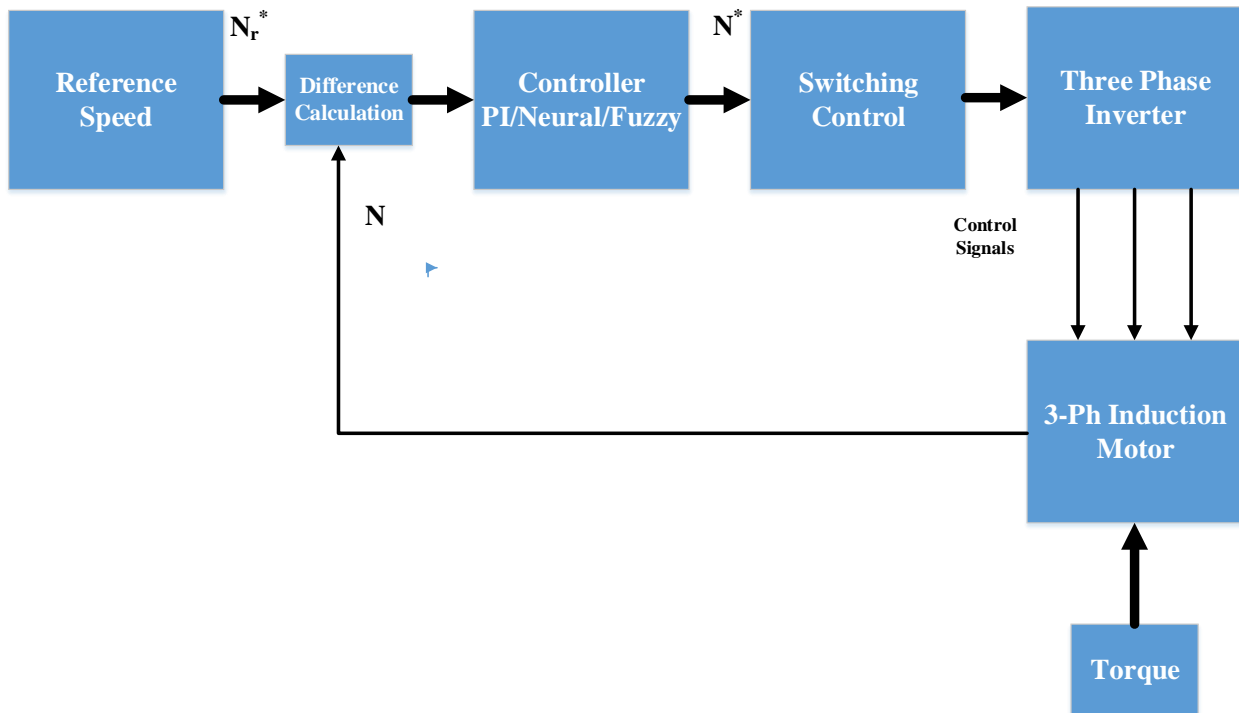


Figure 6.4: Schematic diagram of the system implemented for speed control

As a hardware prototype and proof of concept, we implement the open loop v/f scheme for controlling the speed of a three phase induction motor. Figure 6.4 shows the schematic block diagram for implementing hardware prototype for the same.

### 6.2.1 Development of Power Circuit of Inverter fed Induction motor control



A voltage source inverter for 3 phase, 3 level configuration is suitably developed with 12 MOSFET switches and Input DC Link capacitance. Bridge Rectifier fed by single phase AC supply is used as the input DC source for inverter. Figure 6.5 shows the laboratory hardware prototype of the 3 phase inverter made using 12 switches.

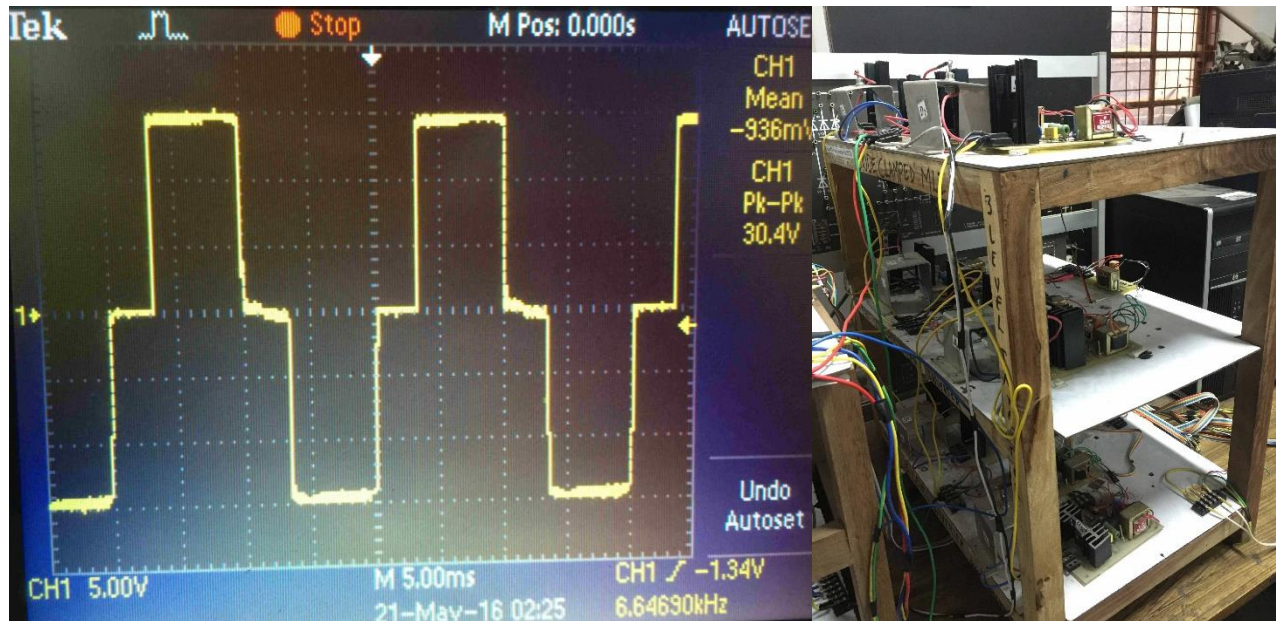


Figure 6.5: 3 Phase - 3 Level Voltage source Inverter

### 6.2.2 Snubber Circuit

Switching high current in short time gives rise to voltage transients that could exceed the rating of the MOSFET. Snubbers are therefore needed to protect the switch from transients. Snubber circuit for MOSFET is shown in Figure 6.6. The diode prevents the discharging of the capacitor via the switching device, which could damage the device due to large discharge current. An additional protective metal oxide varistor (MOV) is used across each device to protect against over voltages across the devices.

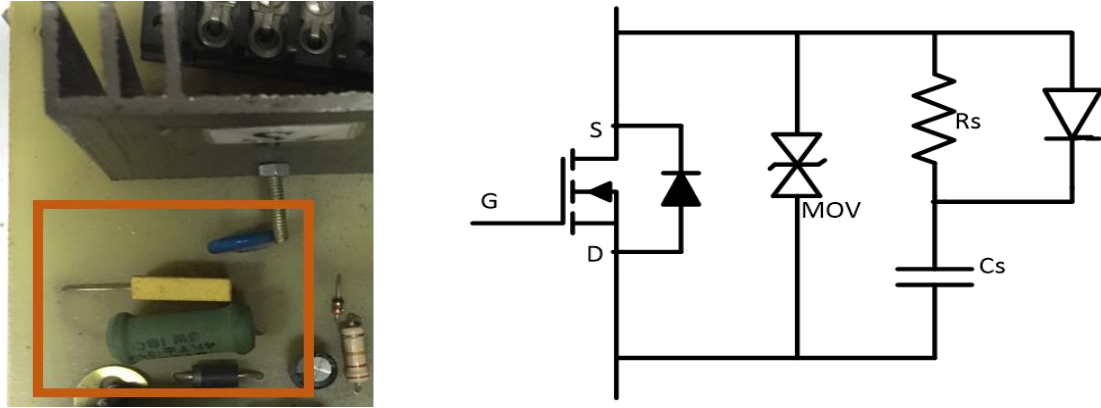


Figure 6.6: Snubber circuit for MOSFET protection and its hardware implementation in laboratory

### 6.3 Measurement of System Parameters

For measuring accurate and reliable parameters of a system in closed loop or open loop operation of various systems, the measurement devices must have:

- High accuracy
- Galvanic isolation between high and low voltage side,
- Ease of installation
- Linearity and fast response, etc.

In order to implement and verify the hardware, we require to measure following signals:

- Line currents using current sensor circuits
- Line voltages using voltage sensor circuits

Ac source currents are sensed using PCB mounted Hall Effect current sensors (HTP 50). It has the transformation ratio of 1000:1; hence its output is scaled properly to obtain the desired value to meet the control requirements. Figure 6.7 shows the schematic circuit used for development of current sensor PCB for procuring signals from the power circuit. Further, Figure 6.7 even shows the laboratory prototype implementation for the same.

AC source voltages  $v_{sa}$ ,  $v_{sb}$  and  $v_{sc}$  (phase to neutral) are required to generate the unit current sine vectors ( $e_{sa}$ ,  $e_{sb}$  and  $e_{sc}$ ) in phase with the respective source voltages. Only sensing two voltage are sufficient for three phase three wire system, but all the three voltages are sensed to avoid the delay introduced due to the subtraction circuit. Figure 6.8 shows the schematic circuit used for development of voltage sensor PCB for procuring signals from the power circuit. Further, Figure

6.8 even shows the laboratory prototype implementation for the same. Note that, in laboratory implementation, an LV 25 voltage sensor has been used due to ease of availability

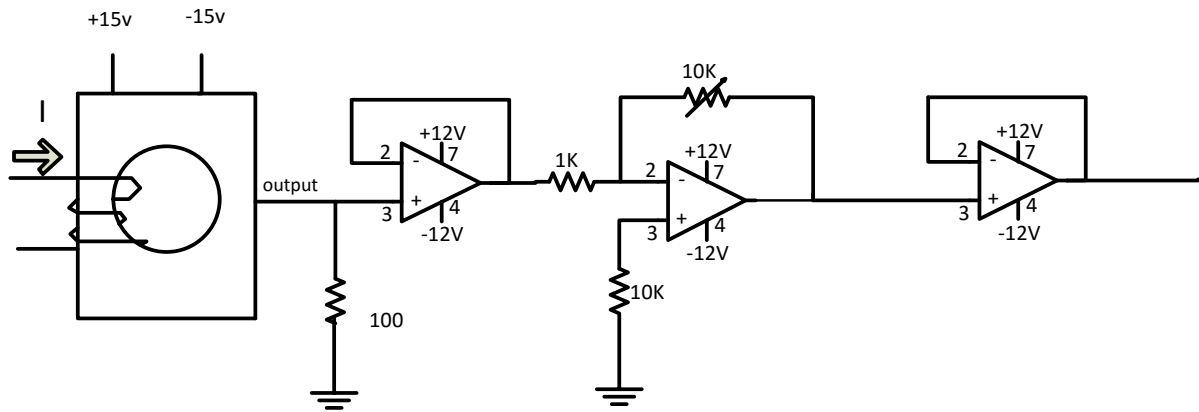


Figure 6.7: AC current sensor circuit

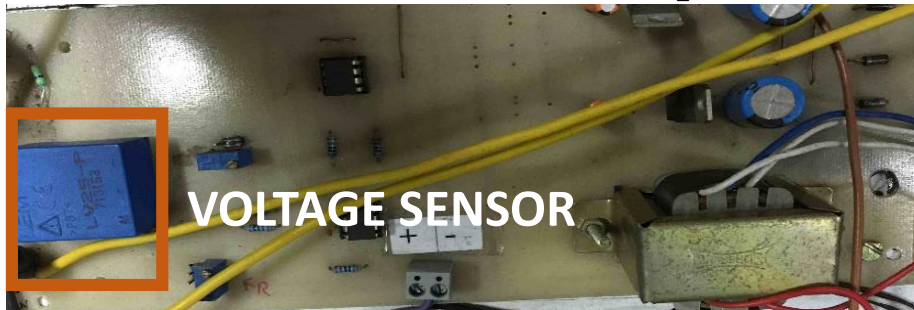
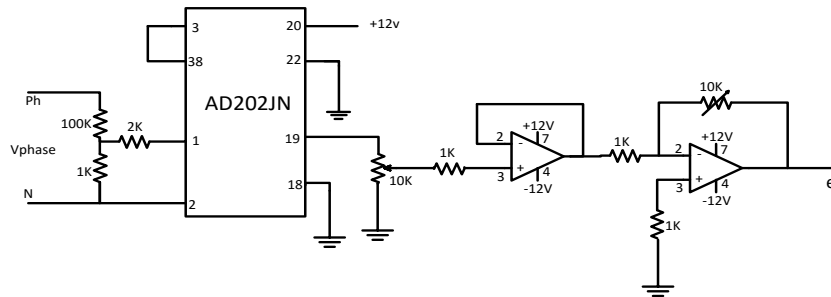


Figure 6.8: AC voltage sensing circuit

## 6.4 Control Hardware

### 6.4.1 Pulse Amplification and Isolation Circuit

The pulse amplification circuit for MOSFET is shown in figure 6.9. The optocoupler MCT-2E provides necessary isolation between the low voltage isolation circuit and high voltage power circuit. The pulse amplification is provided by the output amplifier transistor 2N2222.

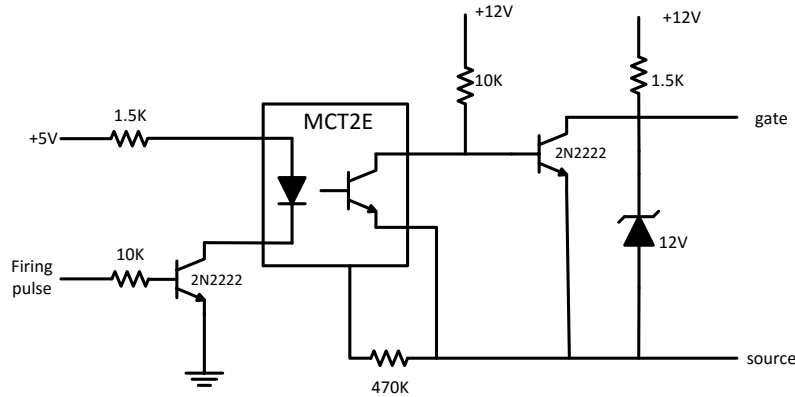


Figure 6.9: Pulse Amplification and Isolation Circuit

### 6.4.2 Controller realization and PWM generation

FPGA SPARTAN 3E is used to realize the controller part of the hardware. The role of FPGA in this application is to take input, the voltage and frequency and apply control algorithms, be it PI or Neural or Fuzzy to generate required mechanism and produce the switching waveforms/signals that are then fed into each of the 12 gates of voltage source inverter. Figure 6.10 shows the image of FPGA used in the realization. Further it highlights 4 switches that can have 2 states (0/1) indicating the modulation index in 16 steps that can be fed manually.

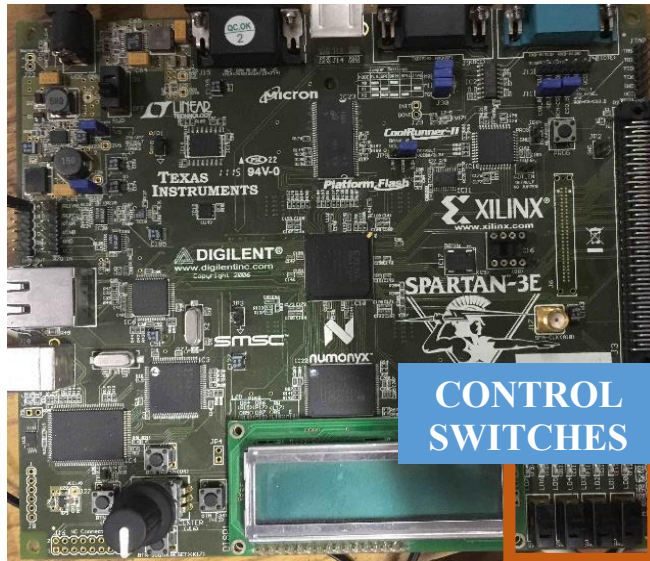


Figure 6.10: FPGA used in hardware and the control switches

## 6.5 Power Supplies

DC regulated supplies (+12v gnd -12v) are required for providing biasing to various circuits like pulse amplification and isolation circuits, hysteresis controller and voltage detectors etc. using IC's 7812 for +12v, IC 7912 for -12v.

The circuit diagram of the power supply is as shown in following figure.

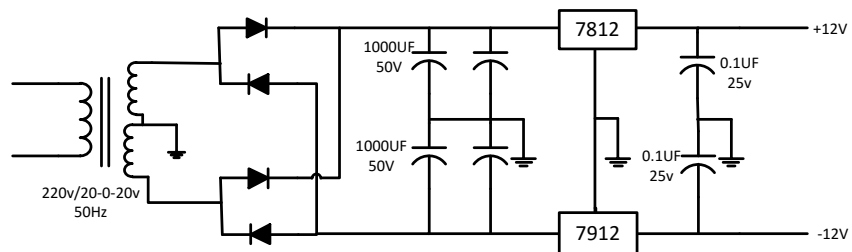


Figure 6.11: Connection diagram for power supplies -12,0,+12v

## 6.6 Overall Setup

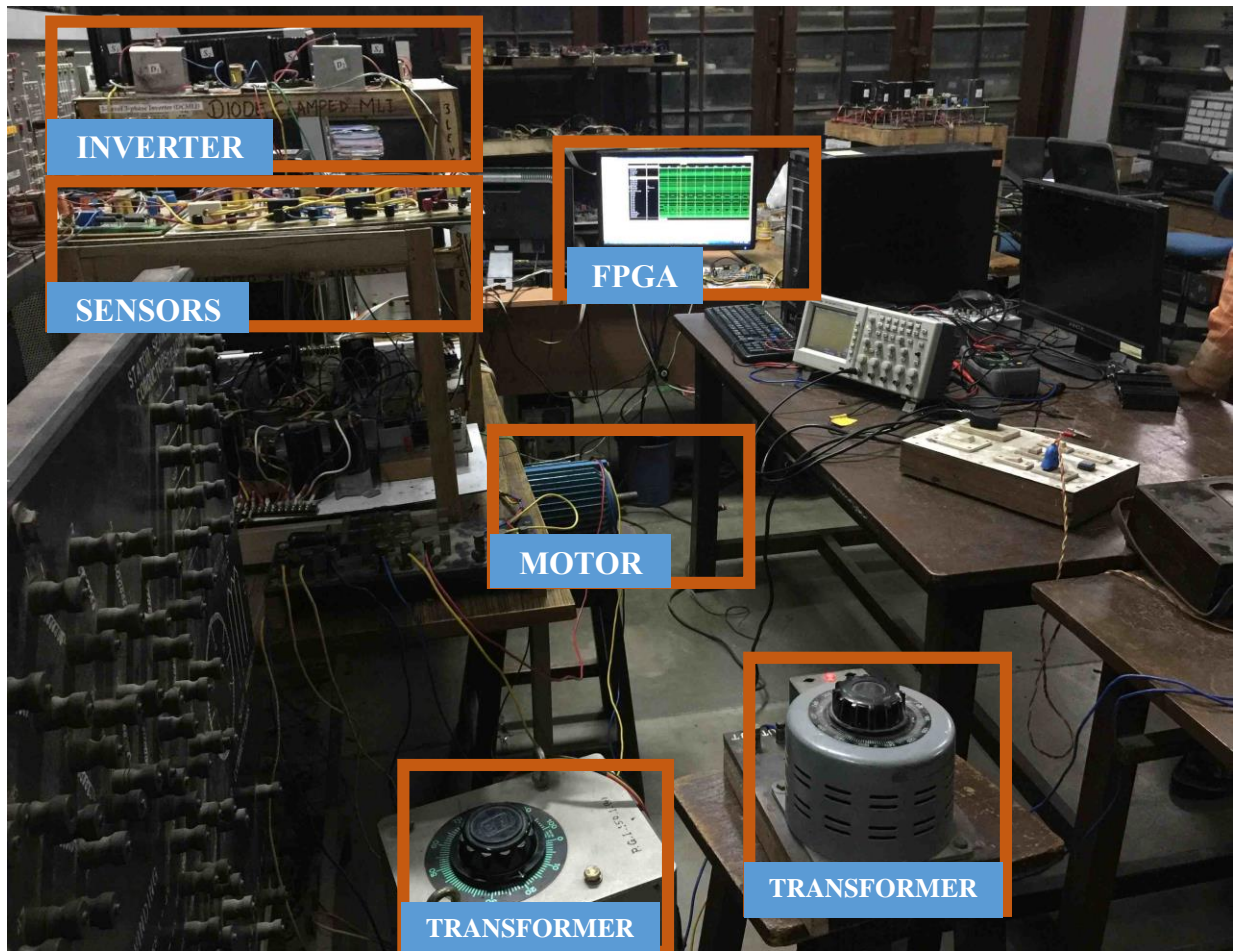


Figure 6.12: Image showing the overall setup of the hardware evaluation

Figure 6.12 shows the overall arrangement for implementing and verification of voltage source inverter fed 3 phase induction machine. Also labelled are the parts of the circuit. Namely auto transformers, 3 phase induction machine, 3 level voltage source inverter, FPGA setup acting as controller, sensors for measurement of currents and voltages. We can further see a Single Pull Double Throw switch and a 3 phase auto transformer.

Initially the 3 phase induction machine is run at around 100 Volts using the 3 phase auto transformer and at run time, the switch is thrown towards the inverter output thus shifting the motor input source to 3 phase inverters. This has been done as a protection measure to avoid the high surge currents during the starting of induction machine which the hardware prototype of inverter might not sustain.

# References

---

1. Xin Yao, "Evolving artificial neural networks," in *Proceedings of the IEEE*, vol.87, no.9, pp.1423-1447, Sep 1999
2. Narendra, Kumpati S., and Kannan Parthasarathy. "Identification and control of dynamical systems using neural networks." *Neural Networks, IEEE Transactions on* 1.1 (1990): 4-27.
3. Zadeh, Lotfi A. "Fuzzy sets." *Information and control* 8.3 (1965): 338-353.
4. Jang, Jyh-Shing Roger, Chuen-Tsai Sun, and Eiji Mizutani. "Neuro-fuzzy and soft computing: a computational approach to learning and machine intelligence." (1997).
5. Arvindan, A. N., V. K. Sharma, and M. Subbiah. "Selective harmonic elimination in a microprocessor based single-phase DC-AC inverter with switch realizations." *Power Electronics, 2006. IICPE 2006. India International Conference on.* IEEE, 2006.
6. Sun, J., and H. Grotstollen. "Pulsewidth modulation based on real-time solution of algebraic harmonic elimination equations." *Industrial Electronics, Control and Instrumentation, 1994. IECON'94., 20th International Conference on.* Vol. 1. IEEE, 1994.
7. Sirisukprasert, Siriroj, Jih-Sheng Lai, and Tian-Hua Liu. "Optimum harmonic reduction with a wide range of modulation indexes for multilevel converters." *Industrial Electronics, IEEE Transactions on* 49.4 (2002): 875-881.
8. Maia, Helder Z., et al. "Adaptive selective harmonic minimization based on ANNs for cascade multilevel inverters with varying DC sources." *Industrial Electronics, IEEE Transactions on* 60.5 (2013): 1955-1962.
9. Saied, Basil M., Shefa Dawwd, and Ahmad S. Al-Soufi. "FPGA based selective harmonic elimination pulse width modulation technique." *Design and Test Workshop (IDT), 2009 4th International.* IEEE, 2009.
10. Taghizadeh, H., and M. Tarafdar Hagh. "Harmonic elimination of cascade multilevel inverters with nonequal DC sources using particle swarm optimization." *Industrial Electronics, IEEE Transactions on* 57.11 (2010): 3678-3684.

11. Balasubramonian, M., and Venkiteswaran Rajamani. "Design and Real-Time Implementation of SHEPWM in Single-Phase Inverter Using Generalized Hopfield Neural Network." *Industrial Electronics, IEEE Nirvanas on* 61.11 (2014): 6327-6336.
12. Banaei, Mohamad Reza, and Pouya Asadi Shayan. "Solution for selective harmonic optimisation in diode-clamped inverters using radial basis function neural networks." *IET Power Electronics* 7.7 (2014): 1797-1804.
13. Bose, Bimal K. "Intelligent control and estimation in power electronics and drives." *Electric Machines and Drives Conference Record, 1997. IEEE International. IEEE, 1997.*
14. Bose, Bimal K. "Expert system, fuzzy logic, and neural network applications in power electronics and motion control." *Proceedings of the IEEE* 82.8 (1994): 1303-1323.
15. Patel, Hasmukh S., and Richard G. Hoft. "Generalized techniques of harmonic elimination and voltage control in thyristor inverters: Part I--harmonic elimination." *Industry Applications, IEEE Transactions on* 3 (1973): 310-317.
16. Arvindan, A. N., V. K. Sharma, and M. Subbiah. "Selective harmonic elimination in a microprocessor based single-phase DC-AC inverter with switch realizations." *Power Electronics, 2006. IICPE 2006. India International Conference on. IEEE, 2006.*
17. Sun, J., and H. Grotstollen. "Pulsewidth modulation based on real-time solution of algebraic harmonic elimination equations." *Industrial Electronics, Control and Instrumentation, 1994. IECON'94., 20th International Conference on. Vol. 1. IEEE, 1994.*
18. Bose, Bimal K. "Neural network applications in power electronics and motor drives—An introduction and perspective." *Industrial Electronics, IEEE Transactions on* 54.1 (2007): 14-33.
19. Maia, Helder Z., et al. "Adaptive selective harmonic minimization based on ANNs for cascade multilevel inverters with varying DC sources." *Industrial Electronics, IEEE Transactions on* 60.5 (2013): 1955-1962.
20. Saied, Basil M., Shefa Dawwd, and Ahmad S. Al-Soufi. "FPGA based selective harmonic elimination pulse width modulation technique." *Design and Test Workshop (IDT), 2009 4th International. IEEE, 2009.*
21. Holmes, D. G., and A. Kotsopoulos. "Variable speed control of single and two phase induction motors using a three phase voltage source inverter." *Industry Applications Society Annual Meeting, 1993., Conference Record of the 1993 IEEE. IEEE, 1993.*



22. Mir, Sayeed A., Donald S. Zinger, and Malik E. Elbuluk. "Fuzzy controller for inverter fed induction machines." *Industry Applications, IEEE Transactions on* 30.1 (1994): 78-84.
23. Kazmierkowski, Marian P. "Control strategies for PWM rectifier/inverter-fed induction motors." *Industrial Electronics, 2000. ISIE 2000. Proceedings of the 2000 IEEE International Symposium on*. Vol. 1. IEEE, 2000.
24. Suetake, Marcelo, Ivan N. da Silva, and Alessandro Goedel. "Embedded DSP-based compact fuzzy system and its application for induction-motor speed control." *Industrial Electronics, IEEE Transactions on* 58.3 (2011): 750-760.
25. Eltamaly, Ali M., A. I. Alolah, and Basem M. Badr. "Fuzzy controller for three phases induction motor drives." *Autonomous and Intelligent Systems (AIS), 2010 International Conference on*. IEEE, 2010.